NOVEL SOLVENT SYSTEMS FOR THE DEVELOPMENT OF SUSTAINABLE TECHNOLOGY

A Thesis
Presented to
The Academic Faculty

by

Laura Christine Draucker

In Partial Fulfillment
of the Requirements for the Degree
Doctor of Philosophy in the
School of Chemical and Biomolecular Engineering

Georgia Institute of Technology
August 2007

NOVEL SOLVENT SYSTEMS FOR THE DEVELOPMENT OF SUSTAINABLE TECHNOLOGY

Approved by:

Dr. Charles A. Eckert, Advisor
School of Chemical and Biomolecular Engineering
Georgia Institute of Technology

Dr. Wm. James Fredrick, Jr.
School of Chemical and Biomolecular Engineering
Georgia Institute of Technology

Dr. Charles L. Liotta, Co-Advisor
School of Chemistry and Biochemistry
Georgia Institute of Technology

Dr. Arthur J. Ragauskas
School of Chemistry and Biochemistry
Georgia Institute of Technology

Dr. Amyn S. Teja
School of Chemical and Biomolecular Engineering
Georgia Institute of Technology

Date Approved: June 20th, 2007

“ She refused to let common sense cloud her judgment”

ACKNOWLEDGEMENTS

I thank my advisors, Dr. Chuck Eckert and Dr. Charlie Liotta, for all their guidance and support throughout the past four years. I would particularly like to thank Chuck for actually reading my entrance essay and believing I had something more to offer then what my undergraduate GPA and GRE scores showed. Even when I wasn't sure I could make it Chuck always believed in me, and for that I will be forever grateful. I would also like to thank the rest of my committee: Dr. Amyn Teja, Dr. Jim Fredrick, and Dr. Art Ragauskas for their kind words, ideas, and advice.

My experience at Georgia Tech would not have been nearly as enjoyable if it wasn't for the other members of the Eckert/Liotta Group. Thanks to Deborah (a.k.a. Photoshop genius), I always had pretty figures for my papers, chemicals to work with, and a smiling face to talk to if I was confused by any weird Georgia Tech rules. I am thankful to everyone that helped me with my research; fellow graduate students Malina Janakat, Michael Lazzaroni, Megan Donaldson, Tori Blasucci, Michelle Kassner, Ryan Hart, and all the undergraduate assistances that helped along the way. I would have probably never finished if it wasn't for the help of all our post-docs, especially Jason Hallet, Chris Kitchens, and David Bush. I was lucky enough to have many of my group members as good friends, and I would not have survived without our walks to Starbucks to let off steam. Furthermore, I have to thank Georgia Tech for merging with IPST my first year; although it wasn't the best situation for many involved, it helped me meet some of my closest friends during graduate school, and introduced me to an industry I had practically no knowledge of beforehand.

I am a very lucky girl to have such wonderful friends and family that helped keep me sane during graduate school. They all believed in me, probably more then I believed in myself when I first started this grad school thing, and have been there for all the highs and lows. My mom and dad have been nothing but supportive and proud of me, and I hope they realize how much I appreciate that. I also owe a huge thank you to my grandmother Verna Draucker and my late grandfather Lewis (Buddy) Draucker. They made it financially possible for me to attend Villanova University where I received a wonderful undergraduate education, and my grandmother continued to make my life as a graduate student a little easier with some pocket money and a handwritten note every month or so that meant so much to me.

And finally, I have to thank Marcus - who has truly seen me at my worse, totally stressed and worrying about way to much, and who wants to marry me anyway ☺

TABLE OF CONTENTS

LIST OF TABLES

LIST OF FIGURES

SUMMARY

Sustainable development in chemical engineering offers technical, industrially relevant solutions to environmental and economic issues. This work focuses on three specific issues; improving solvent selection and reducing costly experimentation, improving catalyst recovery while reducing reaction time, and producing commercial viable biofuels by cost effective pretreatments and valuable side product extractions. Novel solvent systems are a sustainable solution because they provide the ability to replace costly solvents with cheap, benign, and recyclable systems. Specifically, this work investigated the use of one novel solvent system, Gas Expanded Liquids (GXL).

When a solvent is exposed to a gas in which it is miscible at modest pressures and temperatures, the liquid solvent becomes expanded, providing a unique tunable and reversible solvent with properties that can be much different then that of the solvent itself. If you apply this gas to a mixture of two liquids of a solid dissolved in a liquid phase, it can often provide a miscibility switch, aiding in separation, crystallization, and recovery of products or catalysts. In this work several different applications for organic solvents expanded with carbon dioxide were studied including miscibility switches for catalyst recycle, pretreatment of biomass for improved bio-ethanol production, and extraction of valuable chemicals from lignin waste in the pulp and paper industry. Solid solubility models to improve solvent selection and predict unique solvent mixtures during crystallization were also studied. The results reported here show promise for the use of GXL novel solvent systems and solid solubility models in many sustainable applications.

CHAPTER I

INTRODUCTION

In the past several years, the term ‘sustainable’ has been used to describe many concrete things: development, energy, growth, etc. However, the concept behind sustainability is acutely abstract, blurring the line between enabling a society to prosper while also preserving natural resources for future generations. Today, environmental issues have come to a head with fears of climate change, unsafe food supplies, and unaffordable fuel dominating the headlines. The general public is looking to the government and scientific community for answers on ways to preserve their environment and ultimately, their way of life.

For scientific researchers in the chemical engineering field, sustainable development can be achieved two ways. First, we can develop new, sustainable technologies to replace or complement existing processes. Some examples of these technologies include those that reduce waste (liquid, solid, and gaseous emissions), use non-toxic or renewable feedstocks, require less energy, implement more solvent and/or catalyst recycle, and use less processing water. Second, we can develop technologies that create new, sustainable products. The best example of this is the development of biofuels that can adequately replace petroleum as the United State’s primary transportation fuel. The challenge for both of these research endeavors is developing technologies that are environmentally sustainable and economically viable. In this work, we research ways to add sustainability to both new and existing processes with novel solvent systems.

The first two chapters look at ways to improve existing processes. In Chapter II we seek an improved methodology for the design of solvents and solvent mixtures for separations, especially purification of solids by crystallization. We report new data for the solubility of 4 multi-functional solids: 3-nitrophthalimide, 5-fluoroisatin, 2-amino-5-nitrobenzophenone, and benzimidazole. We used these data to regress new MOSCED model parameters for these solids. The MOSCED activity coefficient model uses regressed parameters to predict the infinite dilution activity coefficient, which can then predict solid solubility in a wide range of solvents and solvent mixtures. The ability to use thermodynamic models to predict solubility of complex solutes provides a new paradigm for the selection of both pure and mixed solvents. Solvent selection is a costly process which often wastes time, money, and valuable chemicals. A model like MOSCED that requires a small set of experimental data to determine a large number of solvent and solvent-mixture possibilities can reduce the negative environmental impact of wasted experimental materials while ultimately saving money. The MOSCED model is proven here to work for complex solutes, which is often a challenge for other existing solid solubility models.

In Chapter III we study the phase behavior of several fluorous/organic liquid/CO_2 systems to assess the ability of a CO_2 cosolvent to improve the reaction rate and recycle capability of fluorous biphasic catalysis. Homogeneous catalysts offer many advantages over heterogeneous catalysts such as higher activities and selectivities. However, recovery of homogeneous catalysts is often complicated by difficulties in separating these complexes from the reaction products. The use of gaseous carbon dioxide (CO_2) as a miscibility switch for organic and fluorous phases has been proposed to overcome this

limitation. By using CO_2 as a cosolvent, polar organic reactants can be homogenized with catalysts immobilized in a fluorous phase without using elevated temperatures. The phase behavior reported here provides the means to determine which fluorous/organic solvent pair would be most sustainable.

The last two chapters investigate ways novel solvent systems could provide sustainability to the development of biofuels via biorefineries and pulp and paper mills. Biorefineries combine the concept of biofuel development with the production of other valuable side-products to increase profitability. This is already done with petroleum production; oil refineries produce significant side products to improve their bottom-line. To succeed in providing cost-competitive biofuels to replace gasoline two economically and environmentally sustainable processes need to be developed; one for biofuels, and the other for valuable side-products. The established pulp and paper industry has many things in common with the proposed biorefinery, and we look at both to determine the best fit for specific innovations.

Chapter IV investigates the isolation and extraction of fine chemicals from waste biomass in the pulp and paper mill. We demonstrate a technique for extracting the high-value added chemicals vanillin and syringaldehyde from lignin using a novel CO_2-expanded organic solvent (gas-expanded liquid). This method offers several economic advantages – low operating costs, easy recycle of organic solvents, use of a renewable feedstock, and a way to produce chemicals without wasteful synthesis. Furthermore, this technique demonstrated the ability to produce high-value chemicals ($5-25/lb) from a waste source that is presently being burned for a fuel value of 2-3 cents/lb. We believe

this process will spark interest in developing other sustainable techniques to extract fine chemicals from renewable waste streams.

Chapter V applies the same gas-expanded liquid solvent system to biofuel production, most specifically to the development of a cost-effective pretreatment process for bio-ethanol production from lignocellulosic biomass. When converting lignocellulosic biomass material to bio-ethanol, pretreatment is needed to penetrate the biomass matrix and improve yields. However, even with substantial amounts of research devoted to this problem, a cost-effective and environmentally benign solution has yet to be reported. In this chapter we pretreated several types of lignocellulosic biomass with gas-expanded liquids to determine their effect on the biomass matrix. Finally, Chapter VI offers several recommendations for future work in sustainable development, focused mostly on the development of commercially viable biofuels.

CHAPTER II

EXPERIMENTAL DETERMINATION AND MODEL PREDICTION OF SOLID SOLUBILITY OF MULTI-FUNCTIONAL COMPOUNDS IN PURE AND MIXED NON-ELECTROLYTE SOLVENTS

Introduction

Knowledge of solid-liquid equilibria is of clear importance for the design of separation processes; especially cooling-, evaporative-, and anti-solvent crystallization. There is a strong need to develop better models for predicting these behaviors, especially in the cases of nonideal complexing systems[1] and systems with multifunctional molecules[2].Using models to predict the desired solvent or solvent mixture for a process has many positive impacts on industry. Not only will it reduce the cycle time for the development of new chemical processes by avoiding costly experiments[2]; using models permits comparison of different solvent characteristics and facile choice between process considerations such as manufacturing performance, safety, and solvent recovery and recycle[3]. There are many cases where mixtures of multiple solvents lead to better separations than pure solvents; however, the large number of available solvent mixtures makes thorough experimental testing nearly impossible. Therefore, predicting accurately the performance of such mixtures would be a powerful tool for solvent selection; but, it also constitutes an even greater challenge for solubility models[4-6] compared to predictions for pure solvents. The goal of this study is to facilitate efficient solvent selection by the

development of a good predictive technique for estimating solubility over a wide range of both pure and mixed solvents.

Modified UNIFAC[7-9] has been shown to be a good predictor of solid-liquid equilibria, but many current molecules of interest such as pharmaceuticals, pharmaceutical precursors, and agricultural chemicals have groups with missing UNIFAC interaction parameters and therefore can not be predicted accurately[3]. Another research group used computer-aided molecular design framework for the selection of solvent for crystallization[10]; however, the UNIFAC model was used to evaluate liquid-phase activity coefficients, which results in difficulties with complex systems for the reasons just described[11]. The Hansen solubility model does a good job predicting solid-liquid equilibria for some systems, however Hansen cannot predict negative deviations from ideality and may perform poorly for associated and solvating systems[12]. Since one generally seeks solvents with a low activity coefficient to give high solubility, this is a major drawback of the Hansen method. Mobile Order Theory[13] is also sometimes used to predict solid solubility[14], although it has been shown to work poorly for polar solvents[15].

The MOSCED activity coefficient model[16], like the Hansen solubility parameter model, is an extension of Hildebrand solubility parameter theory and has been applied recently to the prediction of solid solubility in various pure and mixed solvents[12]. Four descriptors for the whole molecule, which are empirically assigned to dispersion, polarizability, dipolarity, and hydrogen-bond or Lewis bonding, are required for each component. In this study the model is further applied to the correlation and prediction of newly-measured solubility values of some interesting and mostly unstudied multi-functional solids. The application of the MOSCED model in this work leads to a new

paradigm for solvent selection via thermodynamic models with minimal experimental data.

The solids used to study the MOSCED model include 3-nitrophthalimide, 5-fluoroisatin, 2-amino-5-nitrobenzophenone, and benzimidazole; the structures of which are shown in Figure 2-1. These particular solutes were chosen for their complexity; i.e. they have multiple functional groups and structures that are not amenable to group contribution techniques such as UNIFAC. Data for these types of solutes are scarce in the literature; most of the non-electrolyte solubility data in the literature are for polynuclear aromatic hydrocarbons. The interactions in solution resulting from the structures and functionalities of these compounds should be a strong test for any model, and we examine the MOSCED model for correlative and predictive capabilities. The organic solvents studied were chosen to represent nonpolar, polar aprotic, aromatic, halogenated, and associated compounds. These solvents were expected to give a good indication of the possible solute-solvent interactions as well as to provide a wide range of solubility values for each solid. The solubilities of each solid were measured in pure solvents, as well as in several mixtures that had the potential to produce a synergistic effect on the solubility – which in this work we define as the existence of an extremum in the solubility plotted vs. solvent composition.

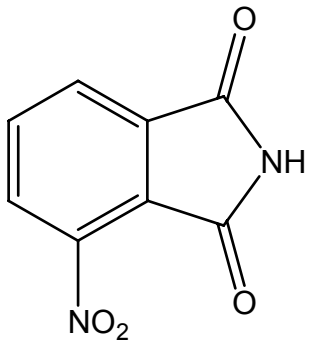

3-nitrophthalimide

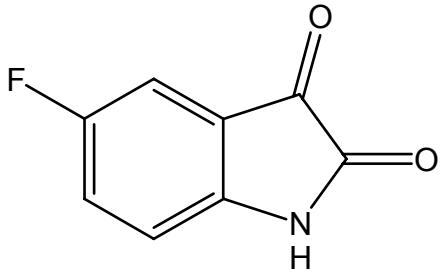

5-fluoroisatin

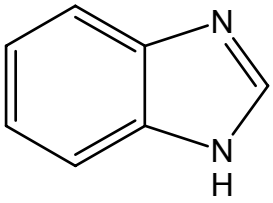

benzimidazole

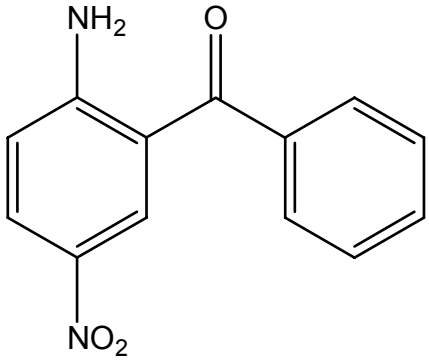

2-amino-5-nitrobenzophenone

Figure 2-1**. Structures of the solid compounds studied.**

The two most prevalent methods for measuring solid-liquid equilibria are the synthetic method (or indirect)[6] and the analytical (or direct sampling) method[17]. For very low solubilities similar to those presented in this paper, the analytical method has been proven effective[18]. Acree and coworkers have used this method in their solubility measurements of polyaromatic solids in organic solvents using an ultraviolet detector[1]. This analytical technique is superior in cases where the solubility is low, but it is limited to solvents that do not have UV signatures. In this study, the solid-liquid equilibria data were measured with the direct sampling method and analyzed using a GC-FID for direct composition analysis. This technique offers several advantages; the capability to prepare simultaneously the equilibrium mixtures of the solutes in all the solvents, the ability to

analyze with an automatic sampler, and the means to avoid limiting the type of solvents available to study.

Experimental Procedures

Materials

The following chemicals were obtained from commercial sources and were used as received.

Chemical	Supplier	Grade and Purity	
2-amino-5-nitrobenzophenone	Acros		98
5-fluoroisatin	Acros		98
3-nitrophthalimide	Acros		97
benzimiazole	Acros		98
benzyl	Aldrich		98
phenanthrene	Aldrich		98
methanol	Aldrich	HPLC grade	99.93
ethanol	Aldrich	Anhydrous	99.5
2-propanol	Aldrich	Anhydrous	99.5
2-butanone	Aldrich		99.8+
ethyl acetate	Fisher		99.9
1,4-dioxane	Aldrich		99.+
nitromethane	Aldrich		98.7
acetonitrile	Aldrich	HPLC grade	99.93
N,*N*-dimethylformamide	Aldrich	Anhydrous	99.8
benzyl alcohol	Aldrich		98
chlorobenzene	Aldrich		99
dichloromethane	Riedel-deHaën		99.8
chloroform	Aldrich		99.8
heptane	Aldrich	HPLC grade	99
cyclohexane	Aldrich	Anhydrous	99.5
toluene	Aldrich	Anhydrous	99.8

Apparatus and Methods

Two experimental methods were used to determine equilibrium solubility of the solids in organic solvents. For the first method, solid and solvent were added to glass vials which were sealed with a plastic lined cap (Fisher, 02-912-058) and placed in a isothermal water bath (VWR Scientific Products, 1296) controlled to ±0.1 K. The

solutions were agitated for three to five days to ensure equilibrium was reached. A sample of known volume of the saturated liquid phase was removed from the vial using a volumetric pipette, and the sample volume and mass were recorded accurate to ±0.005 cm^3 and ±0.05 g respectively. The sample was diluted with a known volume of acetone, up to a 25:1 ratio, and the concentration of the sample was determined using GC-FID with a calibration of response to concentration. The uncertainty in concentration calculated from propagation of error is ± 8.5 percent. To validate this method, we measured the solubility of benzil and phenanthrene in several different solvents. Comparison with literature data[19, 20] are shown in Table 2-1. While some variations exceed the precision reported and/or our standard deviations (determined from multiple measurements), the excesses are minor and deemed to be acceptable given the possible variations with purity and technique.

Table 2-1. Experimental solubility vs. literature values using the dilution method for benzil and phenanthrene at 298 K.

Solute	Solvent	x^{exp}	x^{lit}	AD† / %
benzil	methanol	0.00738	0.00783	-5.7
benzil	2-propanol	0.00837	0.00831	0.7
benzil	ethyl acetate	0.13768	0.14550	-5.4
benzil	toluene	0.13474	0.15040	-10.4
benzil	cyclohexane	0.01107	0.01068	3.7
phenanthrene	methanol	0.00543	0.00589	-7.8
phenanthrene	ethanol	0.01282	0.01114	15.1
phenanthrene	cyclohexane	0.03943	0.03648	8.1
phenanthrene	1-octanol	0.05672	0.05418	4.7
phenanthrene	ethyl acetate	0.13443	0.14990	-10.3
phenanthrene	1,4-dioxane	0.21352	0.21650	-1.4

† $\mathrm{AD} = \left(x^{\mathrm{exp}} - x^{\mathrm{lit}}\right) / x^{\mathrm{lit}}$

For sparingly soluble solids, a second method was used that varied slightly from the above method. Equilibrium vials were prepared in the same way and placed in vials with a pierceable septum top. The sample vials were placed in a temperature-controlled

sample tray and agitated periodically for three days. The sample tray was attached directly to an automatic sampler on the gas chromatograph, and samples were taken from the equilibrium vials and injected directly on the GC column to be analyzed by FID. To validate this method, the solubility of anthracene in several solvents was compared to literature values[21], and the results are shown in Table 2-2. The largest deviations are for the solubility in hexane and methanol. We believe our measurement to be more reliable for hexane since it gives the right trend when comparing to cyclohexane. For the solubility in methanol, the discrepancy is perhaps due to reaching the detection limits in our method. These two methods were used interchangeably to determine the solubility of all four solids in the various solvents and solvent mixtures.

Table 2-2. Experimental solubility vs. literature values using the direct sampling method for anthracene at 298 K.

Solute	Solvent	x^{exp}	x^{lit}	AD / %
anthracene	hexane	0.00122	0.00157	-22
anthracene	cyclohexane	0.00150	0.00157	-5
anthracene	toluene	0.00713	0.00736	-3
anthracene	dioxane	0.00698	0.00838	-17
anthracene	methanol	0.00034	0.00025	35
anthracene	acetone	0.00376	0.00432	-13
anthracene	tetrahydrofuran	0.01384	0.01204	15

The melting point of the four solids was determined using a Mettler-Toledo melting point apparatus accurate to ± 0.05 K. The enthalpy of fusion at the melting point for all the solids was determined using differential scanning calorimetry (Netzsch STA409) at a heating rate of 5°C/min under nitrogen flow. This machine was calibrated against Netzsch supplied standards, and the uncertainty is estimated to be ±10 %. Our enthalpy of fusion for benzimidazole agreed with literature values[22, 23].

Experimental Results, Modeling, and Discussion

Pure solvents

The solubility of benzimidazole, 3-nitrophthalimide, 5-fluoroisatin, and 2-amino-5-nitrobenzophenone in 12 to 14 pure solvents can be found in Table 2-3. The uncertainty was estimated to be ± 9%, determined from the standard deviations of repeated experimental measurements. In general, all four compounds are very soluble in DMF and rather insoluble in alkanes and chlorinated compounds, showing negative and positive deviations from ideality respectively. 3-Nitrophthalamide and 5-fluoroisatin, which have similar structures (aromatic backbone with withdrawing group, two carbonyls, and acidic amine), give similar trends over the complete range of solvents. In alcohols, benzimidazole gives negative deviations while 3-nitrophthalimide, 5-fluoroisatin, and 2-amino-5-nitrobenzophenone give large positive deviations. We believe this is due to the basic character of benzimidazole, which would accept more hydrogen bonding from alcohols compared to the other solids.

Table 2-3. Measured solute physical properties and regressed MOSCED parameters with the Wilson g^E model.

Solute	T_m (K)	ΔHfus (kJ/mol)	λ	τ	α	β
benzimidazole	444	22.7	16.21	4.22	12.15	11.12
2-amino-5-nitrobenzophenone	440	37.9	14.06	8.12	7.29	1.83
3-nitrophthalimide	487	34	15.21	8.81	13.1	5.63
5-fluoroisatin	498	29.6	16.71	6.76	6.93	5.8

Heat of Fusion

As previously mentioned, the heat of fusion values for each solute were measured using a differential scanning calorimetry (DSC) under nitrogen flow. The data reported

here vary from previously reported data[24], which were measured by DSC exposed to air and therefore less accurate. Two different modeling techniques were used in an attempt to model the heat of fusion; Mobile Order and Disorder Theory (MOD)[25] and an entropy of melting approximation using the rotational symmetry number and the molecular flexibility number (termed the Yalkowsky model) [26]. Table 2-4 shows the comparison of each model prediction to the experimental heat of fusion data taken for this study. It can be seen that the MOD model does a poor job predicting the experimental data; however, the Yalkowsky model predicts quite well and is reasonably simple to use.

Table 2-4. Comparison of experimental heat of fusion (kJ/mol) to the MOD and Yalkowsky model predictions.

Solute	Experimental	MOD Model[25]	Yalkowsky Model[26]
benzimidazole	22.7	38.3	23.6
3-nitrophthalimide	34.0	27.5	34.0
5-fluoroisatin	34.0	53.3	34.3
2-amino-5-nitrobenzophenone	37.9	28.7	30.6

MOCSED Model

The MOSCED model calculates infinity dilution activity coefficients by the expression shown in Table 2-5. As previously mentioned, four descriptors for the whole molecule are required for each component; the dispersion parameter λ, the polarity parameter τ, the acidity parameter α, and the bascity parameter β. Upon original conception of this model, the λ and τ parameters were correlated to the refractive index and skeletal carbon atoms of each solute and solvent respectively[16]. To allow for the model's use over a wide range of solutes and solvents, the most recent version of

MOSCED fits all 4 parameters to pure component experimental solubility data[12]. Because the descriptors represent specific interactions of the compound, it is possible to justify the magnitude of the parameters based on physical and chemical characteristics. The induction parameter q, which is a measure of the dipole-induced dipole energy, is typically equal to 1 unless compounds have large dispersion parameters, such as aromatic and halogenated compounds. For aromatic compounds q is set to 0.9, and for halogenated compounds it is varied for the best fit (typically between 0.9-1).

Table 2-5. MOSCED model.

$$\ln \gamma_2^{\infty} = \frac{v_2}{RT}\left[(\lambda_1 - \lambda_2)^2 + \frac{q_1^2 q_2^2 (\tau_1 - \tau_2)^2}{\psi_1} + \frac{(\alpha_1 - \alpha_2)(\beta_1 - \beta_2)}{\xi_1}\right] + d_{12}$$

$$d_{12} = \ln\left(\frac{v_2}{v_1}\right)^{aa} + 1 - \left(\frac{v_2}{v_1}\right)^{aa}$$

$$aa = 0.953 - 0.00968\left(\tau_2^2 + \alpha_2\beta_2\right)$$

$$\alpha_T, \beta_T = (\alpha_{293}, \beta_{293})\left(293/T\right)^{0.8} \qquad \tau_T = \tau_{293}\left(293/T\right)^{0.4}$$

$$\psi = POL + 0.011\alpha_T\beta_T$$

$$\xi = 0.68(POL - 1) + \left[3.24 - 2.4\exp\left(-0.023(\alpha_o\beta_o)^{1.5}\right)\right]^{(293/T)^2}$$

$$POL = q^4\left(1.15 - 1.15\exp\left(-0.02\tau_T^3\right)\right) + 1$$

For this work, MOSCED model parameters were regressed using the experimental solubility data measured in pure solvents. This data is shown in Appendix A, Table A-1. The four parameters are adjusted to minimize the average error in the calculated solubility for all pure solvents[12]. The solubility is calculated from equation 1[27] where ΔH_{fus} is the enthalpy of fusion at the melting point temperature T_m, R is the universal gas constant, ΔC_p is the difference in heat capacity of the sub-cooled liquid and crystalline solute, γ_s is the activity coefficient of the solid in solution, x_s is the equilibrium concentration of the solid in solution, and x^{ideal} is the ideal solubility independent of the solvent. The finite concentration activity coefficients are calculated from a 2-parameter

g^E model where the parameters match infinite dilution activity coefficients predicted by MOSCED. We tested both the Wilson and UNIQUAC g^E models when regressing the parameters and predicting the mixed solvent behavior. We found that both behaved in similar fashion for pure solvents; however, the UNIQUAC model did not always predict reasonably the finite concentration activity coefficients when the two predicted infinite dilution activity coefficients were less then 1, i.e. there was a pronounced finite concentration minimum. It was also shown in the literature [18] that the Wilson model correlates better then UNIQUAC for benzimidazole in solvents with positive deviations from ideality. We therefore chose to show only the regressions with the Wilson model. An example regression of benzimidazole solid solubility in 2-butanone at 298 °K with the MOSCED-Wilson parameters is located in Appendix B.

$$x^{ideal} = x_S \gamma_S = \exp\left[\frac{-\Delta H_{fus}}{R T_m} \left(\frac{T_m}{T} - 1 \right) - \frac{\Delta C_p}{R} \left(\ln \frac{T_m}{T} - \frac{T_m}{T} + 1 \right) \right] \qquad (1)$$

There has been some debate as to the importance of ΔC_p in calculating the ideal solubility of a solid[28-31]. Very few literature values are available for ΔC_p because it is difficult to measure[32], and hence, the following two assumptions are commonly used: setting $\Delta C_p = 0$ or setting it equal to ΔS_{fus}. Pappa et al. conclude that the accuracy of these assumptions compared to using an estimation technique is dependent on the functionality of the solute[28]. The ΔC_p of benzimidazole has been measured by Domańska and Bogel-Łukasi[33], and we compared the experimental and predicted solubilities in both pure and mixed solvents using this ΔC_p, $\Delta C_p = 0$, $\Delta C_p = \Delta S_{fus}$ (which was consistent with the reported value). Our results were similar to the literature on this subject; no single approximation works best for all cases, making ΔC_p more like an adjustable parameter

then a physical property. Therefore, we chose to use $\Delta C_p = 0$, keeping our model as simple as possible.

Second-order phase transitions were not observed in our DSC measurements and are not included in the solubility calculation as was done by Domańska et al.[18]; however, the effort required to understand and measure these transitions often cannot be justified for screening purposes. Furthermore, their effect on the calculated result is likely to be small and within experimental uncertainty.

A graphic representation of benzimidazole solubility in pure solvents as compared to the ideal solubility and the MOSCED predictions is shown in Figure 2-2. Figures 2-3, 2-4, and 2-5 show the experimental versus predicted pure solubility data for 3-nitrophathalimide, 5-fluorosatin, and 2-amino 5-nitrobenzophenone respectively. In these figures, points that fall on the solid line represent a perfect fit between the experimental and predicted values. The model tended to under predict the solubility of each solute in benzyl alcohol, nitromethane, and dichloromethane. Specifically, 3-nitrophthalimide solubility in DMF was under predicted, and the prediction of most alcohols in 5-fluoroisatin was poor.

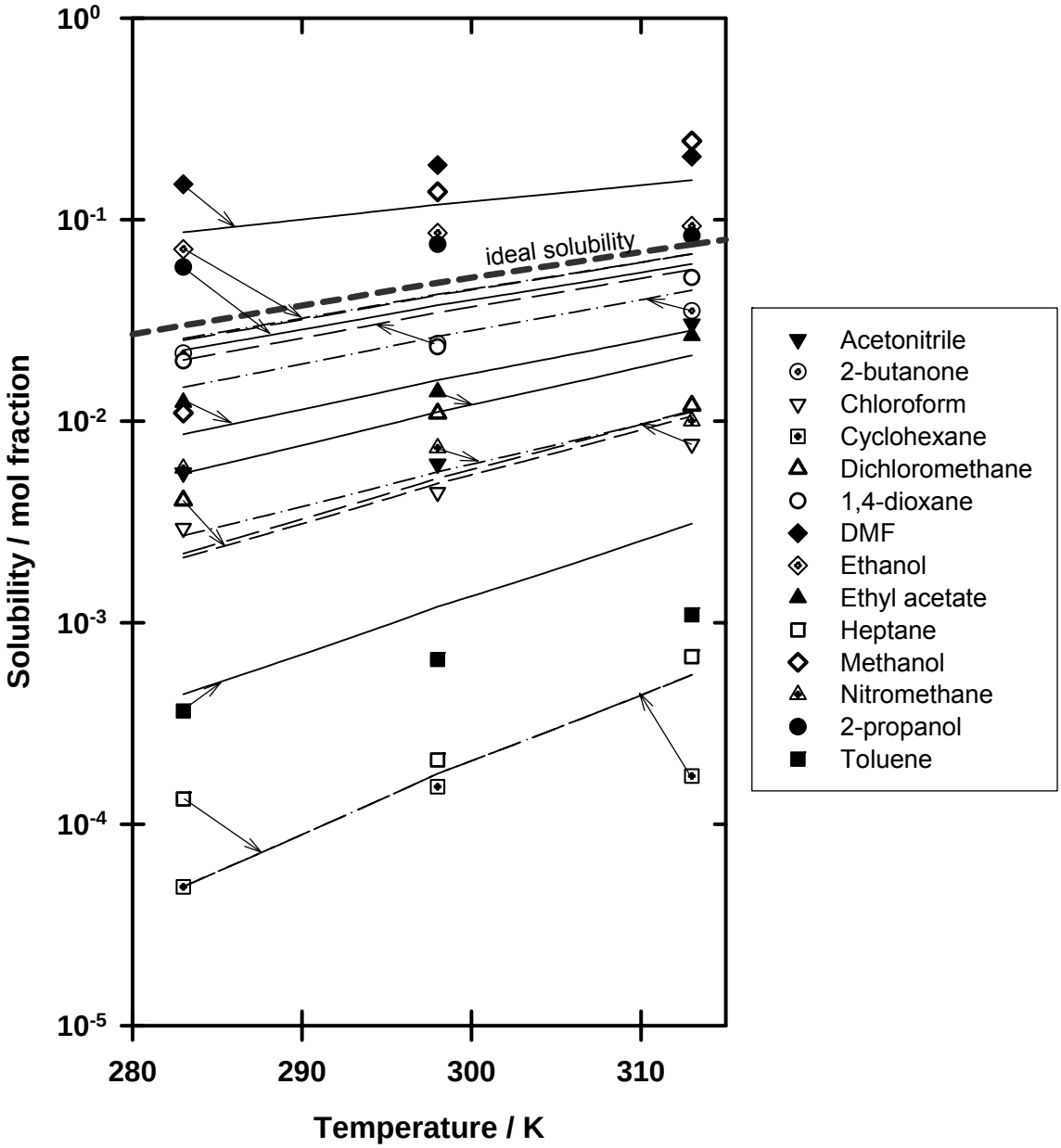

Figure 2-2. Mole fraction solubility of benzimidazole versus temperature in several solvents: symbols, experimental data from this work; lines, predictions with MOSCED + Wilson using parameters in Table 2-3.

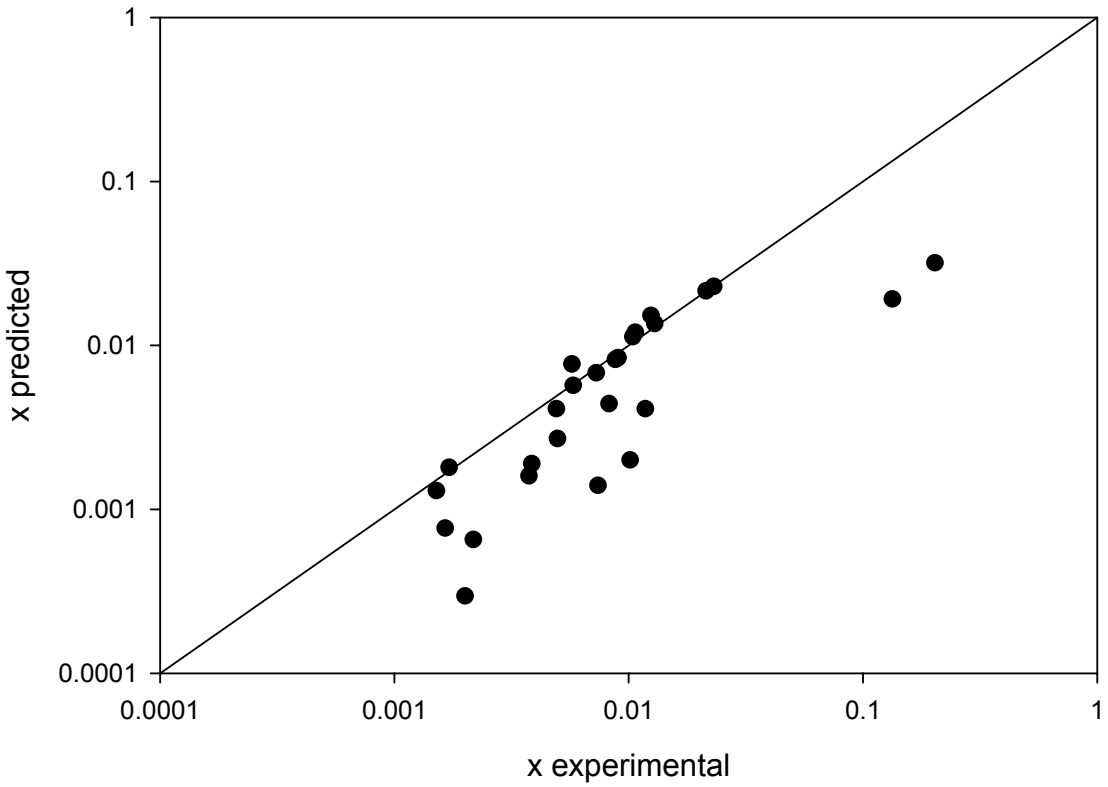

Figure 2-3. Mole fraction solubility of 3-nitrophthalimide in various solvents from 283 to 313 K versus MOSCED predictions.

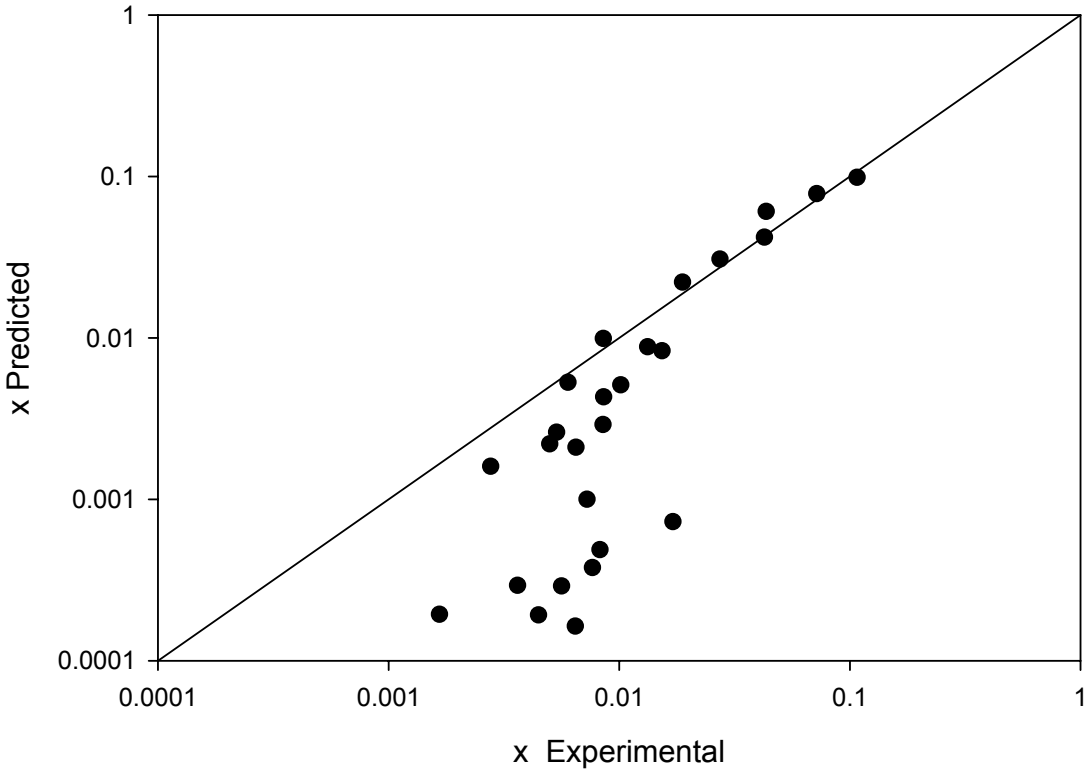

Figure 2-4. Mole fraction solubility of 5-fluoroisatin in various solvents from 283 to 313 K versus MOSCED predictions.

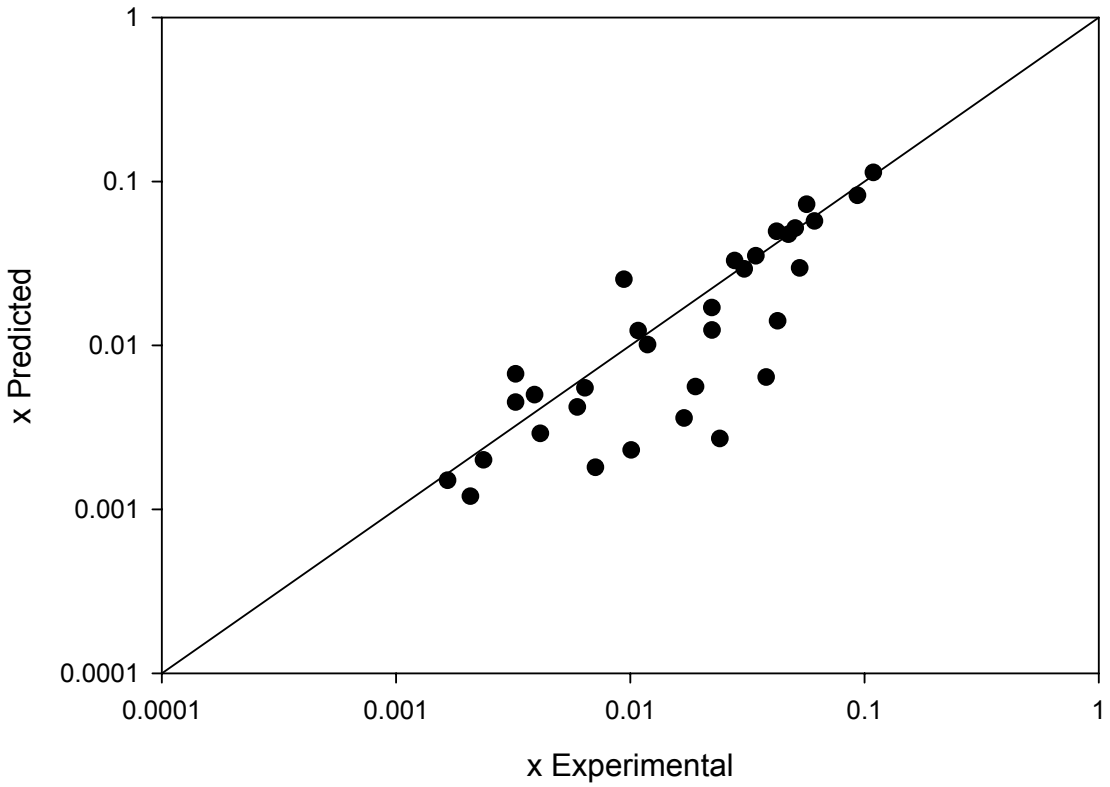

Figure 2-5. Mole fraction solubility of 2-amino-5-nitrobenzophenone in various solvents from 283 to 313 K versus MOSCED predictions.

Overall, the model correlated best the solubility in the polar and hydrogen-bond acceptor solvents like DMF and dioxane, and reasonably well the moderately low solubility in alcohols. MOSCED tended to fit the solubility poorly if the experimental solubility didn't change linearly with temperature, i.e. the solubility was very similar at 283 and 298 K but then increase significantly at 313 K. We found that when this was the case, removing one of the temperatures from the regression improved the fit for that particular solvent. The parameters, while empirical, make some intuitive chemical sense. All four compounds are approximately the same size, so the λ values are all similar. Benzimidazole, with its imine functionality, has the highest β. The low α and β for 2-amino-5-nitrobenzophenone are probably due to the intramolecular hydrogen-bonding

between the arylamine and the carbonyl. However, we do not understand why the α for 5-fluoroisatin would be much less than that of 3-nitrophthalamide since they both have a secondary amine. This could be a problem the model has accounting for the higher activity coefficient of 5-fluoroisatin in DMF.

As one test of our regression parameters, we predicted the solubility behavior for benzimidazole in dichloromethane, toluene, and 1-chlorobutane to compare with experimental data reported by Domańska et al[18]. This comparison is shown in Figure 2-6. The trends in the data are correctly predicted by the MOSCED model using the Wilson g^E expression; however, the deviation between predicted and experimental values is high. Although our predictions are not exact, we are able to correctly capture the relative solubility behavior. We believe the model's ability to qualitatively match these data to be significant, particularly considering that 1-chlorobutane was not included in the data set used to determine the MOSCED model parameters, and that the literature temperature range for all three solvents covers temperatures 40 K higher than the temperatures used in determining the parameters. It should be emphasized that the model is used here to predict behavior without regression or correlation of the data with which it is being compared; rather, predictions are made using model parameters obtained by regression of other data (in Table A-1). This example illustrates how the model can be used as a screening tool to sort solvents according to relative solubility and quickly eliminate candidate solvents that are not likely to be effective (i.e. toluene and 1-chorlobutane in Figure 2-6). A short list of candidates can then be tested experimentally to determine more accurately which solvent is best. This will save experimental time and effort as

well as give the process designer more solvent options than would be feasible with experimental measurements alone[3].

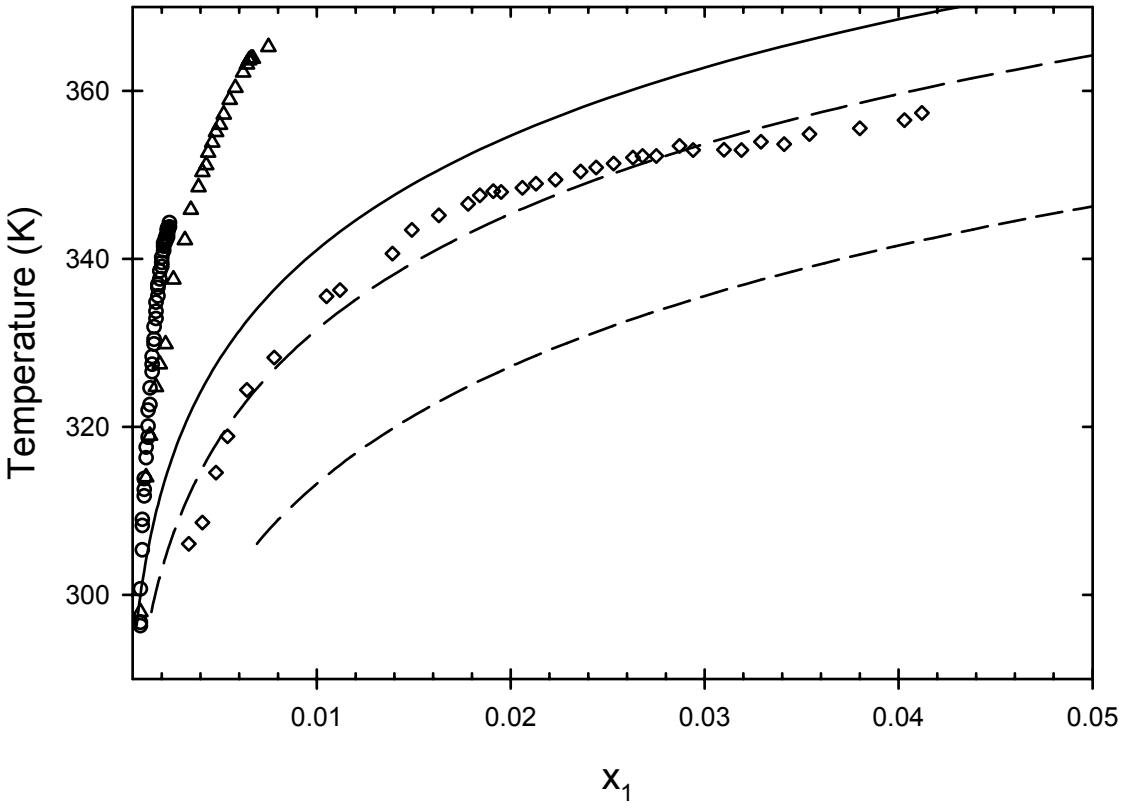

Figure 2-6. Benzimidazole (1) solubility versus temperature in ○, 1-chlorobutane; Δ, toluene; and ◊, dichloromethane; from Ref. 18; lines predicted with MOSCED + Wilson; this work.

Mixed Solvents

The solubility data in mixtures of ethanol + ethyl acetate, 1,4-dioxane + 2-butanone, 2-propanol + nitromethane, and N,N-dimethylformamide (DMF) + chloroform are found in Appendix A, Table A-2. Solvent mixtures have been shown to exhibit positive synergetic effects on solubility, i.e. the mixture provides enhanced solubility compared to pure solvents alone[34]. Mixtures resulting in negative synergetic effects have

also been observed[35]. This data shows that solvent mixtures including alcohols tend to show positive synergistic effects, while mixtures of DMF and chloroform were not observed exhibiting such effects. The solubility of 2-amino-5-nitrobenzophenone did not show any positive synergistic effects with any of the selected solvent pairs, but did show negative synergistic effects when one of the pair was an alcohol. This was not observed in the other solutes, and we believe this difference in solubility is a result of the intermolecular hydrogen bonding within the solute, as previously discussed.

Although predictions were performed for each solute in all four solvent mixtures, only the following three are discussed in detail: benzimidazole, 3-nitrophthalimide, and 5-fluorosatin in mixtures of 2-propanol and nitromethane, which are shown in Figures 2-7, 2-8, and 2-9 respectively. All three of these solutes show an extremum – a higher solubility in the mixture then in either of the pure solvents alone, and the MOSCED model is able to capture this behavior. It appears that if the model were forced to match the experimental solubility in each pure solvent, the model would predict better the correct phase behavior for the mixed solvent. It also appears that if the solubility in the pure solvent was difficult to fit then predicting that solvent in a mixture is even more challenging, which is the case with 2-butanone as seen in Table A-2. If dichloromethane was predicted in a mixture we believe a similar problem would occur due to a poor fit of the pure solubility. It is important to note that these systems are purely predictive; using the parameters regressed previously with pure solvent data. The ability of this model to capture this behavior in mixtures allows the separation designer to choose between a wide range of solvents and an even larger range of solvent mixtures.

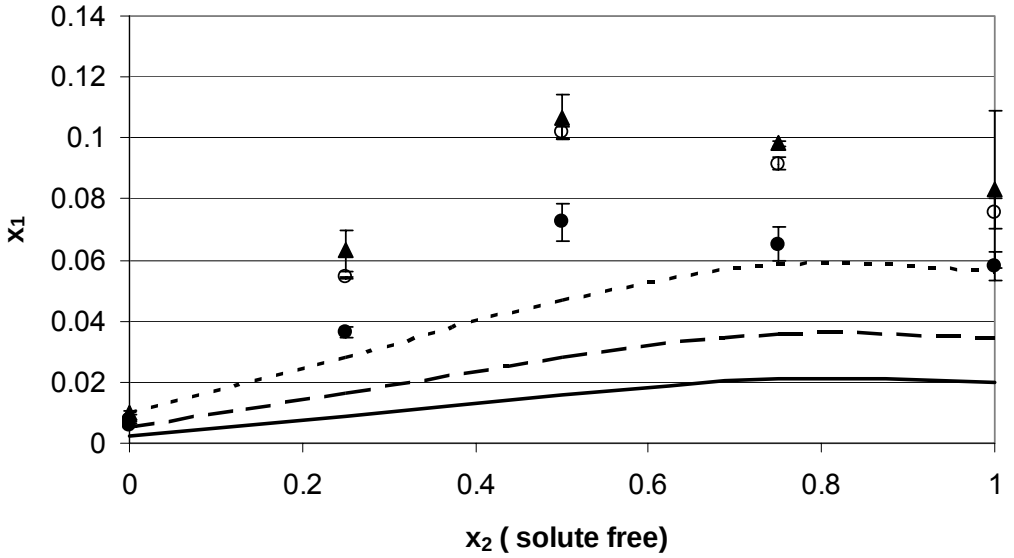

Figure 2-7. Benzimidazole (1) solubility in mixtures of 2-propanol (2) and nitromethane (3): ●, 283 K; ○, 298 K;▲, 313 K; this work; lines predicted with MOSCED + Wilson.

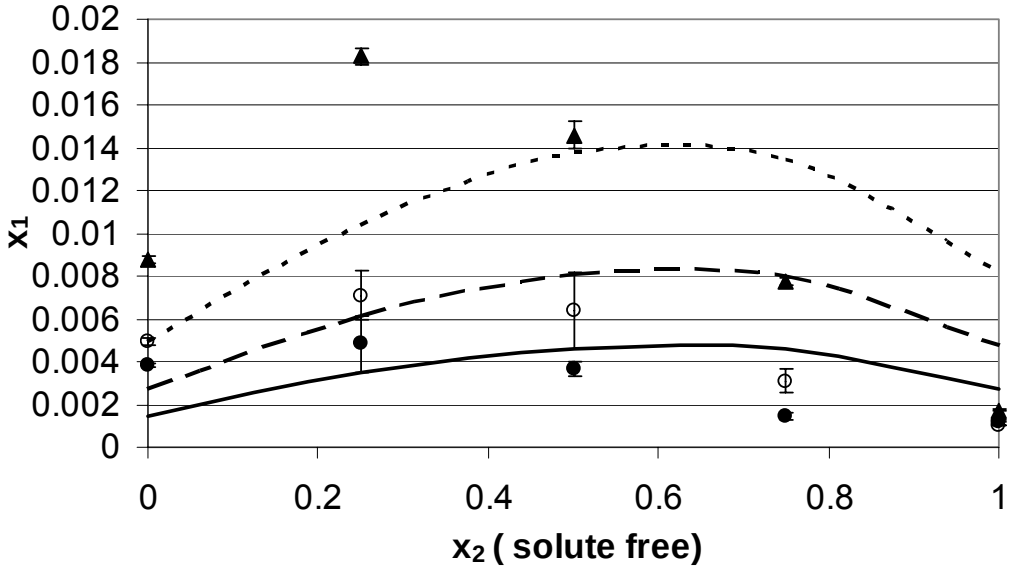

Figure 2-8. 3-nitrophthalimide(1) solubility in mixtures of 2-propanol (2) and nitromethane (3): ●, 283 K; ○, 298 K; ▲, 313 K; this work; lines predicted with MOSCED + Wilson.

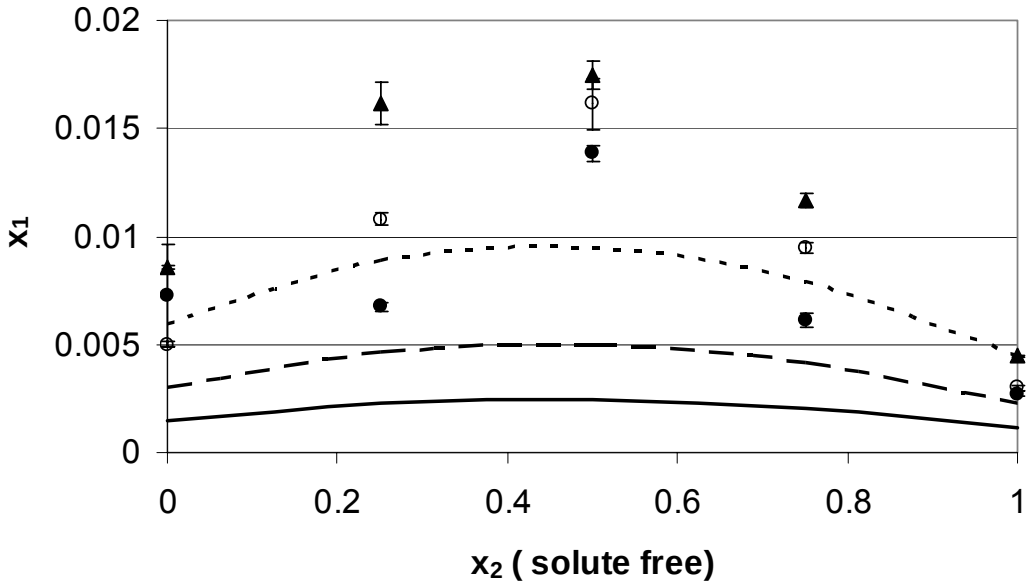

Figure 2-9. 5-fluoroisatin(1) solubility in mixtures of 2-propanol (2) and nitromethane (3): ●, 283 K; ○, 298 K;▲, 313 K ; this work; lines predicted with MOSCED + Wilson.

The graphical representation of model predictions in the other solvent mixtures is located in Appendix C. Overall, the predictions follow the same trend as previously discussed; they predict well qualitatively, and the predictions are more accurate with better pure solvent predictions. An extremum was seen in the mixture of ethanol and ethyl acetate with benzimidazole and the mixture of dioxane and 2-butanone with 3-nitrophthalimide. All solutes in the DMF/chloroform mixture showed better solubility in DMF, producing a positive linear trend based on DMF mole fraction. The model was less accurate in predicting the trends between the solutes in dioxane/2-butanone, most specifically with 2-amino-5-nitrbenzophenone. This may be due to the similarities in dioxane and 2-butanone in that they are both polar and basic, and therefore should have similar solute solubility (which is seen in most cases). However, since the model tends to

overestimate the pure solubility in 2-butanone (as previously described), the overall trend does not match in the mixture.

The uncertainty of experimental measurements is fairly large, particularly when solubility is low, and comparison with predicted values should take this into account. Also, small errors in the heat of fusion data can have a large impact on calculations at temperatures far from the melting point. Furthermore, unlike VLE, easily measured and correlated properties such as vapor pressure do not dominate the calculation.

Conclusions

The solubilities of four multi-functional solid compounds were measured in a variety of organic solvents at several temperatures and in four binary mixed solvent systems. The MOSCED model was relatively successful at correlating the solubilities with few exceptions. The pure component descriptors were found to match the intuitive chemical/physical sense of the pure compounds. The model was also able to predict correctly the existence of maxima in solubility of mixed solvents, and matched the experimental solubility in some cases. In addition, the parameters regressed in this study were used successfully to predict data from the literature.

The ability to predict trends in solubility for complex solutes is the key to rapid and economical solvent selection. We have shown in this work that once a small set of solubility data is taken and MOSCED parameters are regressed, the solubility trend of any solvent or solvent mixture can be predicted as an aid to screening solvents and solvent blends for dissolving or crystallizing complex multi-functional solutes. In this regard, the model provides a useful way of reducing the list of candidate solvents to a

manageable size, quickly screening out solvents that are not likely to be effective and therefore minimizing experimental effort. This can be an important development toward increasing R&D productivity and reducing the time and cost involved in developing new chemical processes.

References

1. Taylor, P. G.; Tran, A. M.; Charlton, A. K.; Daniels, C. R.; Acree, W. E., Jr. Solubility in Binary Solvent Mixtures: Anthracene Dissolved in Alcohol + Carbon Tetrachloride Mixtures at 298.2 K. *J. Chem. Eng. Data* **2003,** 48, 1603-1605.

2. Gupta, S. K.; Olson, J. D. Industrial Needs in Physical Properties. *Ind. Eng. Chem. Res.* **2003,** 42, 6359-6374.

3. Frank, T. C.; Downey, J. R.; Gupta, S. Quickly screen solvents for organic solids. *Chem. Eng. Prog.* **1999,** 95, 41-61.

4. Domańska, U. Solubility of 2,5-Dimethylphenol and 3,4-Dimethylphenol in Binary Solvent Mixtures Containing Alcohols. *Fluid Phase Equilib.* **1988,** 40, 259-277.

5. Domańska, U. Solubility of *n*-Alkanols (C_{16}, C_{18}, C_{20}) in Binary Solvent Mixtures. *Fluid Phase Equilib.* **1989,** 46, 223-248.

6. Domańska, U. Vapor-Liquid-Solid Equilibrium of Eicosanoic Acid in One- and Two-Component Solvents. *Fluid Phase Equilib.* **1986,** 26, 201-220.

7. Lohmann, J.; Gmehling, J. Solid-Liquid Equilibria for Seven Binary Systems. *J. Chem. Eng. Data* **2001,** 46 333-336.

8. Ahlers, J.; Lohmann, J.; Gmehling, J. Binary Solid-Liquid Equilibria of Organic Systems Containing Different Amides and Sulfolane. *J. Chem. Eng. Data* **1999,** 44, 727-730.

9. Lohmann, J.; Röpke, T.; Gmehling, J. Solid-Liquid Equilibrium of Several Binary Systems with Organic Compounds. *J. Chem. Eng. Data* **1998,** 43, 856-860.

10. Karunanithi, A. T.; Achenie, L. E. K.; Rafiqul, G. A Computer-Aided Molecular Design Framework for Crystallization Solvent Design. *Chem. Eng. Sci.* **2006,** 61, 1247-1260.

11. Weidlich, U.; Gmehling, J. A Modified UNIFAC Model. 1. Prediction of VLE, h^E, and γ. *Ind Eng Chem Res* **1987,** 26, 1372-1381.

12. Lazzaroni, M. J.; Bush, D.; Eckert, C. A.; Frank, T. C.; Gupta, S. K.; Olson, J. D. Revision of MOSCED Parameters and Extension to Solid Solubility Calculations. *Ind. Eng. Chem. Res.* **2005,** 44, 4075-4083.

13. Huyskens, P. L.; Sigel, G. G. Fundamental Questions About Entropy. III. A Kind of Mobile Order in Liquids: Preferential Contact Between Molecular Groups. *Bull. Soc. Chim. Belg.* **1988,** 97, 821-4.

14. Borders, T. L.; McHale, M. E. R.; Powell, J. R.; Coym, K. S.; Hernández, C. E.; Roy, L. E.; Acree, W. E., Jr.; Williams, D. C.; Campbell, S. W. Thermodynamics of Mobile Order Theory: Comparison of Experimental and Predicted Anthracene and Pyrene Solubilities in Binary Alkane + Alcohol Solvent Mixtures. *Fluid Phase Equilib.* **1998,** 146, 207-221.

15. Hansen, H. K.; Riverol, C.; Acree, W. E., Jr. Solubilities of Anthracene, Fluoranthene and Pyrene in Organic Solvents: Comparison of Calculated Values using UNIFAC and Modified UNIFAC (Dortmund) Models with Experimental Data and Values using the Mobile Order Theory *Can. J. Chem. Eng.* **2000,** 78, 1168-1174.

16. Thomas, E. R.; Eckert, C. A. Prediction of Limiting Activity Coefficient by a Modified Separation of Cohesive Energy Density Model and UNIFAC. *Ind. Eng. Chem., Proc. Des. Dev.* **1984,** 23, 194-209.

17. De Fina, K. M.; Sharp, T. L.; Chuca, I.; Spurgin, M. A.; Acree, W. E., Jr.; Green, C. E.; Abraham, M. H. Solubility of the Pesticide Monuron in Organic Nonelectrolyte Solvents. Comparison of Observed Versus Predicted Values Based Upon Mobile Order Theory. *Phys. Chem. Liq.* **2002,** 40, 255-268.

18. Domańska, U.; Pobudkowska, A.; Rogalski, M. Solubility of Imidazoles, Benzimidazoles, and Phenylimidazoles in Dichloromethane, 1-Chlorobutane, Toluene, and 2-Nitrotoluene. *J. Chem. Eng. Data* **2004,** 49, 1082-1090.

19. Fletcher, K. A.; Pandey, S.; McHale, M. E. R.; Acree, W. E., Jr. Solubility of Benzil in Organic Nonelectrolyte Solvents. Comparison of Observed Versus Predicted Values Based Upon Mobile Theory. *Phys. Chem. Liq.* **1996,** 33, 181-190.

20. Hernández, C. E.; De Fina, K. M.; Roy, L. E.; Sharp, T. L.; Acree, W. E., Jr. Solubility of Phenanthrene in Organic Nonelectrolyte Solvents. Comparison of Observed Versus Predicted Values Based Upon Mobile Order Theory. *Can. J. Chem.* **1999,** 77, 1465-1470.

21. Roy, L. E.; Hernández, C. E.; Acree, W. E., Jr. Solubility of Anthracene in Organic Nonelectrolyte Solvents. Comparison of Observed Versus Predicted Values Based Upon Mobile Order Theory *Polycyclic Aromat. Compd.* **1999,** 13, 105-116.

22. Domańska, U.; Kozlowska, M. K.; Rogalski, M. Solubilities, Partition Coefficients, Density and Surface Tension for Imidazoles + Octan-1-ol or + Water or + *n*-Decane. *J. Chem. Eng. Data* **2002,** 47, 456-466.

23. Sabbah, R.; Hevia, R.; Tabet, D., Inter & Intramolecular Energy Bonds for Benzimidazole. *Thermochimica Acta* **1998,** 313, 1-7.

24. Lazzaroni, M. J., Optimizing Solvent Selection for Separation and Reaction. Georgia Institute of Technology, Atlanta, 2004.

25. Chickos, James S.; Nichols, Gary, The Estimation of Melting Points and Fusion Enthalpies Using Experimental Solubility, Estimated Total Phase Change Entropies, and Mobile Order and Disorder Theory. *J. Chem. Inf. Comput. Sci*., **2002**, 42, 368-374.

26. Jain, Akash; Yang, Gang; Yalkowsky, Samuel H., Estimation of Total Entropy of Melting of Organic Compounds. *Ind. Eng. Chem. Res*. **2004**, 43, 4376-4379.

27. Prausnitz, J. M.; Lichtenthaler, R. N.; de Azevedo, E. G. *Molecular Thermodynamics of Fluid-Phase Equilibria*. 2nd ed.; Prentice Hall: Englewood Cliffs, N. J., 1986.

28. Pappa, G. D.; Voutsas, E. C.; Magoulas, K.; Tassios, D. P. Estimation of the Differential Molar Heat Capacities of Organic Compounds at Their Melting Point. *Ind. Eng. Chem. Res.* **2005,** 44, 3799-3806.

29. Yalkowsky, S. H. Solubility and Partitioning. 5: Dependence of Solubility on Melting Point. *J. Pharm. Sci.* **1981,** 70, 971-973.

30. Neau, S. H.; Bhandarkar, S. V.; Hellmuth, E. W. Differential Molar Heat Capacities to Test Ideal Solubility Estimations. *Pharm. Res.* **1997,** 14, 601-605.

31. Mishra, D. S.; Yalkowsky, S. H. Ideal Solubility of a Solid Solute: Effect of Heat Capacity Assumptions. *Pharm. Res.* **1992,** 9, 958-959.

32. Gracin, S.; Brinck, T.; Rasmuson, A. C. Prediction of Solubility of Solid Organic Compounds in Solvents by UNIFAC. *Ind. Eng. Chem. Res.* **2002,** 41, 5114-5124.

33. Domańska, U.; Bogel-Łukasik, E. Solubility of Benzimidazoles in Alcohols. *J. Chem. Eng. Data* **2003,** 48, 951-956.

34. Gordon, Leonard J.; Scott, Robert L. Enhanced Solubility in Solvent Mixtures. I. The System Phenanthrene-Cyclohexane-Methylene Iodide. *Journal of the American Chemical Society.* **1952,** 74, 4138-4140.

35. Domańska, U.; Kniaz, K. Solubility of Normail Alkanoic Acids in Selected Organic-Binary Solvent Mixtures. Negative Synergetic Effect. *Fluid Phase Equilib.* **1990,** 58, 211-227.

CHAPTER III

FLOUROUS/ORGANIC/CO_2 PHASE BEHAVIOR TO IMPROVE HOMOGENEOUS CATALYST RECOVERY

Introduction

About 85% of catalytic processes are heterogeneous, primarily because of the ease of separation and reuse of the catalyst. But in many cases, especially asymmetric synthesis, only a homogeneous catalyst will give the rates and especially the selectivity needed. The problem of course is that these are in fact homogeneous. Since catalysts are often costly and/or toxic, some recycle scheme is needed.

In the past decade or so, many chemists have used a scheme called "fluorous biphasic chemistry," capitalizing on the mutual immicibility of fluorous phases with most organics[1-5]. In this scheme, the catalyst is made fluoro-phillic, generally by fluorination of the ligands. Many types of fluorous phase catalysts have been synthesized, e.g. Wilkinson's catalyst [1], Vaska's complex [2], Oxidation catalysts [3-5], as well as many for chiral reactions [6-10]. The partitioning of many of these catalysts in fluorous biphasic systems has also been studied [11]. Normally the reactant and product are in the organic phase and the catalyst in the fluorous phase, allowing facile recycle by mere decantation. However, mass transfer limitations in biphasic systems often limit overall reaction rate. The catalyst and substrate are contacted either by intense agitation or by heating to increase mutual miscibility, and both methods have their limitations.

Shaking a small separatory funnel may work for a chemist in the laboratory, but does not scale well for real applications. For heating to work either the temperature rise

must be quite large (often resulting in racimization or the loss of thermally labile substances), or there must be a bit of mutual solubility at ambient temperature to start with. In the latter case, this solubility results in losses of the fluorous compound on decantation, which is generally both economically and environmentally prohibitive. In spite of the large number of research papers on fluorous biphasic chemistry, the authors know of no current industrial applications. A more feasible alternative for contacting is needed.

As an alternative, CO_2 can be used to induce miscibility of fluorocarbon-hydrocarbon mixtures, even those involving polar compounds such as methanol or N,N-dimethylformamide [12]. The schematic in Figure 3-1 visualizes how the addition of CO_2 can generate a homogeneous reaction with a heterogeneous recovery. Because the addition of CO_2 eliminates the need to induce mixing with heat, this alternative reduces VOC emissions and provides an avenue for thermally labile reactions to be run under homogeneous conditions. Depressurization of the system releases the CO_2 and the phase splits. With this scheme, CO_2 is used as a "switch" to turn homogeneous phase behavior "on" and "off". This creates a medium for homogeneous reactions, wherein the reactants are in intimate contact with the catalyst, greatly enhancing the reaction rate and selectivity [13], while maintaining the facile separation of the original biphasic system containing immobilized catalytic components.

Figure 3-1. Schematic of CO_2-enhanced fluorous biphasic chemistry.

Phase behavior provides essential information for the development of reactions using CO_2-expanded fluorous biphasic chemistry. When considering any type of novel catalytic recycle system, minimizing cost is essential. For this process, an optimal system would have a fluorous and organic phase with minimal mutual miscibility, becomes miscible with minimal CO_2 pressure, and then separates completely when CO_2 is removed. Two different sets of phase behavior were studied here in an effort to understand where this phenomenon can be useful and how well it can be predicted. We first studied the ternary and constituent binary systems of perfluorohexane + CO_2 + methanol, perfluorohexane + CO_2 + toluene, and perfluorohexane + CO_2 + acetone to evaluate the effect of different organic solvents. We then compared the perfluorohexane +CO_2 + methanol phase behavior to that of two commercially available fluorocarbons, FC-75 and FC-43, in the same solvent system. The data reported here can be used to estimate which fluorous-solvent systems would be most cost-efficient for a specific reaction.

Experimental Procedures

Materials

Methanol (HPLC grade, 99.9%), acetone (HPLC grade, 99.9%), toluene (reagent grade, 99.5%), and perfluorohexane (99%) were obtained from Sigma-Aldrich and used as received. Carbon dioxide (SFC Grade, 99.99%) was obtained from Airgas Inc. and was further purified to remove trace water using a Matheson (Model 450B) gas purifier and filter cartridge (Type 451). FC-75 and FC-43 are manufactured by 3-M. FC-75 is a mixture of two components (90% 1-(nonafluorobutyl)-1,2,2,3,3,4,4-nonafluorotetrahydrofuran and 10% perfluorooctane) with slightly different molecular weights but very similar physiochemical properties making it very difficult to separate the two by conventional methods. FC-43 is reported to be 99.5% tri(nonafluorobutyl)-amine with impurities of physiochemically identical isomers[14].

Binary Perfluorohexane-Organic Liquid-Liquid Measurements

For each of the perfluorohexane-organic binary pairs, mutual solubilities were determined by adding 10 mL of each component to a sealed 35 mL vial. The system was thermostatted at 313 K by immersion in an oil bath placed upon a hot plate. The mixture was stirred for one hour with a Teflon-coated magnetic stir bar, and then allowed to settle for 10 minutes prior to sampling. 100 μL samples were withdrawn from each phase and diluted for analysis by GC-FID (HP 6890 Series**,** HP-5 column). The perfluorohexane-rich phase was weighed and diluted 1:10 by volume in FC-72 (mixed perfluorohexane isomers, AMS Chemical Company) while the organic-rich phase was weighed and diluted 1:10 by volume in hexanes (Sigma-Aldrich). The temperature of the oil bath was monitored using a high-precision mercury thermometer (Fisher) with an accuracy of ±

0.05 K. The reproducibility in GC-FID measurements was determined to be within 1 percent for all systems. The sample volume and dilution solvent volumes were measured using an analytical balance with an accuracy of ±0.0001 g (Denver Instrument M-220). GC-FID calibration curves were constructed using standards acquired from Sigma-Aldrich.

Mutual Solubility Pressures of the Fluorous and Organic Phase with CO_2

This procedure, developed by Hallett[14], determines what is often referred to as the miscibility pressure of CO_2-enhanced solvent systems. In short, equal volumes of fluorous and organic solvents were added to a Jergurson model pressure cell (described in detail in Chapter IV). CO_2 was added to the system initially by an ISCO Model 500D syringe pump until the phases begin to merge. Concurrently, the air bath around the cell was set to the desired operating temperature, monitored using an Omega-K-type thermocouple and controlled using an Omega CN76000 PID controller. The system was allowed to equilibrate, and CO_2 was added via a hand syringe pump to accurately pinpoint the pressure at which the fluorous and organic phases became miscible. The hand pump could also remove CO_2, allowing the system to be cycled several times to accurately determine the miscibility pressure. This procedure was repeated 2-3 times for each fluorous-organic system, and the pressures reported were determined within ± 0.02 MPa.

Ternary Vapor-Liquid-Liquid Equilibria Measurements

The apparatus and procedure was the same as that reported by Lazzaroni et al [15], and a schematic of the apparatus is located in Figure 3-2. The precision-bore sapphire cell (50.8 mm o.d. × 25.4 ± 0.0001 mm i.d. × 203.2 mm L) was loaded with known amounts

of fluorous (±0.05 g), organic (±0.05 g), and carbon dioxide (±0.04 g). The total volume was then adjusted to reach the desired pressure (± 10 kPa) using an o-ring sealed piston. The contents of the cell were agitated by rocking the cell 180 degrees for approximately 5 minutes, and then after 1 hour had elapsed, the height of each phase (±0.1 mm) was measured with a micrometer cathetometer. With 3 phases present at a given temperature and pressure, the mole fractions in each phase are independent of overall composition. Three loadings with different overall compositions are required to solve for the unknowns [16]. For the measurements reported, there were between 5 and 8 different loadings for improved accuracy. Additionally, the composition of the vapor phase was assumed from binary data available for perfluorohexane, methanol, toluene, and acetone in CO_2 at comparable pressures and temperatures. For FC-43 and FC-75, it was assumed that the vapor phase consisted only of methanol and CO_2 based on vapor pressure data[14]. The molar volume of the vapor phase was assumed to be that of pure CO_2, since the composition is never less than 95 % CO_2. A detailed procedure for the safe use of the sapphire cell pressure vessel is located in Appendix D.

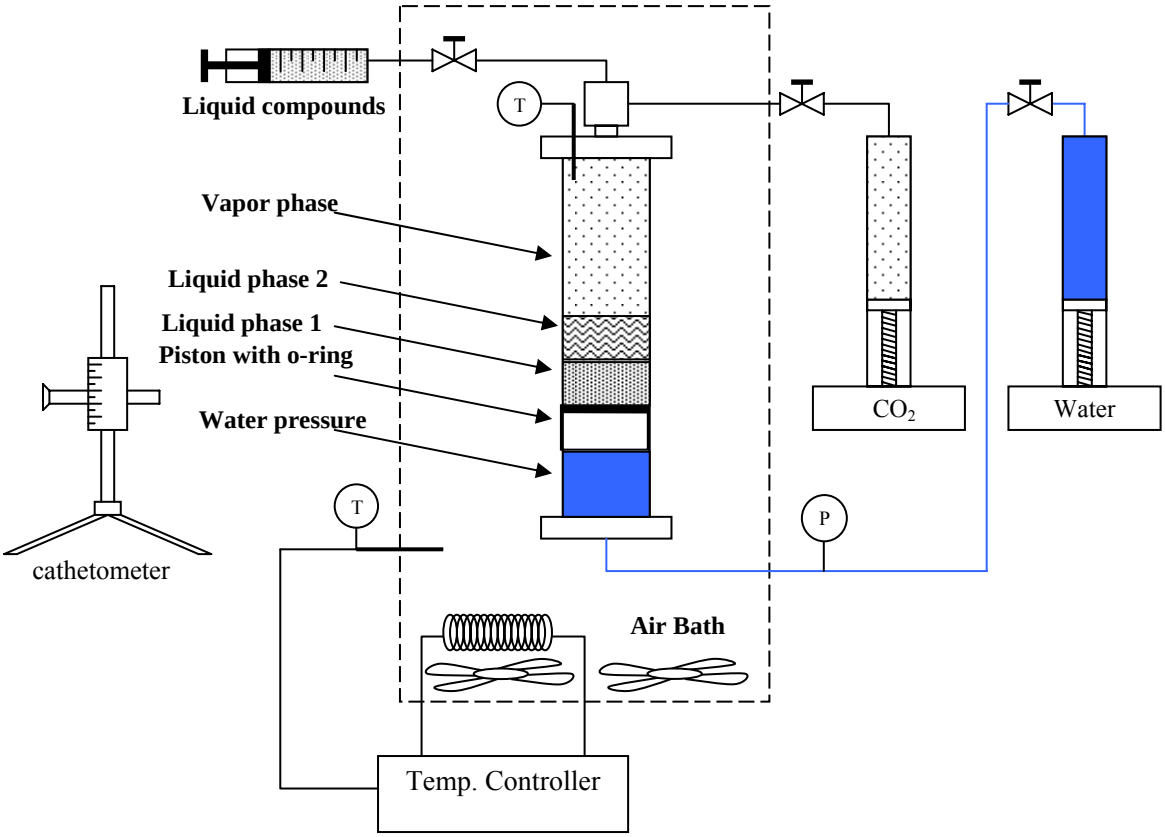

Figure 3-2. Schematic of experimental apparatus[15].

Results and Discussion

Perfluorohexane Phase Behavior

All phase behavior data taken for this study are located in Appendix E. Figure 3-3 shows the ternary phase diagram for CO_2 + perfluorohexane (PFH) + MeOH at 313 K and total pressures from 2.21 MPa to 5.5 MPa. Each tie-line is also in equilibrium with a vapor phase that is 95 to 98 percent CO_2 not represented on the graph. The points on the right side of the graph represent the composition of the denser, fluorous-rich phase and those on the left represent the less dense, methanol-rich phase. With no CO_2 pressure, these two liquids are almost totally immiscible. As can be seen, little of the perfluorohexane is extracted into the less dense phase even at 5.5 MPa with a CO_2 mole

fraction of 0.42. From the left side of the curve, it is evident that methanol is being extracted into the fluorous-rich phase, although at 5.5 MPa, this phase is actually mostly CO_2 (x_{CO2}=0.66). Thus, it appears that CO_2 is acting as cosolvent that extracts methanol into the fluorous rich phase.

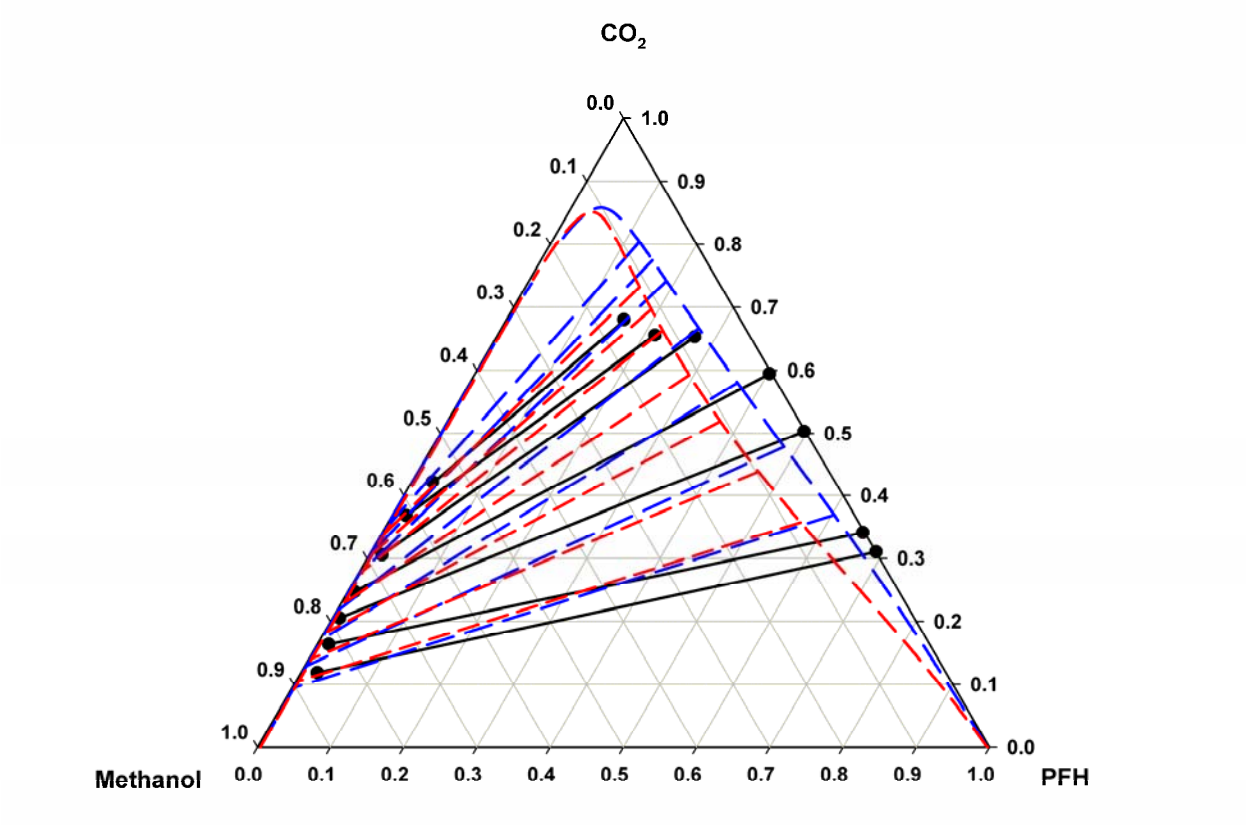

Figure 3-3. Liquid-liquid equilibria for perfluorohexane (PFH) + CO_2 + methanol at 313 K: experimental data, this work (•); modeling, PT-MKP (– – –), PR-HV-UNIQUAC (- - -).

It was observed that the organic phase shrank in size with increasing CO_2 pressure. Since CO_2 dissolves more readily in perfluorohexane than it does in methanol, it is reasonable that more methanol would be extracted into this phase than perfluorohexane into the methanol-rich phase. This type of behavior is expected for two solvents that have significantly different solubilities in a common cosolvent (significantly

different binary bubble point curves with CO_2), as is the case for polar organic solvents combined with a fluorous solvent.

In contrast, for solvents such as acetone or toluene that dissolve CO_2 more readily than methanol, a different type of behavior is seen (shown in Figure 3-4 and Figure 3-5, respectively). In each case, the miscibility pressure is much less then with methanol, as shown in Table 3-1. Although this behavior would seem to be economically beneficial, the acetone and toluene systems have other disadvantages. Table 3-2 shows the mutual solubility of the three organics in PFH at 313 K and ambient pressure, and acetone and toluene have significant mutual solubility before the addition of CO_2. This mutual solubility indicates that less CO_2 will be needed to induce miscibility (as proven by our data). It also means, however, that some of the organic and fluorous solvents will be unable to be recycled even before the reaction process, which is a disadvantage for both environmental and economic reasons as previously discussed. Furthermore, in Figures 3-4 and 3-5, it can be seen that the points on the right hand side (the fluorous-rich phase) become increasingly less fluorous-rich with a small amount of CO_2. Therefore, it would also be necessary to greatly reduce the pressure in order to achieve a separation efficient enough to prevent significant fluorous solvent losses after the reaction. This is not the case in Figure 3-3, where with methanol, the possibility exists for efficient solvent separation (i.e. <1% fluorous solvent in the organic) by decreasing the pressure only slightly from the miscibility pressure. We have determined that compression costs for CO_2 in similar systems tend to be a large contributor to overall operating costs, and that the difference between compressing back to ambient pressure versus 1 MPa can cut that cost in half (as described in detail in Chapter IV). Therefore we feel methanol is the best

choice compared to toluene and acetone for a cost-effective process. However, we recognize that for some fluorous biphasic reactions high CO_2 concentrations could be detrimental, and in these cases acetone or toluene may be the better solvent choice. Future work in this area should include a more detailed economic analysis based on specific reactions to accurately determine the optimal solvent.

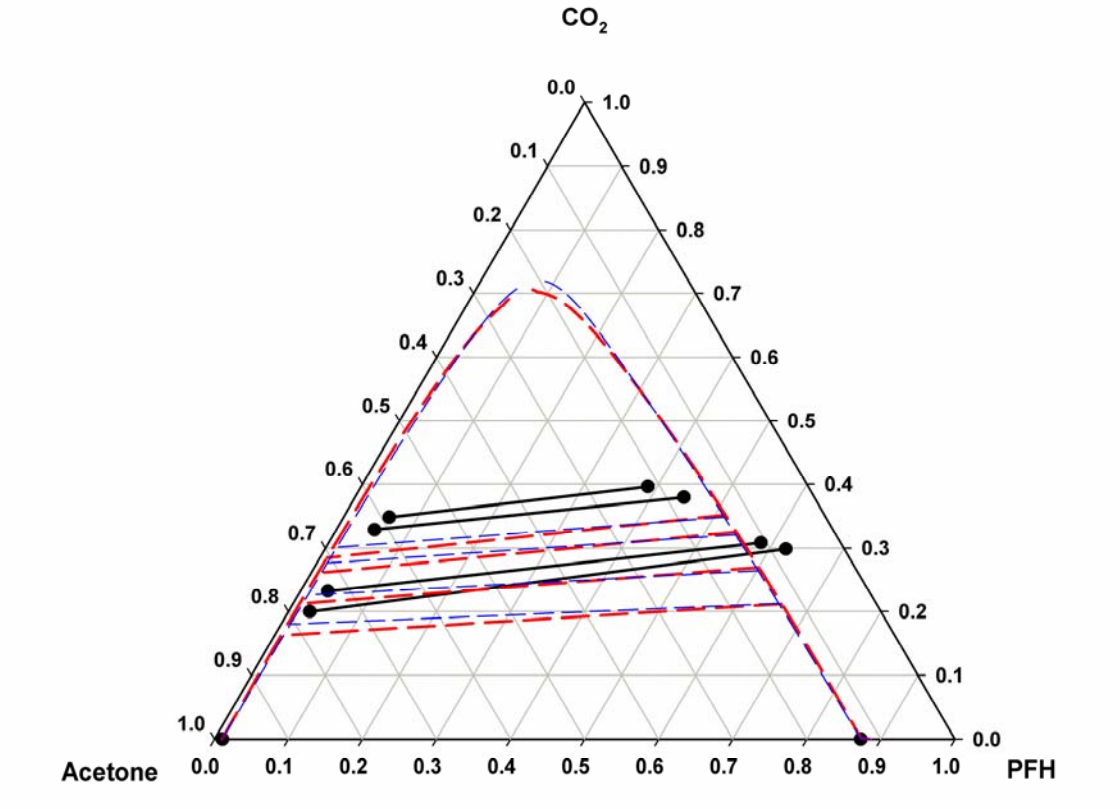

Figure 3-4. Liquid-liquid equilibria for perfluorohexane (PFH) + CO_2 + acetone at 313 K. Experimental data, this work (•); modeling, PT-MKP (– – –), PR-HV-UNIQUAC (- - -).

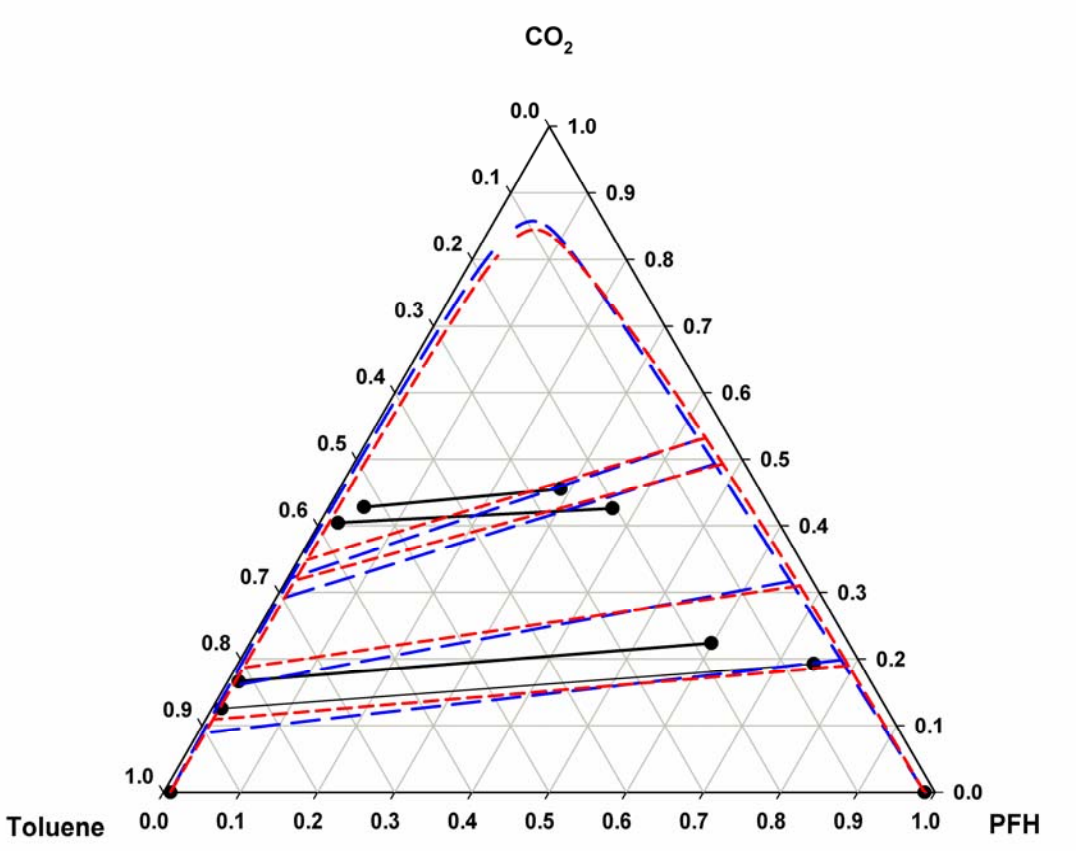

Figure 3-5. Liquid-liquid equilibria for perfluorohexane (PFH) + CO_2 + toluene at 313 K. Experimental data, this work (•); modeling, PT-MKP (– – –), PR-HV-UNIQUAC (- - -).

Table 3-1. Miscibility pressure with CO_2 for PFH with methanol, acetone, and toluene at 313 K.

Organic Component	Pressure (MPa)
Methanol	5.64
Acetone	2.24
Toluene	3.78

Table 3-2. Mutual solubility data for PFH (1) + organic (2) at 313 K.

Organic	x_1 (organic)	x_2 (fluorous)
toluene	0.0093	0.0136
methanol	0.0041	0.0033
acetone	0.0107	0.1274

We chose to evaluate the Patel-Teja [17] (MKP mixing rules [18]) and Peng-Robinson (Huron-Vidal-UNIQUAC mixing rules [19]) equations of state for predicting the measured vapor-liquid-liquid equilibria. The pure component parameters are listed in Table 3-3, and the interaction parameters, which were regressed to binary data only, are listed in Table 3-4. While neither model performed quantitatively, they both gave the correct qualitative behavior. The predictions were best for methanol + perfluorohexane + CO_2, which we believe is due to the liquids remaining "immiscible" even at relatively high concentrations of CO_2. The predicted plait point for all three ternary systems had a much higher CO_2 composition than was measured, which can be expected since liquid-liquid equilibria at ambient pressures is a severe test of any thermodynamic model, and in this case, the model is also required to give the correct pressure dependence of the CO_2 composition in the liquid phase.

Table 3-3. Pure component parameters for the Patel-Teja and Peng-Robinson equations of state.

Component	T_c **/ K**	P_c **/ bar**	ω	ζ_c	F
carbon dioxide	304.21	73.8	0.224	0.311	0.71153
perfluorohexane	451	18.6	0.514	0.316	1.11845
Methanol	512.5	80.84	0.566	0.273	0.96983
Toluene	591.75	41.08	0.264	0.306	0.76945
Acetone	508.2	47.01	0.307	0.282	0.70854

Table 3-4. Binary interaction parameters.

System *i* + *j*		MKP		HV-UNIQUAC		Data source
I	***J***	k_{ij}	l_{ij}	u_{ij}	u_{ji}	
carbon dioxide	perfluorohexane	0.057	-0.069	515.1	394.5	Ref 20
carbon dioxide	methanol	0.049	0.029	575.2	117.4	Ref 21
carbon dioxide	toluene	0.099	0.056	341.5	130.7	Ref 22
carbon dioxide	acetone	-0.005	0	278.2	-130.9	Ref 23
perfluorohexane	methanol	0.245	-0.650	3558.6	376.3	This work
perfluorohexane	toluene	0.233	-0.157	1110.6	-34.6	This work
perfluorohexane	acetone	0.179	-0.060	804.8	188.5	This work

FC-43 and FC-75 Phase Behavior

Upon completion of the perfluorohexane ternary phase behavior, we compared the methanol and PFH phase behavior to that of two commercially available fluorocarbons. Figures 3-6 and 3-7 show the ternary phase diagrams for CO_2 + FC-43 + MeOH and CO_2 + FC-75 +MeOH at 313 K, respectively. Table 3-5 compares the miscibility pressures of these fluorocarbons in methanol with PFH. In general, all three fluorocarbons behave similarly in systems with methanol and CO_2, which leads to the conclusion that the phase behavior is most affected by the interaction between the organic solvent and CO_2. Ternary phase behavior data for FC-75 was more difficult to obtain, which we contribute to the large percentage of impurities present. Modeling was not performed on this data due to poor performance of existing vapor-liquid-liquid equilibria models on the perfluorohexane phase behavior. As new thermodynamic models are developed, future work would apply those models to the ternary data presented here.

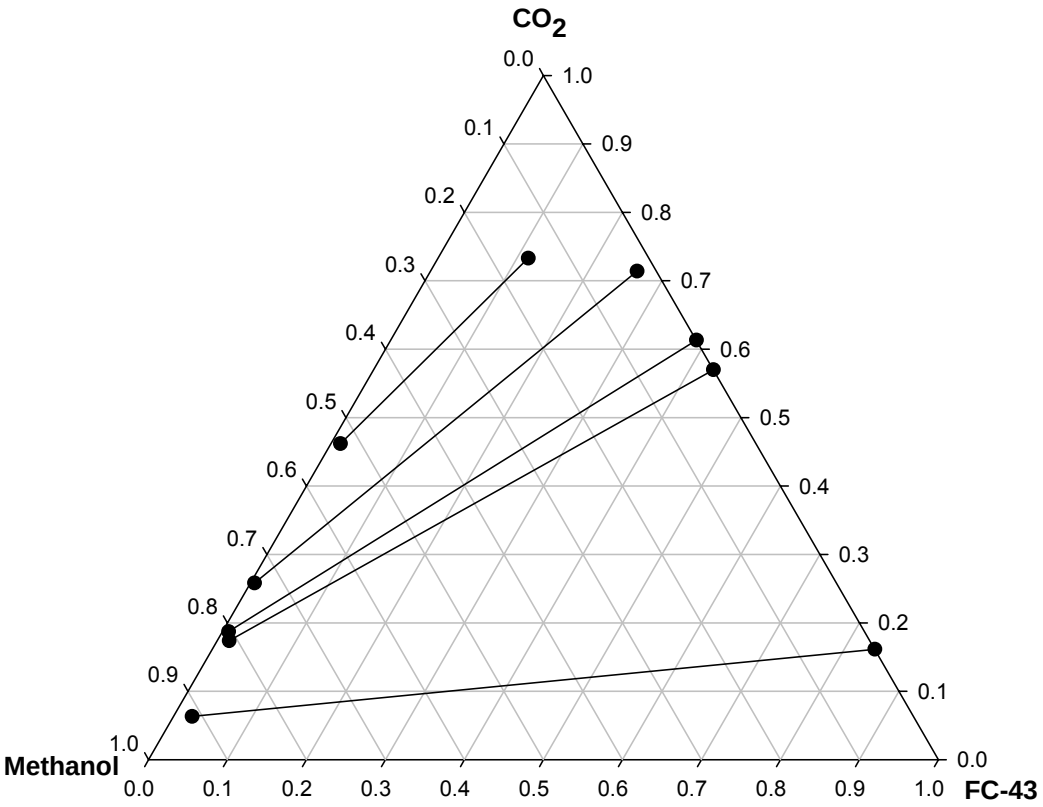

Figure 3-6. Liquid-liquid equilibria for FC-43 + CO_2 + methanol at 313 K.

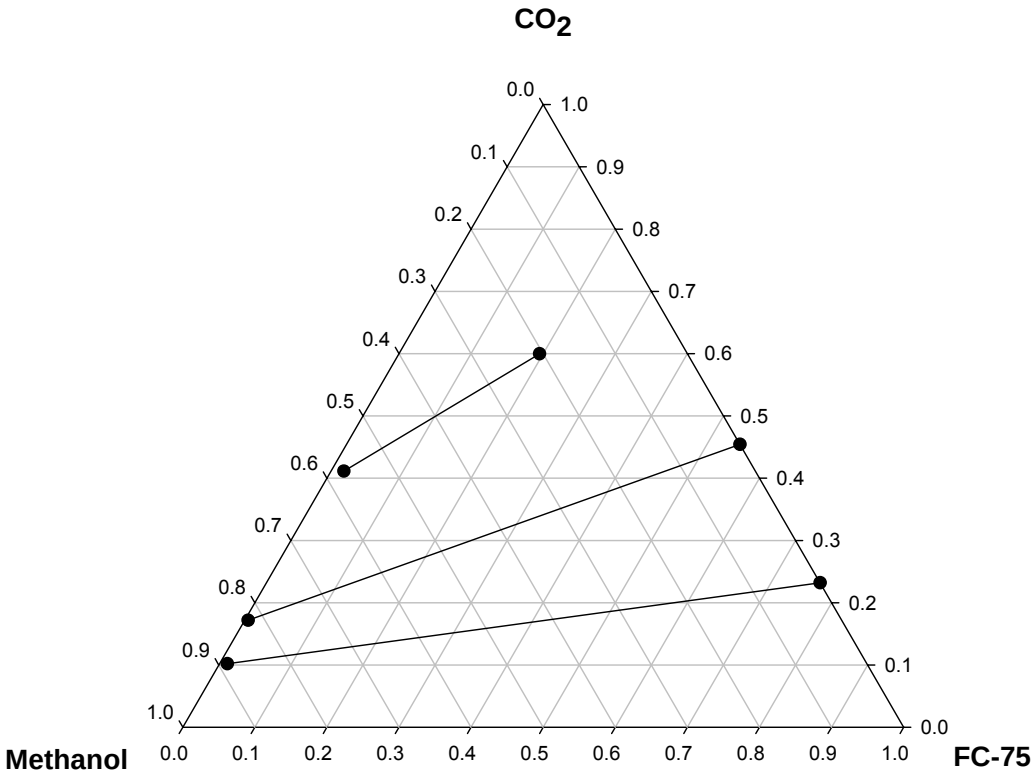

Figure 3-7. Liquid-liquid equilibria for FC-75 + CO_2 + methanol at 313 K.

Table 3-5. Miscibility pressure with CO_2 for methanol with PFH, FC-43, and FC-75 at 313 K.

Fluorous Component	Pressure (MPa)
PFH	5.64
FC -43	6.39
FC – 75	5.84

Assuming that a specific reaction would produce comparable yields and reaction rates in each of these fluorocarbon-methanol-CO_2 systems, FC-75 would be the economic choice for this process. Although PFH has the lowest miscibility pressure with methanol, PFH is not produced on an industrial scale and is extremely volatile, making it expensive and difficult to work with. FC-43 required more CO_2 to reach miscibility with methanol and therefore would have higher compression costs. However, when looking at specific

reactions, it will be imperative to use organic solvents that are miscible with the reactants and products, and fluorous solvents that are not. Furthermore, the catalyst used will need to be insoluble in the organic phase and resistance to negative affects from CO_2 pressure. These issues, together with data presented here, will all need to be considered before ultimately determining which systems are cost-effective.

Conclusions

New data for evaluating fluorous + organic + CO_2 solvent systems for homogeneous reaction with heterogeneous separation are reported. The data shows that the best catalyst and fluorous recovery is with the methanol ternary system. Perfluorohexane, FC-43, and FC-75 all show similar phase behavior in methanol, indicating that organic-CO_2 interactions can be used to predict the success of these CO_2-enhanced fluorous biphasic systems. However, to determine accurately an optimal organic-fluorous system, specific details about the reaction need to be known. Methanol-fluorous systems require high CO_2 concentrations in the liquid phase, which could change the reaction rates. In cases where high concentrations of CO_2 need to be avoided, the acetone or toluene ternary system would be preferred. These new data provide insight into solvent selection for fluorous biphasic reactions.

References

1. Richter, B.; Spek, A. L.; van Koten, G.; Deelman, B. J., Fluorous Versions of Wilkinson's Catalyst. Activity in Fluorous Hydrogenation of 1-Alkenes and Recycling by Fluorous Biphasic Separation. *J. Am. Chem. Soc.* **2000,** 122, 3945-3951.

2. Guillevic, M. A.; Rocaboy, C.; Arif, A. M.; Horváth, I. T.; Gladysz, J. A., Organometallic Reactivity Patterns in Fluorocarbons and Implications for Catalysis: Synthesis, Structure, Solubility, and Oxidative Additions of a Fluorous analogue of Vaska's Complex, trans-Ir(CO)(Cl)[P(CH2CH2(CF2)5CF3)3]2. *Organometallics* **1998,** 17, 707-717.

3. Betzemeier, B.; Cavazzini, M.; Quici, S.; Knochel, P., Copper-Catalyzed Aerobic Oxidation of Alcohols Under Fluorous Biphase Conditions. *Tet. Lett.* **2000,** 41, 4343-4346.

4. Pozzi, G.; Cavazzini, M.; Quici, S., Metal Complexes of a Tetraazacyclotetradecane Bearing Highly Fluorinated Tails: New Catlaysts for the Oxidation of Hydrocarbons Under Fluorous Biphase Conditions. *Tetrahedron Letters* **1997,** 38, (43), 7605-7610.

5. Ravikumar, K. S.; Barbier, F.; Bégué, J.-P.; Bonnet-Delpon, D., Manganese (III) Acetate Dihydrate Catalyzed Aerobic Epoxidation of Unfunctionalized Olefins in Fluorous Solvents. *Tetrahedron* **1998,** 54, 7457-7464.

6. Birdsall, D. J.; Hope, E. G.; Stuart, A. M.; Chen, W.; Hu, Y.; Xiao, J., Synthesis of Fluoroalkyl-Derivatised BINAP Ligands. *Tet. Lett.* **2001,** 42, 8551-8553.

7. Maillard, D.; Pozzi, G.; Quici, S.; Sinou, D., Asymmetric Hydrogen Transfer Reduction of Ketones Using Chiral Perfluorinated Diimines and Diamines. *Tetrahedron* **2002,** 58, (20), 3971-3976.

8. Nakamura, Y.; Takeuchi, S.; Okumura, K.; Ohgo, Y.; Curran, D. P., Recyclable Fluorous Chiral Ligands and Catalysts: Asymmetric Addition of Diethylzinc to Aromatic aldehydes Catalyzed by Fluorous BINOL-Ti Complexes. *Tetrahedron* **2002,** 58, (20), 3963-3969.

9. Pozzi, G.; Cavazzini, M.; Cinato, F.; Montanari, F.; Quici, S., Enantioselective Catalysis in Fluorinated Media - Synthesis and Properties of Chiral Perfluoroalkylated (Salen)manganese Complexes. *Eur. J. Org. Chem.* **1999**, 1947-1955.

10. Tian, Y.; Chan, K. S., An Asymmetric Catalytic Carbon-Carbon Bond Formation in a Fluorous Biphasic System Based on Perfluoroalkyl-BINOL. *Tet. Lett.* **2000,** 41, 8813-8816.

11. Barthel-Rosa, L. P.; Gladysz, J. A., Chemistry in Fluorous Media : A User's Guide to Practical Considerations in the Application of Fluorous Catalysts and Reagents. *Coord. Chem. Rev.* **1999,** 190-192, 587-605.

12. West, K. N.; Hallett, J. P.; Jones, R. S.; Bush, D.; Liotta, C. L.; Eckert, C. A., CO_2-Induced Miscibility of Fluorous and Organic Solvents at Ambient Temperatures. *Ind. Eng. Chem. Res.* **2004,** 43, 4827-4832.

13. Jessop, P. G.; Ikariya, T.; Noyori, R., Homogeneous Catalysis in Supercritical Fluids. *Chem. Rev.* **1999,** 99, 475-493.

14. Hallett, J. P. Enhanced Recovery of Homogeneous Catalysts Through Manipulation of Phase Behavior. Georgia Institute of Technology, Atlanta, 2003.

15. Lazzaroni, M. J.; Bush, D.; Jones, R.; Hallett, J. P.; Liotta, C. L.; Eckert, C. A., High-pressure phase equilibria of some carbon dioxide-organic-water systems. *Fluid Phase Equilibria* **2004,** 224, 143-154.

16. Fontalba, F.; Richon, D.; Renon, H., Simultaneous Determination of Vapor-Liquid Equilibria and Saturated Densities up to 45 MPa and 433 K. *Rev. Sci. Instrum.* **1984,** 55, 944.

17. Patel, N. C.; Teja, A. S., A New Cubic Equation of State for Fluids and Fluid Mixtures. *Chem. Eng. Sci.* **1982,** 37, 463-473.

18. Mathias, P. M.; Klotz, H. C.; Prausnitz, J. M., Equation-of-state mixing rules for multicomponent mixtures: the problem of invariance. *Fluid Phase Equilibria* **1991,** 67, 31-44.

19. Orbey, H.; Sandler, S. I., *Modeling Vapor-Liquid Equilibria: Cubic Equations of State and Their Mixing Rules*. Cambridge University Press: New York, 1998.

20. Lazzaroni, M.; Bush, D.; Brown, J. S.; Eckert, C. A., High Pressure Vapor-Liquid Equilibria of Some Carbon Dioxide + Organic Binary Systems. *J. Chem. Eng. Data* **2005,** 50, 60-65.

21. Ohgaki, K.; Katayama, T., Isothermal Vapor-Liquid Equilibrium Data for Binary Systems Containing Carbon Dioxide at High Pressures: Methanol-Carbon DIoxide, n-Hexane-Carbon Dioxide, and Benzene-Carbon Dioxide Systems. *Journal of Chemical and Engineering Data* **1976,** 21, (1), 53-55.

22. Fink, S. D.; Hershey, H. C., Modeling the Vapor-Liquid Equilibria of 1,1,1-Trichloroethane + Carbon Dioxide and Toluene + Carbon Dioxide at 308, 323, and 353 K. *Industrial & Engineering Chemistry Research* **1990,** 29, (2), 295-306.

23. Adrian , T.; Maurer, G., Solubility of Carbon Dioxide in Acetone and Propionic Acid at Temperatures between 298 K and 333 K. *Journal of Chemical and Engineering Data* **1997,** 42, (4), 668-672.

CHAPTER IV

TUNABLE SOLVENTS FOR FINE CHEMICALS FROM THE BIOREFINERY AND PULP AND PAPER MILL

Introduction

The idea that one day fuels will be derived from renewable resources has been around for almost a century[1]. Until recently, however, the cheap and readily available nature of petroleum has put biofuel development on the backburner. In 1999, scientists from the National Renewable Energy Laboratory expressed the need for research and development in cost-efficient bioethanol productive, in the hopes that the cost of biofuels could soon be competitive against historically low petroleum prices[2]. Today, eight years later, we are battling record high petroleum prices still without a sustainable way to produce biofuels on a large scale[3]. Furthermore, there is no end in sight for rising fuel prices; turmoil in the Middle East, natural disasters, and the inevitable total consumption of a non-renewable resource leaves the public anxious to protect our national security and way of life by developing alternative fuels[3, 4]. This anxiety has provoked the writing of many literature reviews discussing ways to make biorefineries (refineries that use biomass feedstocks instead of fossil fuels) commercially viable[1, 3, 5-8].

Innovative plant design, improving the efficiency of bioethanol fermentation, and producing biomaterials from biorefineries are the three main topics of research in improving biofuel production[3, 8]. Innovative plant design focuses on several ways to increase the total amount of biomass available: manipulating photosynthesis to increase source strength[9], genetically engineering plants to promote plant adaptation to

environmental stresses[10], and altering the lignin content of a plant cell wall by coregulation[11]. Improving the efficiency of the bioethanol fermentation focuses mostly on cost efficient ways to pretreat biomass, as discussed in detail in Chapter V. Pretreatment is a necessary tool because it helps breakdown the biomass and makes microbe digestibility efficient; however, it is often viewed as the most expensive step in bioethanol fermentation due to expensive chemicals and high operating costs. The third way to improve the sustainability of a biorefinery involves the production of high value biomaterials, which will be the topic of this chapter.

When converting biomass to bioethanol by fermentation, naturally occurring organisms readily break down only six carbon sugars like glucose, mannose, and galactose[8]. These sugars make up the cellulose and a fraction of the hemicellulose present in biomass[12]. As shown in Table 4-1, less than 60% of typical biomass consists of components useable for bioethanol production; that leaves as waste the lignin, extractives or minor components, and unreacted cellulose and hemicellulose. In the pulp and paper industry, only the cellulose fraction of biomass is used for paper, leaving over half the feedstock components as waste[1]. Typically, this unused biomass is burned for fuel value[2]. However, the use of this "waste" biomass to produce value chemicals is an untapped resource for sustainability in a pulp and paper mill[3]. Use of biomass waste to synthesize fine chemicals has been previously commercialized; vanillin, a compound used frequently in the flavor and fragrance industry, was extracted from the lignin left as waste from the kraft pulping process of wood[13]. However the method used was not practical and created copious amounts of waste; therefore, the last American plant used to recover vanillin from lignin was closed in 1991. This leaves researchers with the task of

developing a more practical and profitable process. Furthermore, residual lignin remaining after valuable chemical extraction could be used as a replacement for natural gas in the paper mill[14], or a feedstock for biofuels beyond ethanol such as renewable diesel[15, 16] or bio-hydrogen[17]. The challenge here is developing cost-effective and environmental friendly techniques for removal and extraction of lignin and valuable chemicals.

Table 4-1: Percent dry weight composition of lignocellulosic feedstocks, adapted from N. Mosier et al.[8]

Feedstock	Cellulose	Hemicellulose	Lignin	Extractives/Minor Components
Cornstover	37.5	22.4	17.6	22.5
Pine Wood	46.4	8.8	29.4	15.4
Popular Wood	49.9	17.4	18.1	14.6

We have developed a cost-efficient way to extract valuable chemicals from lignin using a Gas-Expanded Liquid (GXL). When a gas, typically CO_2, is added to an organic solvent in which it is soluble, the dissolution of that gas provides the solvent with different and tunable properties. The use of GXLs offer several advantages over typical solvents; ease of separation, use of benign gases to reduce the amount of solvent needed, and the ability to tune properties such as solubility, transportability, and polarity[18]. Furthermore, previous work has shown that the addition of CO_2 to small alcohols forms an in situ alkylcarbonic acid[19]. In this work, GXLs are used in a gas anti-solvent (GAS) process[20]; as the amount of CO_2 pressure increases, the solubility of some lignin components in the organic solvent decreases and falls out of solution. Staying in solution are low molecular weight fractions of lignin, which include vanillin and syringaldehyde

(for hardwood lignin). Vanillin is commonly used in the flavor and fragrance industry and is sold for many dollars per pound. Syringaldehyde, which sells for tens of dollars per pound, has been patented for use as a hair and fiber dye as well as a pharmaceutical precursor for obesity and breast cancer treatments[21-23]. Table 4-2 shows the structures of these compounds, as well as their physical properties and estimated price.

Table 4-2. Structure, physical properties, and estimated selling price of vanillin and syringaldehyde.

Component	Structure	T_m °C [a]	ΔH_{fus} (J/g) [a]	Approximate selling price [b]
Vanillin	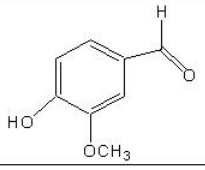	81.4 ± 0.4	154.6 ± 7	5 – 9 $/lb
Syringaldehyde	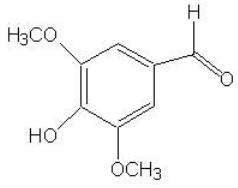	110.8 ± 0.5	163.8 ± 27	27 – 29 $/lb

[a] Measurements take in our lab

[b] Approximation based on World Market Report (1996) for vanillin

For the preliminary experimental work done in this study, purchased organosolv lignin was used as a starting material. However, we base the economic benefits of our preliminary results on removal of these valuable chemicals from the black liquor waste stream in a kraft pulping plant[12]. Although black liquor is a mixture (lignin, degraded hemicellulose, spend white liquor, ash, etc.[12]), several separation techniques have been studied for removing lignin from this stream; the most promising of which include ultrafiltration using ceramic membranes[24], and acid precipitation of lignin using CO_2[25-28]. Both of these techniques have the potential to become cost-effective ways to remove

lignin from kraft black liquor. However, the economic analysis shown here is based on the acid precipitation technique due to the ease at which we believe this process could be combined with GXL extractions. A schematic of what we hope to accomplish is shown in Figure 4-1: the ability to add a small innovation (labeled GXL extraction unit) that will create profit while minimizing disruption of the existing process. Pulp and paper mills are the original lignocellulosic biorefinery; and, with further research in value-added co-products, as well as the use of tall oil, hemicellulose and lignin for biofuels (as discussed in Chapter VI), this industry may have the opportunity to revitalize itself as a leader in renewable products.

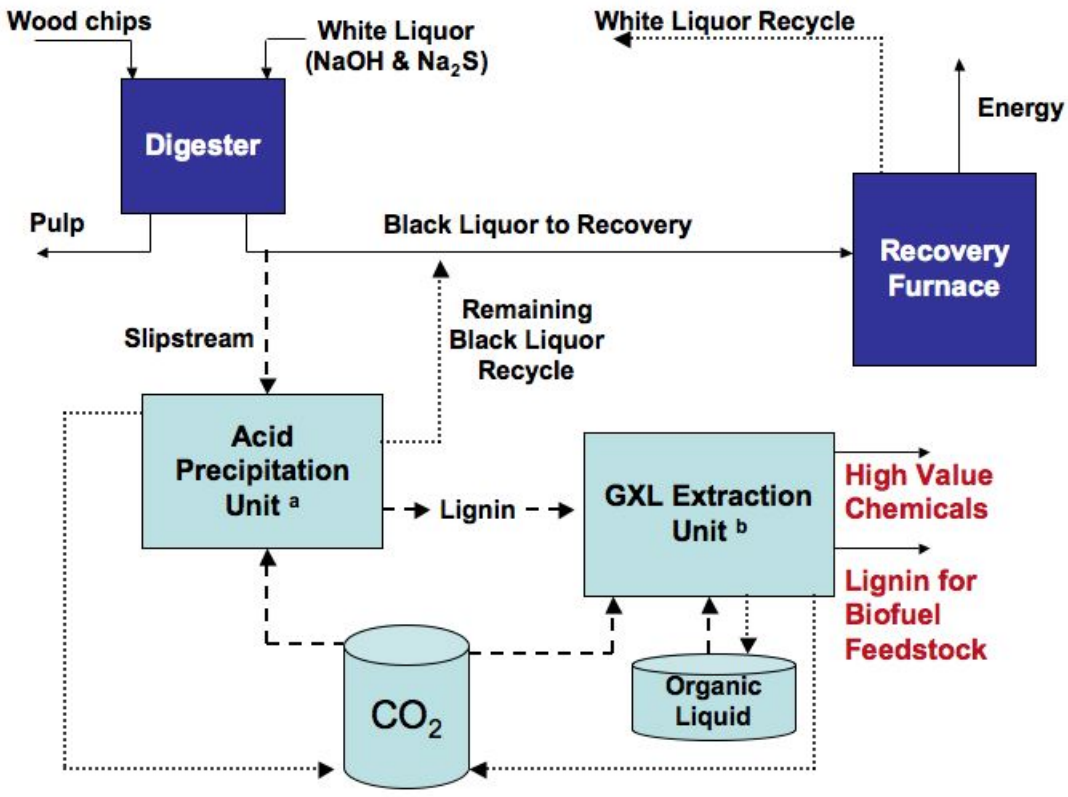

Figure 4-1. Schematic of desired outcome for utilization of GXL valuable chemical extraction into the kraft pulping process[12]; [a] process from literature[27, 28], [b] this work.

Experimental Apparatus and Procedures

Materials

All Chemicals were obtained from Sigma-Aldrich and used as purchased: methanol (HPLC, 99.9%), ethanol (HPLC, 99.9 %), acetone (HPLC, 99.9%), toluene (anhydrous, 99.8%), vanillin (99%), syringaldehyde (98+%), and syringol (99%). The carbon dioxide (SFC/SFE grade) was obtained from Airgas and was filtered prior to use. The melting point and heat of fusion for vanillin and syringaldehyde was determined using a DSC (TX-Q20) at a heating rate of 10 °C/min under nitrogen flow. All work in this study was done using organosolv lignin purchased from Sigma-Aldrich (CAS 8068-03-9, product number 371017). This lignin was recovered using the ethanol-based Alcell® process from a mixture of hardwoods, specifically 50 % maple, 35 % birch, and 15 % poplar[29]. Table 4-3 gives characterization of this lignin, as reported by the research group that produces it commercially for Sigma-Aldrich.

Table 4-3. Properties of mixed hardwood organosolv lignin, adapted from Lora and Glasser (commercial provider to Sigma-Aldrich)[29].

Property	Mixed Hardwood Lignin
Total OH/C_9	1.1 - 1.4
Phenolic OH/C_9	0.3 - 0.6
Methoxyl/C_9	1.0 - 1.3
T_g (°C)	97
Mn ($x10^3$)	0.6
Mw ($x10^3$)	2.1 - 8.0

Procedures

Lignin Solubility

To determine which organic solvent would perform best in the GXL system with lignin, we tested the solubility of lignin in methanol, ethanol, acetone, and toluene. A known but excess amount of lignin was added to a known volume of organic solvent at ambient conditions and allowed to stir overnight to insure saturation. The solution was filtered to remove all undissolved solid, and the solubility of lignin was determined two ways. First, the filtrate and glassware used were dried and weighed on a Deltarange scale (AT261) to determine the amount of lignin in solution. This number was accurate to ±2 grams due to human error associated with gravimetric determinations. Second, a sample of known volume (typically 1 μL using an Eppendorf pipette and weighed for improved accuracy) was taken from the filtered solution. After allowing the solvent to evaporate, the remaining mass was weighed to determine the final lignin solubility. The error between these two methods was between 2-20% over 15 runs.

General GXL Procedure

The GXL extraction process was performed at several temperatures. After following the procedure above, a sample from the filtered solution was taken to determine the concentrations of vanillin and syringaldehyde. All samples taken throughout the experiment were run thru a Hewlett Packard 6890 Gas Chromatograph with Mass Selective Detector 5973 (GC-MS) for peak identification. Calibration curves developed using purchased vanillin and syringaldehyde were used to determine the chemical concentrations, with an error of ±0.01 mg/mL. The small concentrations of vanillin and syringaldehyde present in some of the samples increased the error in

concentration due to the limitations of the equipment. The solution was added to a gas tight syringe, and loaded into an equilibrium cell (Jergurson Model 18T-32) that had been evacuated to remove all air from the system. A schematic of the experimental setup is located in Figure 4-2. The temperature was monitored with a digital temperature controller (Omega CN 76000) accurate to ±0.2 K. Throughout experimentation at ambient temperatures the system remained within ±2 K of 298 K. Carbon dioxide was added to the system by an ISCO 500D syringe pump with a series D controller. CO_2 was added until the first sign of lignin precipitate was noted, and the system was left to equilibrate while periodically being shaken. Once it was insured that equilibrium was reached (±2 hour waiting period with periodic shaking until no pressure change was observed for at least 30 minutes), liquid samples were taken via a Valco 6-port high-pressure sample valve. The valve pulled samples thru a filter from the bottom of the cell to insure the solid precipitate remained in the cell. The sample loop on the valve was calibrated to a volume of 535 μL (±1 μL). After each sample set (three samples at each pressure) the pressure within the system was reduced by a maximum of 0.2 bar, which we deem negligible considering the overall volume of the experimental solution (> 30 mL). Since the organic liquids used expand significantly with the addition of CO_2, the volume of the actual liquid sample (excluding CO_2) removed from the sample loop was determined using previously published binary phase behavior correlated to the appropriate temperature[30]. An additional sample was taken and used to determine the lignin content in the liquid phase at that temperature and pressure (following the gravimetric procedure described previously). After all samples were taken, more CO_2 was added to the system and the procedure was repeated until either the saturation

pressure of CO_2 was reached (below 32 °C) or the dilution of the organic solvent with CO_2 reduced the sample volume below the detection limits of the GC-MS. This procedure was completed at least twice for each set of presented results. To gain a more complete understanding of the results obtained using this method at 25 °C, two other experimental procedures were preformed; staged GXL extractions and GXL extractions over time in a PARR reactor. For all procedures, the solution preparation and analyzes of the GXL phase components remained the same.

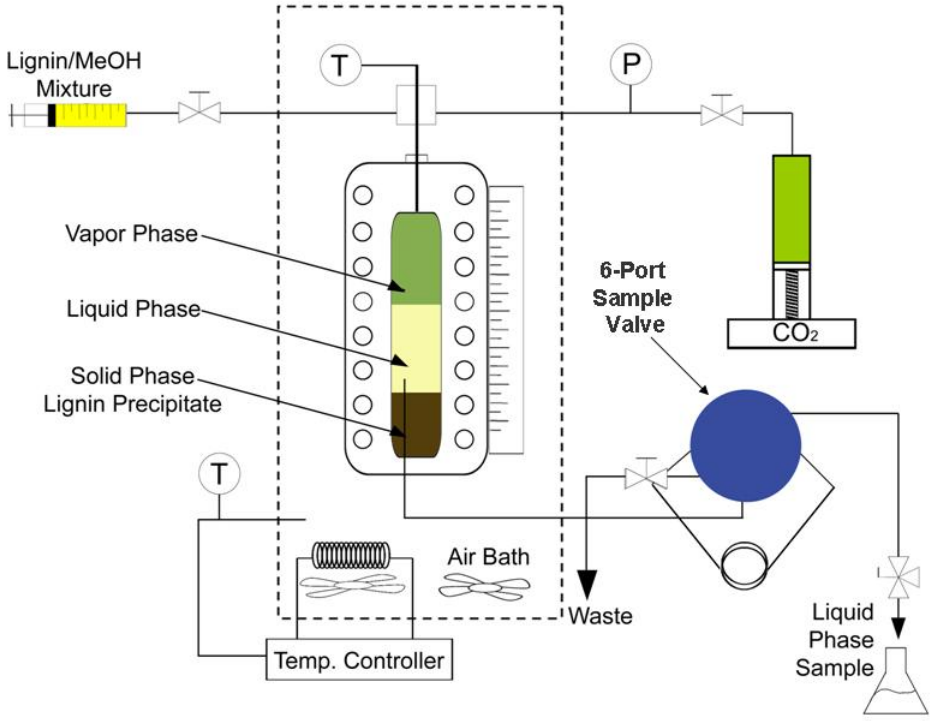

Figure 4-2. Schematic of experimental set-up in the Jergurson model cell.

Timed GXL Procedure

To determine the effect of time on the concentrations of vanillin and syringaldehyde, the lignin-organic liquid solution was added to a PARR reactor

(described in detail in Chapter V). Two runs were performed at different CO_2 loadings. The reactor was stirred continuously, and the pressure and temperature were held constant for 24 hours. Samples of the liquid phase were taken at time intervals throughout the experiment and analyzed for vanillin, syringaldehyde and lignin concentration.

Staged GXL Procedure

The lignin-organic liquid solution was loaded into the Jergurson cell as previously described, and CO_2 was added to the system until lignin began to precipitate. For this experiment, the Valco 6-port high-pressure sample valve was replaced with a standard HIP valve. This was so the entire liquid phase could be removed from the solid precipitate, keeping the pressure constant (to avoid reintroduction of lignin into the liquid phase) by running the ISCO pump continuously throughout the separation. The cell was then cleaned to remove the solid precipitate, evacuated to remove excess solvent and air, and re-loaded with the same liquid phase. This process was repeated 4-6 times, with samples being taken from each liquid phase to determine the vanillin, syringaldehyde, and lignin content.

Results and Discussion

The goal of this work was to prove:

- lignin would precipitation out of solution in a GXL system,
- valuable chemicals could be separated from lignin using this technique, and
- these processes could be profitable when introduced into a kraft pulping plant.

We report here the outcomes of these objectives and future work that could be performed based on these results.

Lignin Solubility in Various Organic Solvents and GXL systems

The first step in determining whether lignin would precipitate in a GXL system was to determine what organic solvents would dissolve lignin. We chose 4 preliminary solvents (methanol, acetone, ethanol, and toluene) based on previously published lignin solubility data[31] and previous experience with GXL systems. The solubility results are located in Table 4-4. Lignin was most soluble in acetone, fairly solubility in methanol and slightly soluble in ethanol. Lignin was not soluble in toluene, and therefore toluene was not used in the GXL experiments.

Table 4-4. Lignin solubility at ambient conditions in several organic solvents.

Solvent	mg/mL
methanol	139 ± 31
ethanol	47 ± 4
acetone	> 250
toluene	Not soluble

The next step in picking an optimal GXL system was to determine the anti-solvent power of CO_2 with methanol, acetone, and ethanol at different temperature. The data for these experiments is located in Appendix G. The addition of CO_2 to all solvent/lignin mixtures resulted in the precipitation of lignin, as expected. The addition of CO_2 to the ethanol/lignin mixture did not cause much lignin to precipitate, which we believe is due to the low initial solubility of lignin in ethanol. This made ethanol a poor choice for this process because more solvent would be needed to dissolve the same amount of lignin; therefore, no more experiments were run with this system. In specific cases the use of ethanol could provide a "natural" method of extracting vanillin which makes for a more valuable product. However, in a kraft pulping process, no processes

downstream of the digester (which uses NaOH and Na_2S) would qualify as natural with or without ethanol as a solvent.

Figure 4-3 shows the effect CO_2 has on the lignin concentration in GX-methanol at various temperatures. Although the data reported in Appendix G are in terms of CO_2 pressure, we used existing methanol-CO_2 phase behavior[30] to estimate the mole fraction of CO_2 at those pressures for a better understanding of the temperature effects. From this figure is it clear that temperature (within 25-48 °C) has little effect on the precipitation of lignin by CO_2.

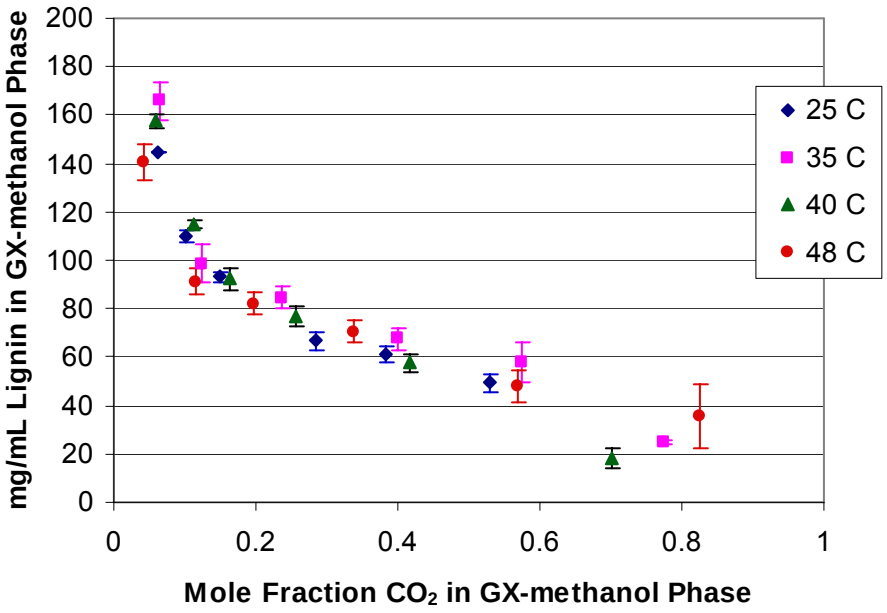

Figure 4-3. CO_2 mole fraction versus lignin concentration in GX-methanol at various temperatures.

Figure 4-4 shows a comparison of the effect CO_2 concentration has on lignin in the GX-methanol and GX-acetone phase at 40 °C. Originally, we hypothesized that the precipitation of lignin would be enhanced by the in-situ acid formed when methanol is expanded with CO_2. From Figure 4-4 we see that there is slightly more precipitation in

the methanol case, but the GX-acetone system (which does not form an in-situ acid) also causes significant lignin precipitation. Therefore it seems the driver for lignin precipitation is not acid formation but rather initial solute-solvent solubility and the addition of non-polar CO_2 to polar solvents.

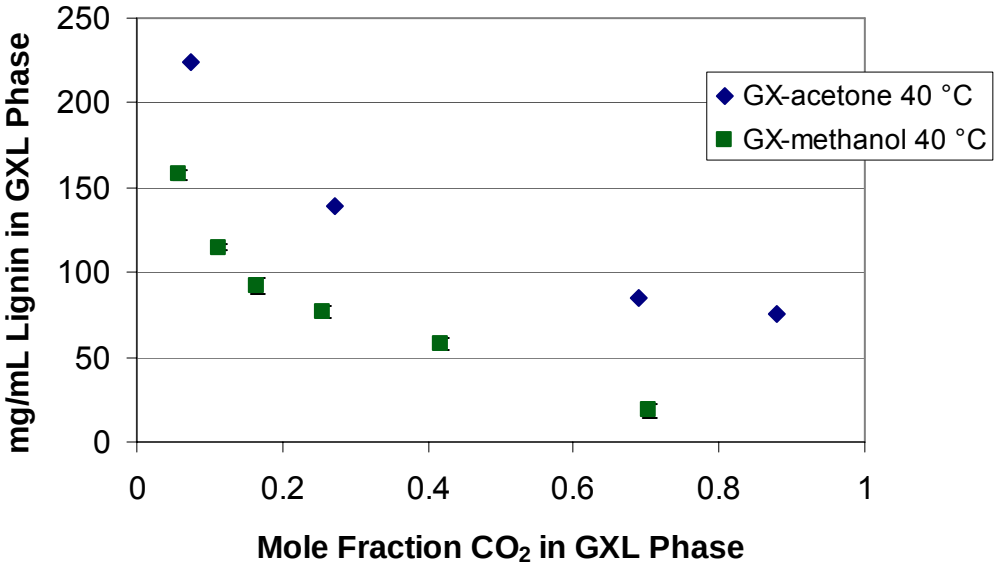

Figure 4-4. CO_2 mole fraction versus lignin concentration in GX-methanol and GX-acetone at 40 °C.

Separation of Valuable Chemicals from Lignin using GXLs

From the first set of experiments, it was determined that we would compare methanol and acetone for use in GXL valuable chemical extractions from lignin. Acetone, however, did not extract high enough concentrations of valuable chemicals from the lignin for accurate detection using our analytical methods. Therefore, the remainder of the results focuses solely on GX-methanol/lignin systems.

During the preliminary determination of valuable chemicals available for extraction (by sampling the liquid phase of a lignin/methanol solution and determining

extractants via GC-MS), syringol, a flavoring agent similar in cost to vanillin was also detected. However, it was difficult to get accurate calibrations with pure syringol, and for simplicity we focused only on vanillin and syringaldehyde. Future work should include determining other valuable chemicals or chemical intermediates that can be extracted from lignin using different solvent systems.

GX-methanol Extractions as 25 °C

All the data taken for the GX-methanol/lignin systems are located in Appendix G. For these results, the reported errors range from 1 to 30% due in combination to inaccuracies of the analytical technique used and composition variations that are inherent when working with natural products. Future work in this area should include a better analytical technique such as liquid chromatography or pyrolysis mass spectrometry to decrease experimental error. Figure 4-5 shows the concentration of valuable chemicals in the GX-methanol phase versus pressure at 25 °C using the "general GXL procedure" as described in the procedure section. This figure shows two interesting results; 3 times more syringaldehyde then vanillin is extracted from the lignin, and both chemicals precipitate out of the GX-methanol phase with increasing pressure. The first result can be explained by the chemical make-up of the hardwood lignin used in this study; hardwood lignin is predominately made up of syringyl units which are oxidized to mostly syringaldehyde and some vanillin[13]. Furthermore, research using the same mixed hardwood lignin showed molar ratios (syringaldehyde to vanillin) of approximately 3 for which is in agreement with our data[32]. Harder to prove is the reason why both vanillin and syringaldehyde begin to fall out of solution after the initial onset of lignin precipitation (around 10 bar). It seemed likely that CO_2 may be acting as an anti-solvent

for these chemicals as well as lignin; however, the vanillin and syringaldehyde concentrations in the lignin/methanol solution are much lower the their maximum solubility in methanol at 25 °C (456.5 mg/mL vanillin and 52.7 mg/mL syringaldehyde) and therefore should not be effected by the addition of CO_2. An attempt to prove this by measuring the cloud point of vanillin and syringaldehyde was made; however, at low concentrations any precipitation was hard to see and at high concentrations of vanillin above the critical point of CO_2 a one-phase system was observed. Some literature has been published on the solubility of vanillin and CO_2; and, although a melting point depression was reported, it is far outside the pressure and temperature ranges studied in this work[33, 34].

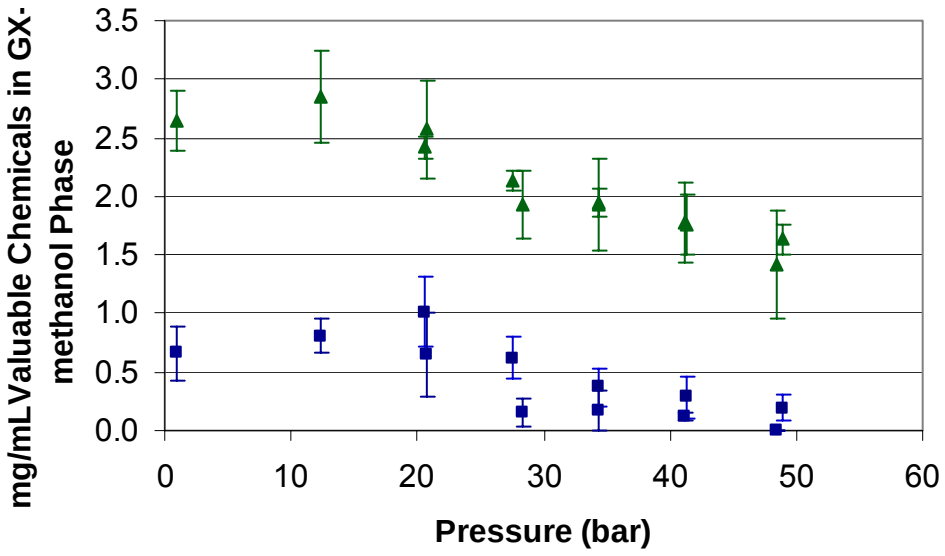

Figure 4-5. Concentration of valuable chemicals in the GX-methanol phase versus pressure at 25 °C using the general GXL procedure; (▲) syringaldehyde, (■) vanillin.

Therefore, more experiments were needed to determine why vanillin and syringaldehyde precipitated out of solution at 25 °C. Figure 4-6 and 4-7 show results for

GX-methanol/lignin systems at 25 °C using the "timed GXL procedure" and the "staged GXL procedure", respectively. From the timed extractions, Figure 4-6 shows that the syringaldehyde concentration decreases within the first 3 hours of exposure to GX-methanol, but then levels off between 3 and 24 hours. For vanillin it seems that, within error, the concentrations are staying relatively constant over time. Figure 4-7 shows constant vanillin and syringaldehyde concentrations at 25 °C when the process is staged.

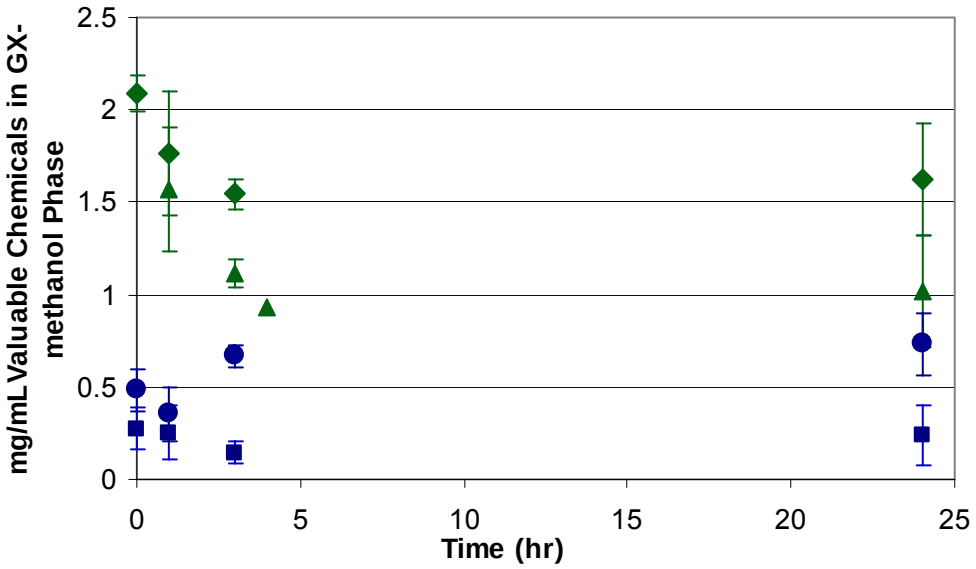

Figure 4-6. Concentration of valuable chemicals in the GX-methanol phase versus time at 25 °C and constant pressure using the timed GXL procedure; (◆) syringaldehyde and (●) vanillin at 18 bar, (▲) syringaldehyde and(■) vanillin at 38 bar.

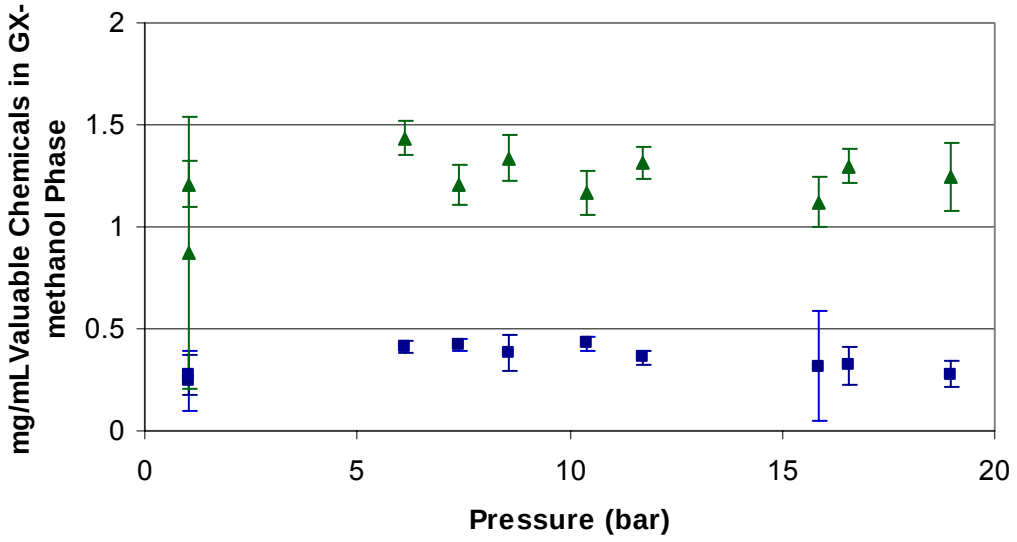

Figure 4-7. Concentration of valuable chemicals in the GX-methanol phase versus time at 25 °C using the staged GXL procedure; (▲) syringaldehyde, (■) vanillin.

These results suggest two conclusions:

- acetal formation between the aldehydes and the alcohol is occurring under the acidic media of GX-methanol at 25 °C, and
- poor mixing in the general procedure accentuates the effect by causing some vanillin and syringaldehyde to drop out of solution with lignin.

It is known that when two equivalents of alcohol are added to an aldehyde an acetal is formed, and that the rate of this reaction is increased by the addition of an acid catalyst[35]. This reaction is shown in Figure 4-8. Literature shows that 76% of vanillin and 93% of syringaldehyde form their equivalent acetals when concentrated sulfuric acid is added to a solution of aldehyde in methanol. Figure 4-9 shows that in 24 hours, approximately 35 % of vanillin was converted to acetal in a solution of just methanol exposed to the atmosphere. When CO_2 was bubbled thru the solution the rate increased as expected, but

the overall conversion remained the same. The results in Figure 4-6 suggest that in this system approximated 25 % of the aldehydes were converted over 24 hours.

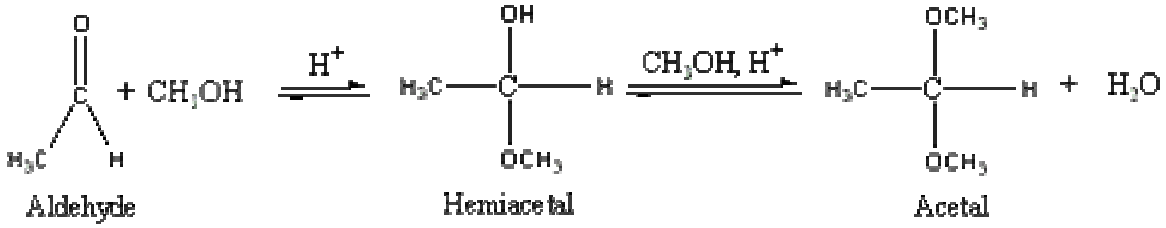

Figure 4-8. Reaction of an aldehyde and alcohol to form acetal[35].

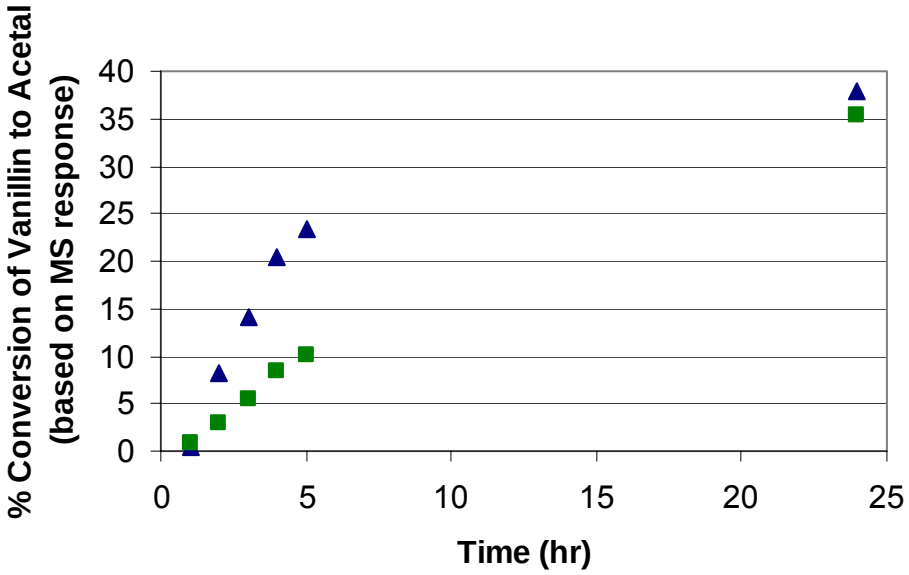

Figure 4-9. Percent conversion of vanillin to acetal versus time at ambient conditions; (▲) bubbled CO_2 and methanol, (■) methanol only.

However, the formation of acetal is not a barrier for the extraction of vanillin and sringaldehyde from lignin using GX-methanol. The acetal reaction is reversible with water, which will always be present when working with wood-based feedstocks. The lower acetal conversions shown here compared to literature reports can be attributed to water present in the system. Furthermore, we are still able to extract vanillin and

syringaldehyde even with the formation of acetal (as shown in Figure 4-6). During the staged runs (Figure 4-7) the liquid phase was removed from the cell and exposed to the atmosphere. This reduced the amount of time the liquid was exposed to the in-situ acid and increased the probably of water entering the system from the air. Excess water drives the acetal reaction towards the left, which is consistent with the constant vanillin and syringaldehyde concentrations in the staged system. We believe that the increased precipitation in Figure 4-5 as compared to Figure 4-6 is due to decreased stirring capability in the Jergurson cell as compared to the Parr reactor. For the other process temperatures studied in this work, the decrease in valuable chemical concentration was not observed outside of experimental error, which we believe is due to reduced in-situ acid strength at higher temperatures.

GX-methanol Extractions at Various Temperatures

Figure 4-10 shows the concentration of valuable chemicals in the GX-methanol phase versus pressure at 40 and 48 °C. As previously discussed, a decrease in concentration with increasing pressure is not seen at elevated temperatures. Although there seems to be a slight decrease in syringaldehyde concentration versus time at 48 °C, we believe this to be essentially constant within experimental error, based on the other results shown. A similar trend was seen at 35 °C for this system, however only one run was successfully completed at that temperature and therefore the results are not reported.

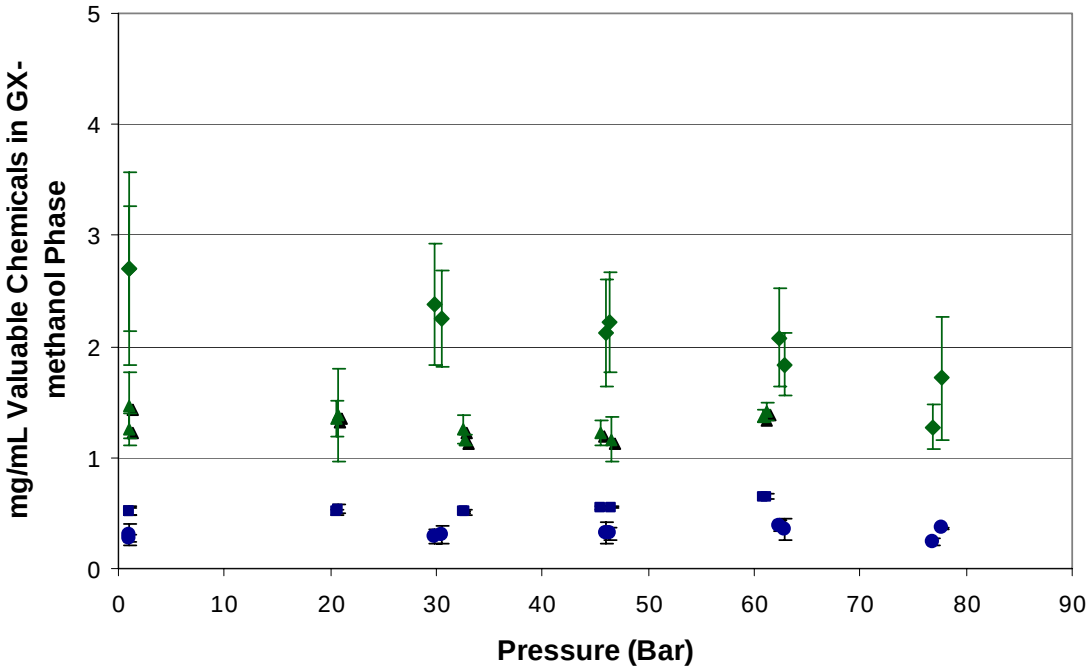

Figure 4-10. Concentration of valuable chemicals in the GX-methanol phase versus pressure using the general GXL procedure; (▲) syringaldehyde and (■) vanillin at 40 °C, (◆) syringaldehyde and (●) vanillin at 48 °C.

Table 4-5 shows the average results for each run, where the data for 25 °C is an average from the staged runs so a constant concentration could be assumed for each temperature. On average, 0.06 % of vanillin and 0.2 % of syringaldehyde was removed from lignin using GX-methanol extraction. More data will need to be taken to adequately prove whether temperature has a positive or negative effect on valuable chemical extraction. Table 4-5 also compares the GX-methanol extraction to three other extraction processes found in the literature[32, 36]. It is clear that, although the literature procedures extract more vanillin and syringaldehyde from lignin, the GX-methanol extraction is a more cost-efficient and environmental friendly process because it requires lower operating temperatures, shorter retention times then conventional heating, and no

chemical oxidation. Furthermore, extracting large amounts of vanillin and syringaldehyde could flood the market, reducing the costs of these chemicals and ultimately lower profits.

Table 4-5. Average amount of valuable chemicals extracted over pressure range (assuming constant concentration). Data from this work compared to literature[32, 36].

Extraction Process	Temperature °C	Vanillin mg/g Lignin	% of total lignin	Syringaldehyde mg/g Lignin	% of total lignin
This Work					
GX-methanol extraction (~ 30 min)	25	2.6 ± 0.7	0.04	9.2 ± 1.3	0.1
	40	3.8 ± 0.2	0.1	8.9 ± 1.1	0.2
	48	2.6 ± 0.4	0.05	15.3 ± 2.9	0.3
Literature					
Nitrobenzene oxidation (10-150 min)[32]	195	---	5.2 - 7.5	---	17.5 - 29.5
Microwave heating (2 N NaOH/15 min)[36]	160	---	5.1	---	---
Conventional heating (2 N NaOH/ 24 hr)[36]	160	---	3.5	---	---

Economic Analysis

The key goal of this work was to prove that GXL extraction could potentially create profit for a paper mill or biorefinery. Table 4-6 shows the estimated net gain for the implementation of GXL extraction into the kraft pulping process. The following assumptions were made:

- The acid precipitation removal of lignin from black liquor was profitable based on the process reported in the literature[28]. Although the lignin price used in Table 4-6 is less then what they report as profitable, we compensate with the additional sale of valuable chemicals.

Table 4-6. Total net gain for sale of vanillin, syringaldehyde, and lignin extracted using GX-methanol. Unless noted, unites in $/day.

Slip Stream	T/ °C	Max Pressure [a] (bar)	Net profit from chemicals	Net profit from Lignin	Cost CO_2 (raw material)	Cost MeOH (5% loss/day)	Compression Cost (1 bar to max) [b]	Compression Cost (10 bar to max) [c]	Total Net Gain per day [b]	Total Net Gain per day [c]
15 % Slip Stream	25	45	17,566	670	3295.52	1767.04	1481	576	11,692	12,597
	40	59.7	17,425	670	2944.64	1767.04	1412	588	11,971	12,795
	48	74.4	28,634	670	2770.92	1767.04	1411	622	23,355	24,144
20% Slip Stream	25	45	23,421	894	4394.6	2356.06	1974	768	15,590	16,796
	40	59.7	23,233	894	3926.76	2356.06	1883	784	15,961	17,060
	48	74.4	38,179	894	3694.56	2356.06	1882	829	31,140	32,193
25 % Slip Stream	25	45	29,277	1,117	5493.68	2945.07	2468	960	19,487	20,995
	40	59.7	29,042	1,117	4907.16	2945.07	2353	980	19,954	21,327
	48	74.4	47,723	1,117	4618.2	2945.07	2352	1037	38,925	40,240

[a]Max pressure normalized to 62 % lignin removal based on CO_2 concentration at given temperature

[b]Assuming that CO_2 is compressed from 1 bar to max pressure

[c]Assuming that CO_2 is compressed from 10 bar to max pressure

- That the lignin remaining after the GXL extraction could be sold for 0.035 $/kg as a feedstock for biofuel. This is the feedstock price given by the National Renewable Energy Laboratory to product profitable biofuels[37].
- That vanillin and syringaldehyde can be sold for 5 and 27 $/lb, respectively.
- That the effect of mass loss on the heat value of black liquor sent to the recovery furnace is not effected when less then 0.15 tonne black liquor/air dried ton pulp is removed for processing[28]. This correlates to a maximum slipstream of 42%.
- The cost of CO_2 is 17.2 $/ton as estimated by the DOE[38]. For this analysis we did not include CO_2 recycle.
- The cost of electricity is 0.05 $/kWh as estimated by the DOE[39].

The results for CO_2 compression costs were determined using an ASPEN-based process design model. The compressor was assumed to have 5 stages, with in-between stage cooling at 25 °C. For simplicity, other then the compressor, no heating or cooling costs were included. This analysis is preliminary and for operating costs only. Once a complete process design is established, a complete economic analysis will need to be performed. However, the positive net gain shown for the preliminary analysis implies that after a certain payback period this process will be profitable. Therefore, Table 4-6 predicts that the addition of lignin and valuable chemical removal from the kraft black liquor stream would be a profitable investment.

Future Work

We have developed a preliminary process for the cost efficient extraction of high value added chemicals from lignin. For this process to be implemented, more work will need to be completed. This work includes, but is not limited to: optimizing pressure and temperature for the process, performing experiments combining the acid precipitation and GXL extraction process, and developing a more accurate analytical technique for determination of lignin and valuable chemical compositions. Another very important aspect of the process that has not been investigated is the separation of vanillin and syringaldehyde downstream of the GXL extraction unit. It can be assumed that this step will have significant impact on the overall economics of the system. Part of this separation scheme will need to include the removal of sulfur from lignin derived from black liquor. Processes have been proposed in the literature; however, a cost-effective and environmental friendly process has yet to be developed[27]. Furthermore, work can be done in removing lignin from biomass before treatment with white liquor. This would avoid the need of acid precipitation, improve the efficiency of the paper mill, and improve the purity of downstream products including biofuels. We also mentioned several other components of biomass that are burned as waste, all of which can offer unique additions to the range of biomaterials produced from biomass. In petroleum refineries many other chemicals are products to help sustain the industry, we need to do the same for biorefineries[3].

Conclusions

We have developed a cost efficient technique for extracting fine chemicals from biomass in an effort to add sustainability to the biorefinery. In this work, we investigated

the preliminary economic impact of adding a GXL extraction unit to a kraft pulping plant. We believe that processes like the one developed here will not only improve the bottom line of the pulp and paper industry, but that valuable chemical extraction will be crucial in the development of a profitable biofuel industry. Biofuels are a necessary part of our future, and the sooner we are able to produce them in an economical viable way we will be one step closer to ending our dependency on non-domestic, non-renewable resources. It is our hope that this innovation, as well as research being performed on other sustainable technologies for commercially viable biorefineries, will help provide cheap, readily available biofuel to our nation.

References

1. Ragauskas, A. J.; Nagy, M.; Kim, D. H.; Eckert, C. A.; Hallett, J. P.; Liotta, C. L., From wood to fuels: Integrating biofuels and pulp production. *Industrial Biotechnology* **2006,** 2, (1), 55-65.

2. Wooley, R.; Ruth, M.; Glassner, D.; Sheehan, J., Process Design and Costing of Bioethanol Technology: A Tool for Determining the Status and Direction of Research and Development. *Biotechnology Progress* **1999,** 15, 794-803.

3. Ragauskas, A. J.; Williams, C. K.; Davison, B. H.; Britovsek, G.; Cairney, J.; Eckert, C. A.; Fredrick, W. J. J.; Hallett, J. P.; Leak, D. J.; Liotta, C. L.; Mielenz, J. R.; Templer, R.; Tschaplinski, T., The Path Forward for Biofuels and Biomaterials. *Science* **2006,** 311, 484-489.

4. Group, N. E. P. D., National Energy Policy. In House, T. W., Ed. 2001.

5. Kamm, B.; Kamm, M., Principles of biorefineries. *Applications of Microbiology and Biotechnology* **2004,** 64, 137-145.

6. Palmqvist, E.; Hahn-Hagerdal, B., Fermentation of lignocellulosic hydrolysates, II: inhibitors and mechanisms of inhibition. *Bioresource Technology* **2000,** 74, 25-33.

7. Zhang, P. Y.-H.; Himmel, M. E.; Mielenz, J. R., Outlook for cellulase improvemnt: Screening and selection strategies. *Biotechnology Advances* **2006,** 24, 452-481.

8. Mosier, N.; Wyman, C.; Dale, B.; Elander, R.; Lee, Y. Y.; Holtzapple, M.; Ladisch, M., Features of promising technologies for pretreatment of lignocellulosic biomass. *Bioresource Technology* **2005,** 96, 673-686.

9. Van Camp, W., Yield enhanced genes: seeds for growth. *Current Opinon in Biotechnology* **2005,** 16, 147-153.

10. Vinocur, B.; Altman, A., Recent advances in engineering plant tolerance to abiotic stress: achievements and limitations. *Current Opinon in Biotechnology* **2005,** 16, 123-132.

11. Boudet, A. M.; Kajita, S.; Grima-Pettenati, J.; Goffner, D., Lignins and lignocellulosics: a better control of syntesis for new and improved uses. *Trends in Plant Science* **2003,** 8, (12), 576-581.

12. Smook, G. A., *Handbook for Pulp and Paper Technology*. 2nd ed.; Angus Wilde Publications: 1992.

13. Hocking, M. B., Vanillin: Synthetic Flavoring from Spent Sulfite Liquor. *Journal of Chemical Education* **1997,** 74, (9), 1055-1059.

14. Thammachote, N.; Watkinson, A. P.; Barr, P. V.; Posarac, D., Combustion of Lignin Mixtures in A Rotary Lime Kiln. *Pulp and Paper Canada* **1996,** 97, (9), 51-55.

15. Prins, M. J.; Ptasinski, K. J.; Janssen, F. J. J. G., From coal to biomass gasification: Comparison of thermodynamic efficiency. *Energy* **2007,** 32, (1248-1259).

16. Ledford, H., Making it up as you go along. *Nature* **2006,** 444, (7), 677-678.

17. Dowaki, K.; Ohta, T.; Kasahara, Y.; Kameyama, M.; Sakawaki, K.; Mori, S., An economic and energy analysis on bio-hydrogen fuel using a gasification process. *Renewable Energy* **2007,** 32, 80-94.

18. Eckert, C. A.; Liotta, C. L.; Bush, D.; Brown, J. S.; Hallett, J. P., Sustainable Reactions in Tunable Solvents. *Journal of Physically Chemistry B* **2004,** 108, 18108-18118.

19. West, K. N.; Wheeler, C.; McCarney, J. P.; Griffith, K. N.; Bush, D.; Liotta, C. L.; Eckert, C. A., In Situ Formation of Alkylcarbonic Acids with CO_2. *Journal of Physically Chemistry A* **2001,** 105, 3947-3948.

20. Clifford, T., *Fundamentals of Supercrtical Fluids*. 1st ed.; New York, 1999.

21. Kunz, M.; Mueller, C. Agents for coloring dyes. 2000.

22. Tagmose, T. M.; Olesen, P. H.; Hansen, T. K. Preparation of hydroxystyryl sulfonyl derivatives for treatment of obesity. 2004.

23. Yamazaki, R.; Nishiyama, Y.; Furuta, T.; Matsuaki, T.; Hatano, H.; Yoshida, O.; Nagaoka, M.; Aiyama, R.; Hashimoto, S.; Sugimoto, Y. Breast cancer resistance protein(BCRP) inhibitor. 2004.

24. Holmqvist, A.; Wallberg, O.; Jonsson, A.-S., Ultrafiltration of Kraft Black Liquor From Two Swedish Pulp Mills. *Chemical Engineering Research and Design* **2005,** 83, (A8), 994-999.

25. Loutfi, H.; Blackwell, B.; Uloth, V., Lignin recovery from kraft black liquor: preliminary process design. *Tappi Journal* **1991**, (January), 203-210.

26. Davy, M. F.; Uloth, V. C.; Cloutier, J.-N., Economic evaluation of black liquor treatment processes for incremental kraft pulp production. *Pulp and Paper Canada* **1998,** 99, (1), 35-39.

27. Olsson, M. R.; Axelsson, E.; Berntsson, T., Exporting lignin or power from heat-integrated kraft pulp mills: A techno-economic comparison using model mills. *Nordic Pulp and Paper Research* **2006,** 21, (4), 476-484.

28. Axelsson, E.; Olsson, M. R.; Berntsson, T., Increased capacity in kraft pulp mills: Lignin separation and reduced steam demand compared with recovery boiler upgrade. *Nordic Pulp and Paper Research* **2006,** 21, (4), 485-492.

29. Lora, J. H.; Glasser, W. G., Recent Industrial Applications of Lignin: A Sustainable Alternative to Nonrenewable Materials. *Journal of Polymers and the Environment* **2002,** 10, 39-48.

30. Chang, C. J.; Day, C.-Y.; Ko, C.-M.; Chiu, K.-L., Densities and P-x-y diagrams for carbon dioxide dissolution in methano, ethanol, and acetone mixtures. *Fluid Phase Equilibria* **1997,** 131, 243-258.

31. Schuerch, C., The Solvent Properties of Liquids and Their Relation to the Solubility, Swelling, Isolation, and Fractionation of Lignin. *Journal of the American Chemical Society* **1952,** 74, 5061-7.

32. Goyal, G. C.; Lora, J. H.; Pye, E. K., Autocatalyzed organosolv pulping of hardwoods: Effect of pulping conditions on pulp properties and characteristics of soluble and residual lignin. *Tappi Journal* **1992**, (February), 110-116.

33. Liu, J.; Kim, Y.; McHugh, M. A., Phase behavior of the vanillin-CO_2 system at high pressures. *The Journal of Supercritical Fluids* **2006,** 39, 201-205.

34. Skerget, M.; Cretnik, L.; Knez, Z.; Skrinjar, M., Influence of the aromatic ring substituents of phase equilibria of vanillins in binary systems with CO_2. *Fluid Phase Equilibria* **2005,** 231, 11-19.

35. Bruice, P. Y., *Organic Chemistry*. Third ed.; Prentice Hall: New Jersey, 2001.

36. Clark, J. H.; Budarin, V.; Deswarte, F. E. I.; Hardy, J. J. E.; Kerton, F. M.; Hunt, A. J.; Luque, R.; Macquarrie, D. J.; Milkowski, K.; Rodriguez, A.; Samuel, O.; Tavener, S. J.; White, R. J.; Wilson, A. J., Green chemistry and the biorefinery: a partnership for a sustainable future. *Green Chemistry* **2006,** 8, 853-860.

37. Elander, R.; Eggerman, T., Process and economic analysis of pretreatment technologies. *Bioresource Technology* **2005,** 96, 2019-2025.

38. http://www.netl.doe.gov/, 2007.

39. http://www.eia.doe.gov/fuelelectric.html, 2007.

CHAPTER V

NOVEL SOLVENTS FOR IMPROVED BIOMASS PRETREATMENT

Introduction

Chapter I discussed briefly the concept of a biorefinery and the need for cost-effective innovations. Chapter IV investigated the use of lignin, a largely wasted component of biomass, to extract valuable chemical side products. This chapter will go into more detail on the benefits of biofuels, and will focus on improving the biorefinery by adding sustainability to biomass pretreatment techniques.

The United States' increasing dependence on oil is of national concern[1]. With domestic oil production decreasing and increasing instability in regions we rely on for oil, the need for alternative and diversified fuel sources is acutely apparent[2, 3]. Fossil fuels, the feedstock for oil, emit copious amounts of greenhouse gases (GHG) including CO_2, all of which could soon be harshly regulated with global warming becoming a growing concern[4-6]. Without substantial innovations in the field of CO_2 sequestration, the use of renewable energy sources will need to increase exponentially to counteract these emissions from fossil fuels and coal[7-9]. Although GHG emissions (excluding CO_2) from power plants, oil refineries, and other industrial facilities are fairly well regulated, the emissions from mobile sources like cars and trucks are much more difficult to control[10]. Of the oil used by the U.S., the transportation sector alone consumed 68% in 2005 as shown in Figure 5-1[11]. Therefore, to reduce the total consumption of oil in this country as well as reduce CO_2 and GHG emissions, the development of commercially available renewable petroleum alternatives is a necessity.

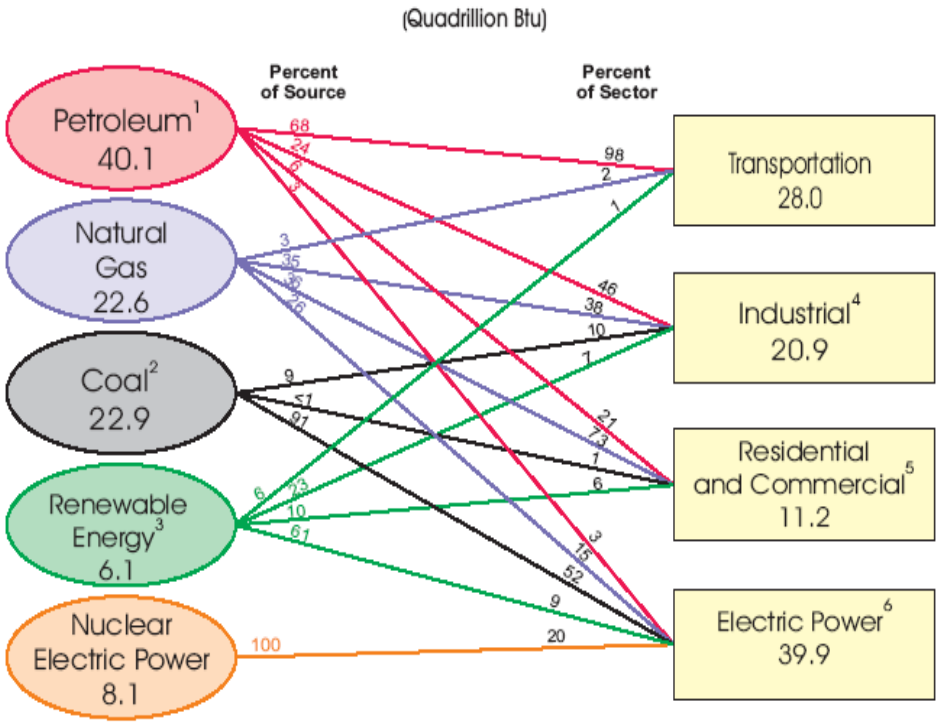

Figure 5-1. Primary energy consumption by source and sector in the US for 2005, as determined by the USDOE Energy Information Administration[11].

Solar energy stored as sugar in biological materials has unique properties, providing a great opportunity for use as a transportation fuel alternative[12]. This sugar can be converted into alcohol-based fuels via hydrolysis and fermentation, and the easiest form of stored sugar to convert is starch[12]. Due to this, most of the renewable transportation fuel produced in this country is ethanol from starch-based corn. However, it has become apparent that using corn for fuel has many disadvantages including ethical concerns, energy use in cultivation, limited positive net environmental impact, and market fluxuations[13]. Furthermore, there is not sufficient land available to cultivate enough corn to make a substantial dent in U.S. oil use. These issues have shifted the focus away from corn ethanol and towards ethanol produced from lignocellulosic materials, which contain sugar in the form of cellulose and hemicellulose. Specifically,

lignocellulosic materials contains on average ~ 40-50% cellulose, a polymer of glucose; ~ 25-35 % hemicellulose, a polymer of five different sugars, 6-carbon hexoses and 5-carbon pentoses; ~ 15-20% lignin; and the remainder resins, oils and extractives[14, 15]. Lignocellulosic materials have several advantages over starch-based biomass; they are abundant throughout the U.S., require little fertilizer or excess water to grow, and are not a viable food source[16]. Some examples of possible lignocellulosic feedstocks include biomass from agriculture (i.e. cornstovers), forestry (i.e. woodmeal/softwood), herbaceous (i.e. switchgrass), and woody (i.e. poplar trees/hardwood) crops[15]. Table 5-1 compares the availability of several lignocellulosic feedstocks and highlights the abundance of cornstovers. It has been estimated that only 40% of the available harvestable cornstovers is needed to produce 3 billion gallons per year of ethanol, a vast improvement over the use of corn alone[17]. Even the president has recognized the advantage of using lignocellulosic materials like cornstovers, switchgrass, and wood for fuel[1]; the challenge here is developing technologies that make the conversion commercially feasible.

Table 5-1. Estimated availability of selected feedstocks[17].

Feedstock Type	Estimated Availability (million dry ton/yr)
Corn Stover	153
Other Agricultural Residues	58
Corn Fiber	4
Energy Crops	70
Wood Coproducts	72

There are three general steps in converting lignocellulosic biomass into ethanol: pretreatment, hydrolysis, and fermentation[18]. Hydrolysis and fermentation are both required for corn-to-ethanol production. Although work is being done in these areas to improve yields and efficiencies, these processes are well-defined compared to biomass pretreatment. Starch, being easy to degrade, does not require pretreatment; however, lignocellulosic materials are much more robust and do require pretreatments to break into the cell wall and expose the cellulose and hemicellulose for further processing, as shown in Figure 5-2[19]. It has been reported that without pretreatment, and using standard hydrolysis and fermentation procedures as determined by the National Renewable Energy Lab (NREL), only 8.5% of xylose (one of the 5-carbon sugars in hemicellulose) and 15.7% of glucose is freed for conversion into fuels[20]. Furthermore, this study also concludes that without close to 100% yields of xylose and glucose, ethanol from lignocellulosic materials will not be competitive in price with oil. This leaves researchers with the task of developing a pretreatment method that meets the following criteria[19]:

- Avoids the need to reduce the size of biomass particles
- Limits the formation of degradation products that inhibit growth of fermentative microorganisms
- Minimizes energy demands or costs
- Maximizes yield of biofuel from feedstocks

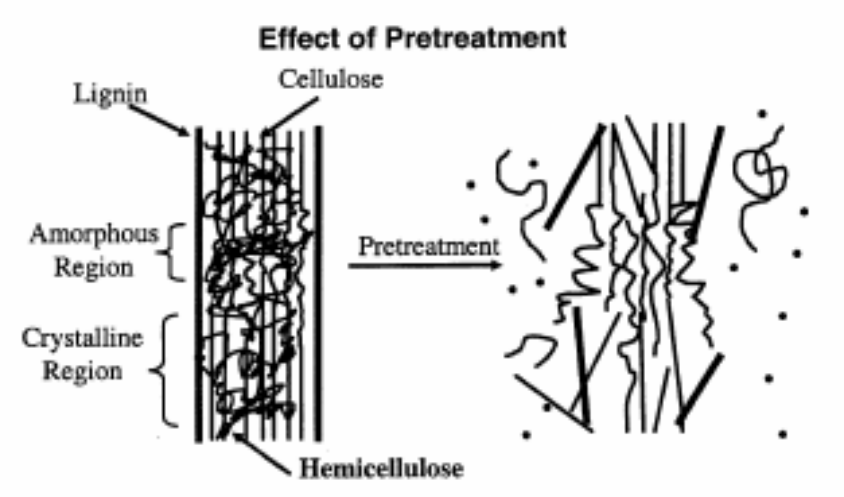

Figure 5-2. Schematic of goals for pretreatment of lignocellulosic material[19, 21].

Consequently, a large amount of work has been done in the field of lignocellulosic biomass pretreatments. To facilitate data compatibility and collaboration in this field, the Biomass Refining Consortium for Applied Fundamentals and Innovations (CAFI) was formed among several universities and the NREL[15]. This unique group performs different pretreatment techniques on the same source of biomass, and the same lab performs the analytical techniques to insure accurate comparisons. These pretreatment techniques involve the use of many different processes and materials: uncatalyzed stream explosion, batch and co-current liquid hot water treatments, and batch and flowthrough dilute sulfuric acid, lime, and ammonia treatments[19]. Their results so far have shown that acidic and basic treatments provide the best sugar yields, but the downstream processing and neutralization of these treatment systems adds unwanted waste and energy use[15]. Outside CAFI, other work being done in this area includes using high pressure combined with acid or base treatments, ionic liquids to dissolve cellulose, and designer enzymes; however, it is clear that new technologies can be discovered to improve the efficiency of this process[22, 23].

CO_2-expanded alcohols, a type of Gas Expanded Liquid (GXL), have several properties that make them an excellent candidate for use in biomass pretreatment. When an alcohol (methanol, ethanol, etc.) is expanded with CO_2, an in-situ alkyl carbonic acid is formed[24]. This could provide similar results as dilute acid pretreatments with the distinct advantage of no downstream neutralization; simply depressurizing the system reverses the acid formation. GXLs are a class of tunable solvents, meaning their solvation properties can be tailored by changing the temperature and/or pressure of the system[25]. A tunable process makes perfect sense when dealing with a variable feedstock like biomass; because each type of biomass will require different degrees of pretreatment, CO_2-expanded alcohols can provide flexibility without requiring different processing equipment or materials. The use of pressure in this system will provide additional penetrating power, which should aid in disrupting the matrix of the biomass and improving the efficiency of the pretreatment. Some proposed pretreatment methods combine pressure treatments with dilute acid to achieve the effect that CO_2-expanded alcohols provide without the caustic chemicals and downstream waste[23]. Furthermore, GXLs can provide a cost-efficient process for pretreatment that would improve the profitability of ethanol produced from lignocellulosic materials.

The current work investigates the ability of CO_2-expanded methanol to penetrate the biomass matrix, separating lignin and extractives from the cellulose and hemicellulose. Figure 5-3 predicts what could be accomplished with this treatment; the extractives and lignin can be further processes to valuable products as shown in Chapter IV, and the cellulose and hemicellulose can be processed into biofuels like ethanol. Methanol is used in this study because it is inexpensive, forms the strongest alkyl

carbonic acid with CO_2, and has reasonable solubility with lignin[26, 27]. In this study cornstovers, switchgrass, and softwood woodmeal (wood chips that have been run thru a mesh), are treated with CO_2-expanded methanol. The cellulose, hemicellulose, lignin and extractive composition of the treated biomass was analyzed to determine if the pretreatment was successful in removing the unwanted components.

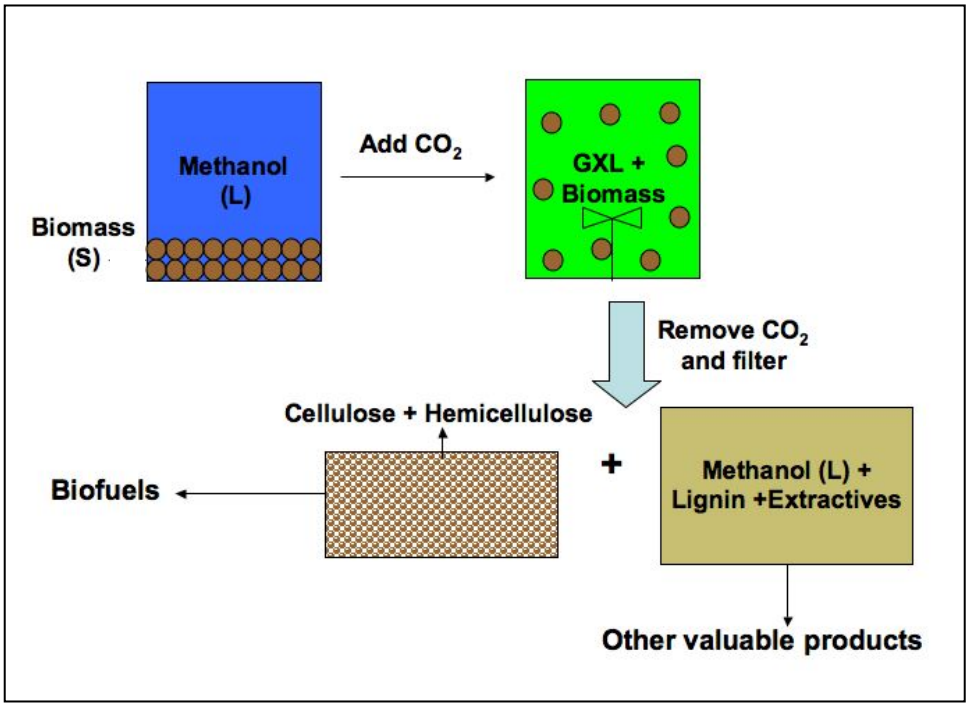

Figure 5-3. Schematic of prospective results: biomass pretreated with CO_2-expanded methanol.

Experimental Apparatus and Procedures

Materials

Pine softwood chips, switchgrass, and cornstovers were received from Dr. Ragauskas' lab in the School of Chemistry and Biochemistry. These biomass materials were run thru a 4.75-mm (No. 4) sieve using a Thomas Wiley Mill to minimize size difference between the feedstocks. Methanol (HPLC grade) was received from Sigma-Aldrich. 98% Sulfuric acid (ACS/FCC), 10% barium chloride titrate, and acetone (ASC)

were received from VWR. Sodium hydroxide pellets were received from Fischer Scientific. The carbon dioxide (SFC/SFE grade) was obtained from Airgas and was filtered prior to use.

Apparatus

All pretreatments were performed in a 300 ml Parr pressure reactor. A known amount of biomass and methanol was added to the reactor, and the reactor was sealed and heated to the desired temperature. CO_2 was added to the system by an ISCO 500D syringe pump with a series D controller until the desired pressure was reached. The reactor stirred at a maximum, steady rate (controlled by a tachometer) until the completion of all runs. The CO_2 was vented from the system, and the reactor was allowed to cool. A schematic or the vessel is shown in Figure 5-4.

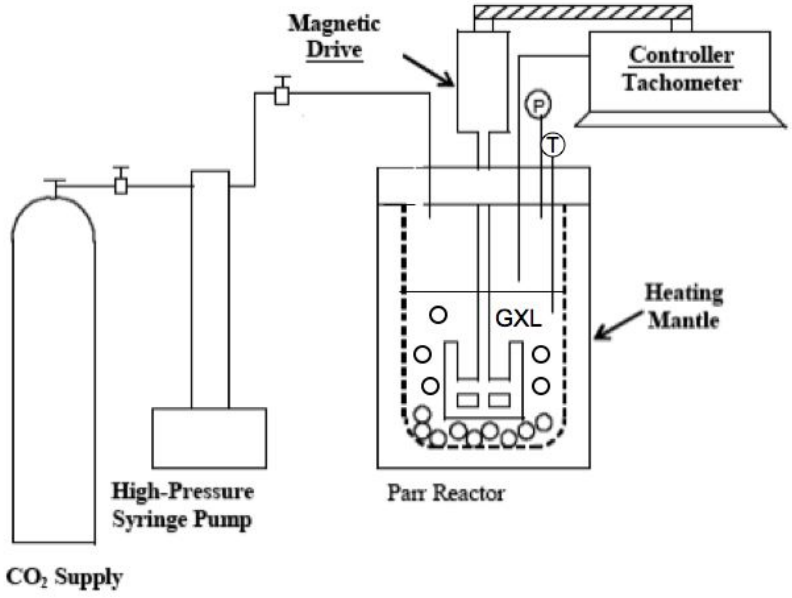

Figure 5-4. Schematic of the reaction apparatus.

Woodchip Extractions

Initial experiments for this project involved treating woodchips, as received, with GX-methanol to determine what type of extractives were removed. First, 15 grams of wood chips and 100 milliliters of methanol was added the reactor with 17.4 bar of pressure at 40 °C. Simultaneously, the same amount of wood chips were treated with just methanol on the bench top and both of the treatments ran for three days. Once the treatments were completed, the biomass was filtered and washed with excess methanol to insure all extractives were collected. Samples were taken from the filtrate and analyzed for peak identification with a Hewlett Packard 6890 Gas Chromatograph with Mass Selective Detector 5973 (GC-MS). A third woodchip pretreatment was performed under 26.6 bar CO_2 pressure and 40 °C for 3 days; however, samples were taken from the system periodically throughout the experiment to determine the effect of time on the extractives present.

Biomass Pretreatments

Determining Mass Loss

Several pretreatments were preformed with woodmeal, switchgrass, and cornstovers to determine the total mass removed during treatment. Pretreatments were performed following the procedure above at 60 °C and 30 bar for 24 hours, and the biomass was washed with excess methanol following removal from the reactor. Both the biomass and the filtrate were placed in pre-weighed containers and allowed to dry for several days. Once the weigh of the dried biomass and filtrate (methanol had evaporated leaving dried extractives) had become constant over time, the final weights were recorded

and mass balances were performed, which were closed with an accuracy of ± 2%. The biomass was further analyzed for composition.

Determining Biomass Compositions

Biomass that had been pretreated with GX-methanol at 60 °C and 30°C was analyzed for composition using the procedure reported by Yang et al[28]. For comparison, untreated biomass was also analyzed.

Extractives

Extractives were removed by Soxhlet extraction[29]. The biomass sample was weighed and added to a Whatman 25mm x 88mm cellulose thimble filter. 60 milliliters of acetone per gram of biomass sample was added to the extraction chamber. Once the system had reached 90 °C it was left to reflux for 3 hours. The biomass sample was removed and dried until a constant weight was obtained. The acetone and extractives were transferred to a crystallization disk where the acetone evaporated. The extracts were dried until a constant weight was obtained, and the mass balance was closed within ± 1%.

Hemicellulose

150 milliliters of 0.5 mol/L NaOH solution (NaOH pellets dissolved in distilled water) was added to 1 gram of extractive-free dried biomass, and the solution was placed in an 80 °C oil bath for 3.5 hours. The biomass sample was filtered and washed with distilled water until no more Na+ was detected (the Ph value of the solution approached 7). The biomass sample was dried to a constant weight, and the recorded weight difference was the hemicellulose content.

Lignin and Cellulose

30 milliliters of 98% sulfuric acid was added for each gram of extractive-free, hemicellulose-free, dried biomass. The solution was held at ambient temperature for 24 hours, and then it was placed in a 100 °C oil bath for 1 hour. The biomass was filtered and washed with distilled water until the sulfate ion in the filtrate was undetectable (via titration with a 10% barium chloride solution). The sample was dried to a constant weight, and the recorded weight difference was the lignin content. The remaining sample can be assumed to be the cellulose content of the original biomass sample.

Results and Discussion

Woodchip Extractions

Table 5-2 shows the components extracted from woodchips after 3 days in GX-methanol, 3 days in methanol only, and 1hr in GX-methanol respectively. Although over 50 peaks were shown on the MS as extractives, the components listed in Table 5-2 were identified with a greater then 97 qualitative match using the HP MS software library. To identify other peaks of interest, pure component samples would need to be run for comparison. The components identified fall under three categories; cyclic extractives, fatty acids, and resin acids. To determine the quantity of these peaks as compared to the extractives as a whole, the peak areas were compared to the total area of the sample on a solvent free basis. This accounts for differences in sample size and instrument sensitivity. The numbers in Table 5-2 are only qualitative assessments; however, they give insight on the approximant amount of each component you can expect to remove at these conditions

from pine woodchips. For more accurate results, calibrations would need to be run on pure components for each desired extractive.

Table 5-2. Extractive components from pine woodchips treated with GX-methanol at 17.4 Bar and 40 ° C for three days, methanol only at ambient pressure and temperature for 3 days, and GX-methanol at 17.4 Bar and 40 °C for 24 hours.

Component	Structure	% in GX-sample (solvent free basis) 3 days	% in BT sample (solvent free basis) 3 days	Average % in GX-sample 1 hr (solvent free basis)
a-pinene		1.2	3.6	0.5
b-pinene		0.3	1.5	0.2
octanoic acid (caprylic acid)	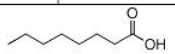	1.1	0.9	0.6
verbenone		0.5	0.5	0.3
nonanoic acid	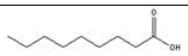 HO_2C-$(CH_2)_7$-Me	1.1	1.1	1.0
vanillin	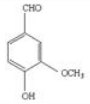	0.2	N/A	0.4
tetradecanoic acid	HO_2C-$(CH_2)_{12}$-Me	0.2	N/A	0.7
hexadecanoic acid (palmitic acid)	HO_2C-$(CH_2)_{14}$-Me	5.0	5.6	4.2
9-octadenoic acid (oleic acid)	$CH_3(CH_2)_7CH=CH(CH_2)_7CO$ OH	9.9	11.5	9.0
resins*		31.6	24.7	14.2

*Resins are shown here as a collective area over a range of residence times (R.T 15-20 minutes).

Although preliminary, these results give us some interesting insight on pine woodchip extractives. Of the peaks identified two of the fatty acids, palmitic and oleic, were the largest contributors to overall area following the resins. These components could be used as value-added products such as surfactants or lubricants[30, 31], and as potential feedstocks for biodiesel and diesel additives[32-34]. Of the resins acids, the most

frequently identified was dehydroabietic acid (structure shown in Table 5-2). Resin acids are known for their toxicity in pulp and paper waste water streams[35]; if they could be removed via pretreatment and used for valuable products such as pesticides or biofuels, pretreatment with GX-methanol could improve profit and reduce waste[36, 37]. Of the other extractives present, vanillin (as discussed in Chapter IV), α-pinene, and β-pinene have value as flavoring agents. Extracting components like vanillin with this process instead of from a black liquor stream would alleviate the need to remove sulfur during purification. If GX-ethanol could be used in place of methanol, this pretreatment would be a "natural" and cheap processing technique for these compounds.

For the components identified, it is clear that GX-methanol does not offer any great advantages over treatment for three days with methanol alone. Vanillin and tetradecanoic acid were not present in the methanol-only extractives, and the pinenes showed greater areas for methanol only; the rest of the components give similar qualitative amounts for both treatments. However, it is interesting to note the qualitative amounts present after treatment with GX-methanol for only 1 hour. To accurately state that methanol alone would not give these results, more control experiments would need to be preformed. However, if after one hour one can remove substantial amounts of palmitic, oleic, and dehydroabietic acids, one could have a potentially efficient process for removing biomaterials for the biorefinery process. Figure 5-5 shows the amount of component extracted versus time during treatment with GX-methanol, and overall most compound areas remain constant. For this particular run, the peak for oleic acid becomes unidentifiable behind the resin peak, which increases over time. Also during this run, acetic acid, which has been identified as an inhibitor for ethanol production when formed

during pretreatment, was identified as an extractive peak[38]. If this type of treatment were to be used as a value-added removal step before biofuel pretreatment, the removal of acetic acid would be beneficial. With calibrations for the specific chemicals and more runs performed, additional information could be obtained from these pretreatments and their benefits more accurately determined.

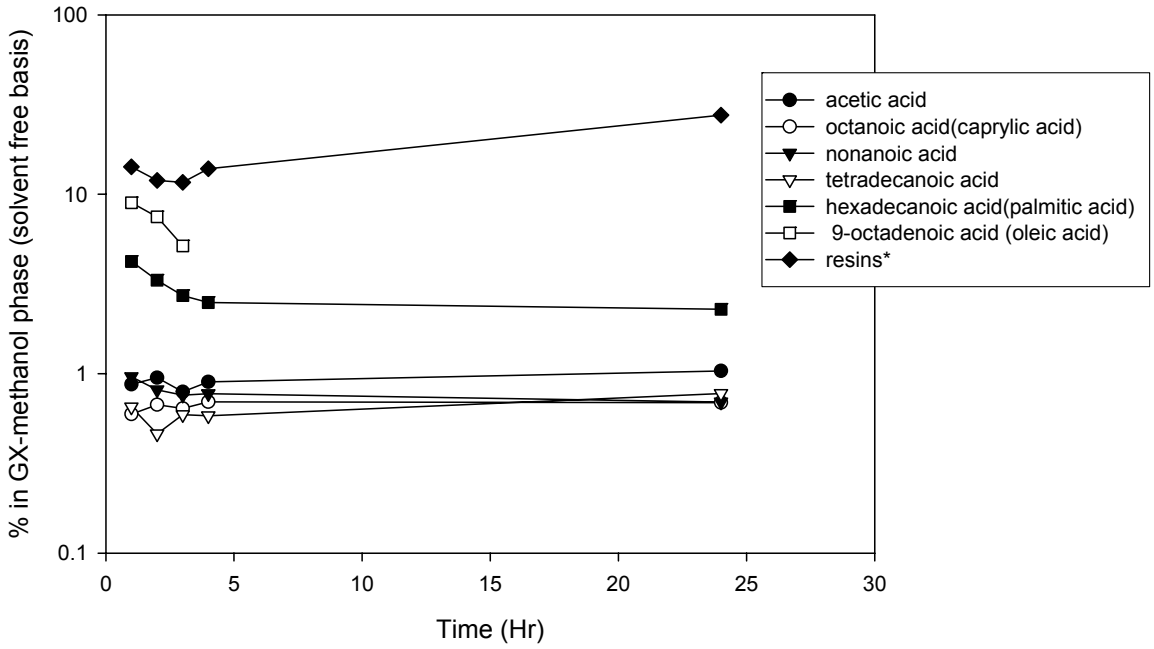

Figure 5-5. Percent component extracted versus time during treatment with GX-methanol at 26.6 bar and 40 °C.

Biomass Pretreatments

Figure 5-6 shows the percent mass loss (based on initial biomass weight) during pretreatment of woodmeal, cornstovers, and switchgrass with GX-methanol at 60 °C and 30 bar for 24 hrs. These results indicate that both switchgrass and cornstovers lose approximately 10 -12% of their mass after treatment with GX-methanol. The woodmeal did not see such a drastic reduction, which we hypothesis is due to the higher lignin content in pine wood (as shown in Table 5-3).

Table 5-3. Literature values for percent dry weight composition of lignocellulosic feedstocks, adapted from N. Mosier et al[19].

Feedstock	Cellulose	Hemicellulose	Lignin	Extractives/Minor Components
Corn Stover	37.5	22.4	17.6	22.5
Pine Wood	46.4	8.8	29.4	15.4
Switch grass	31	20.4	17.6	31

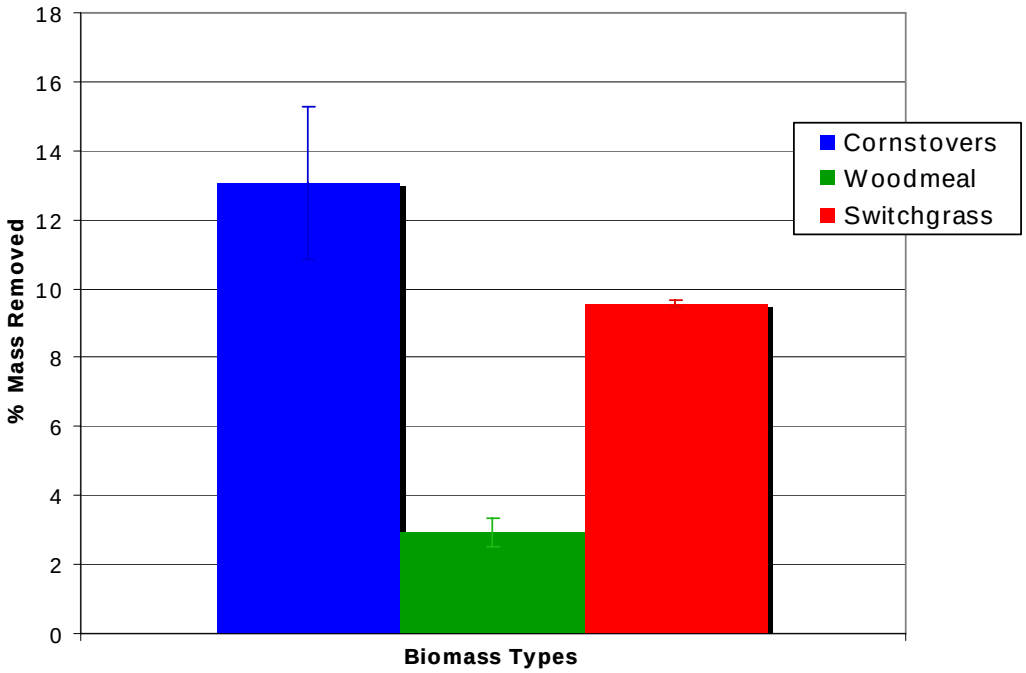

Figure 5-6. Percent total mass removed from several biomass samples after treatment with GX-methanol at 60 °C and 30 bar for 24 hrs.

Table 5-4 shows biomass compositions measured for each biomass type after no treatment, and treatment with GX-methanol at 60 °C for 24 hrs and 30 °C for 3 hrs. It is important to note the discrepancy between the literature data for the dry weight compositions (Table 5-3) and the results we obtained for the untreated samples, most specifically the large difference in extractive concentrations. The soxhlet extraction techniques followed from the literature (as described in the procedure section) seem to

reflux for a much shorter time then other methods available, specifically the NREL method for determination of extractives in biomass[39]. If further work is to be done in this area we suggest following the NREL protocols, if only for a more accurate comparison to the results published by CAFI. However, since all data taken for this work were analyzed by the same procedure (for which error is included), the comparison between treatment techniques is still valid for lignin, hemicellulose, and cellulose compositions.

Table 5-4. Composition of biomass components in both treated and untreated cornstover, woodmeal, and switchgrass samples.

Treatment	% Composition in biomass sample determined after treatment			
	Extractives*	Hemicellulose	Lignin	Cellulose
Cornstover				
No Pretreatment	0.38	51.5±1.3	43.0±0.9	5.1±2.2
GX-Methanol 60 °C/ 24 hr/ 30 Bar	0.04	40.6±2.5	31.6±9.8	27.7±12.3
GX-Methanol 30 °C/ 3 hr/ 40 Bar	0.37	48.4±3.1	42.5±1.8	8.8±1.3
Woodmeal				
No Pretreatment	0.46	9.3±3.0	34.8±16.4	54.5±12.5
GX-Methanol 60 °C/ 24 hr/ 30 Bar	0.03	4.7±0.5	36.5±14.6	58.7±14.0
GX-Methanol 30 °C/ 3 hr/ 50 Bar	0.61	7.80±0.5	34.8±5.5	56.7±5.0
Switchgrass				
No Pretreatment	0.39	44.2±2.8	37.8±1.9	16.8±3.8
GX-Methanol 60 °C/ 24 hr/ 30 Bar	0.04	42.7±0.5	46.8±0.3	10.4±0.1
GX-Methanol 30 °C/ 3 hr/ 55 Bar	0.32	48.7±0.9	30.2±6.6	20.8±5.8
* Error determined via overall mass balance with average error of 0.5 - 7 %				

Figures 5-7, 5-8, and 5-9 show graphically the data presented in Table 5-4 for cornstover, woodmeal, and switchgrass respectively. As previously discussed, it was our hope that GX-methanol would create an acidic media to remove lignin and extractives from the biomass and leave the hemicellulose and cellulose in the solid biomass sample. Only the cornstovers show an increase in cellulose composition after treatment at 60 °C

for 24 hrs, however within the error it seems all biomass samples retain the same lignin, hemicellulose, and cellulose compositions throughout the treatments.

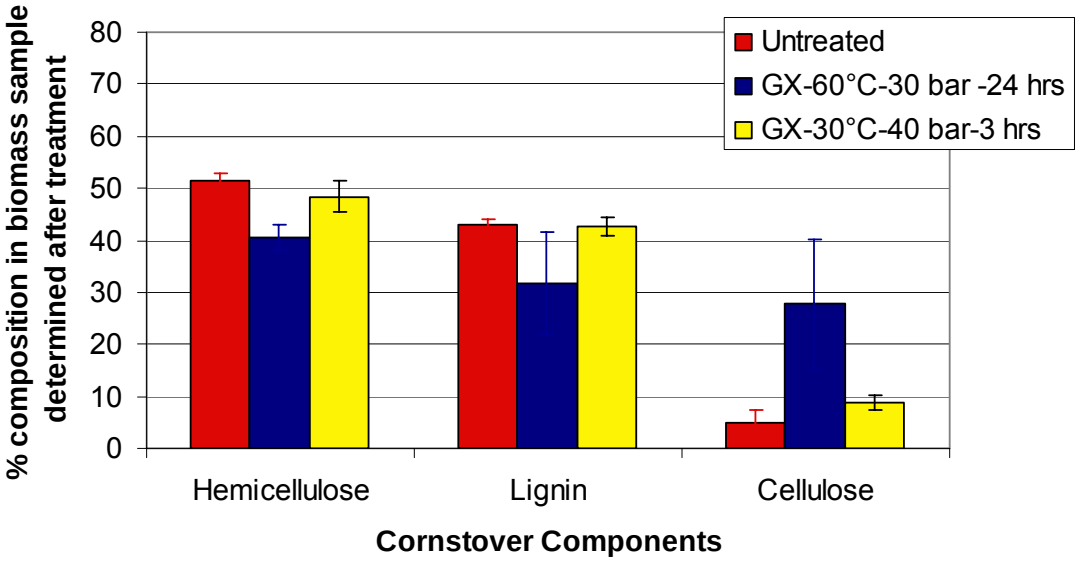

Figure 5-7. Percent hemicellulose, lignin, and cellulose composition in cornstover determined after no treatment, treatment with GX-methanol at 60 °C, 30 bar, and 24 hrs, and treatment with GX-methanol at 30 °C, 40 bar, and 3 hrs.

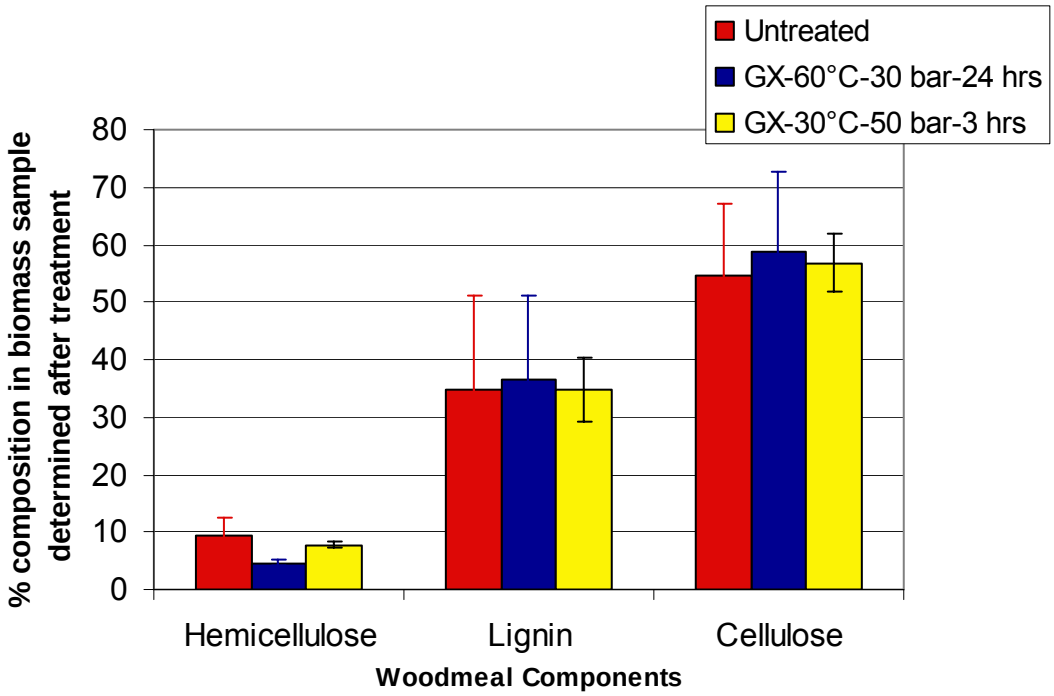

Figure 5-8. Percent hemicellulose, lignin, and cellulose composition in woodmeal determined after no treatment, treatment with GX-methanol at 60 °C, 30 bar, and 24 hrs, and treatment with GX-methanol at 30 °C, 50 bar, and 3 hrs.

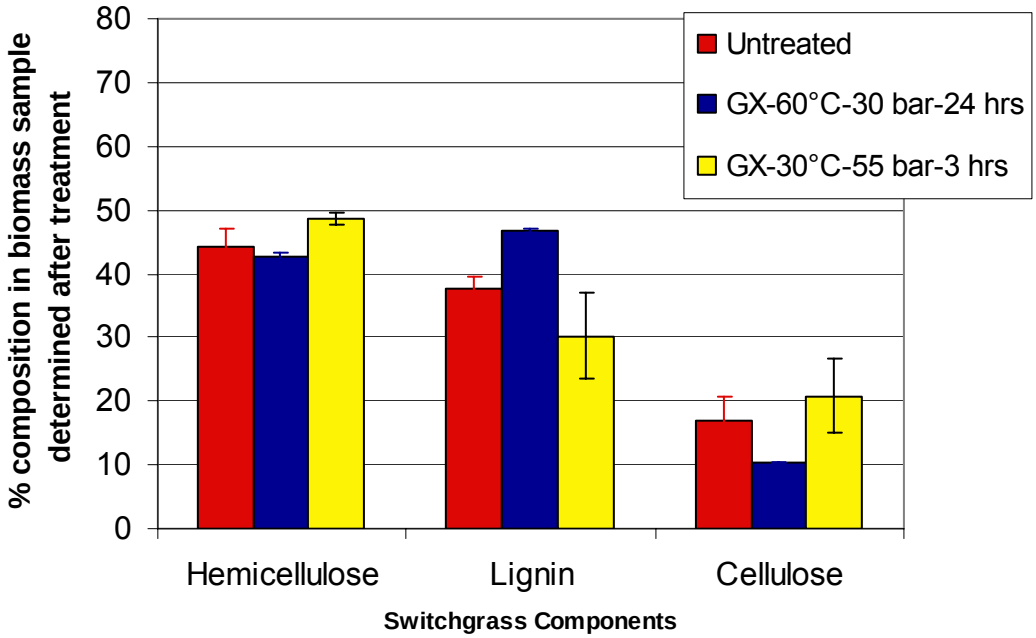

Figure 5-9. Percent hemicellulose, lignin, and cellulose composition in switchgrass determined after no treatment, treatment with GX-methanol at 60 °C, 30 bar, and 24 hrs, and treatment with GX-methanol at 30 °C, 55 bar, and 3 hrs.

From the results shown here, it does not seem that GX-methanol has enough acidic characteristics or penetrating power to accomplish our pretreatment goal. If the acidic nature of GX-methanol did have an effect, we should have seen better results from the 30 °C data (the media is more acidic at lower temperatures); however, this was not the case. Although we did only run the treatment for 3 hours at 30 °C and increasing the treatment time may improve the results, on an industrial scale a 24-hour pretreatment step will most likely not be a cost-effective solution. We also did not see much difference in CO_2 pressures ranging from 30-55 bar, so it can be assumed that under these moderate pressures the biomass matrix is not penetrated. In researching other GXLs that would form an acidic media, we considered methanol expanded with SO_2. The literature shows,

however, that the acid formed is monobasic (pK_a of 6.42)[40], and is therefore a slightly weaker acid then the methylcarbonic acid formed with CO_2 (pK_a of 6.37)[41].

Conclusions

This work shows the effect of gas expanded methanol pretreatments on three different species of lignocellulosic biomass. Although the results do not show promise for the use of this technique as an improvement in bioethanol productions, GXL treatment may be used as a preliminary treatment to remove valuable chemicals. The work preformed here provided some preliminary information on how novel solvent systems may provide profitability to the biorefinery. Future work in the area of novel solvents for biomass pretreatment could include CO_2-enhanced nearcritical water, supercritical CO_2 with an organic co-solvent, or acid treatment with a novel downstream separation, all of which are discussed in more detail in Chapter VI.

References

1. *State of the Union Address*; www.whitehouse.gov, 2007.

2. *BP Statistical Review of World Energy*; BP America Inc., http://www.bp.com/productlanding.do?categoryId=6842&contentId=7021390, 2006.

3. *National Security Consequences of U.S. Oil Dependency*; 58; Council of Foreign Relations,2006.

4. Lewis, N. S., *Chemical Challenges in Renewable Energy*; http://nsl.caltech.edu/files/Energy_Notes.pdf, 2007.

5. Crabtree, G. W.; Whitesides, G. M., Don't Forget Long-Term Fundamental Research in Energy. *Science* **2007,** 315, 796-798.

6. Keer, R. A., Scientists Tell Policymakers We're All Warming the World. *Science* **2007,** 315, 754-757.

7. Schrag, D. P., Preparing to Capture Carbon. *Science* **2007,** 315, 812-813.

8. Hoffert, M. I.; Caldeira, K.; Benford, G.; Criswell, D. R.; Green, C.; Herzog, H.; Jain, A. K.; Kheshgi, H. S.; Lackner, K. S.; Lewis, J. S.; Lightfoot, H. D.; Manheimer, W.; Mankins, J. C.; Mauel, M. E.; Perkins, L. J.; Schlesinger, M. C.; Volk, T.; Wigley, T. M. L., Advanced Technology Paths to Global Climate Stability: Energy for a Greenhouse Planet. *Science* **2002,** 298, 981-987.

9. Pacala, S.; Socolow, R., Stabilization Wedges: Solving the Climate Problem for the Next 50 years with Current Each. *Science* **2004,** 305, 968-972.

10. Cadle, S. H.; Belian, T. C.; Black, K. N.; Minassian, F.; Natarajan, M.; Tierney, E. J.; Lawson, D. R., Real-World Vehicle Emissions: A Summary of the 14th Coordinating Research Council On-Road Vehicle Emissions Workshop. *Journal of the Air & Waste Man Association* **2005,** 55, 130-146.

11. *Annual Energy Review 2005*; DOE/EIA-0384; Department of Energy Energy information Administration,2005.

12. Sanderson, K., A field in ferment. *Nature* **2006,** 444, 673-676.

13. Hill, J.; Nelson, E.; Tilman, D.; Polasky, S.; Tiffany, D., Environmental, economic, and energetic costs and benefits of biodiesel and ethanol biofuels. *Proceedings of the National Academy of Sciences of the United States of America* **2006,** 103, (30), 11206-11210.

14. Smook, G. A., *Handbook for Pulp and Paper Technology*. 2nd ed.; Angus Wilde Publications: 1992.

15. Wyman, C.; Dale, B.; Elander, R.; Holtzapple, M.; Ladisch, M.; Lee, Y. Y., Coordinated development of leading biomass pretreatment technologies. *Bioresource Technology* **2005,** 96, 1959-1966.

16. Schubert, C., Can biofuels finally take center stage? *Nature Biotechnology* **2006,** 24, (7), 777-784.

17. McMillan, J. D.; Kadam, K. L., Availability of corn stovers as a sustainable feedstock for bioethanol production. *Bioresource Technology* **2002,** 88, 17-25.

18. Liu, C.; Wyman, C., The Effect of Flow Rate of Very Dilute Sulfuric Acid on Xylan, Lignin, and Total Mass Removal from Corn Stovers. *Industrial & Engineering Chemistry Research* **2004,** 43, 2791-2788.

19. Mosier, N.; Wyman, C.; Dale, B.; Elander, R.; Lee, Y. Y.; Holtzapple, M.; Ladisch, M., Features of promising technologies for pretreatment of lignocellulosic biomass. *Bioresource Technology* **2005,** 96, 673-686.

20. Elander, R.; Eggerman, T., Process and economic analysis of pretreatment technologies. *Bioresource Technology* **2005,** 96, 2019-2025.

21. Hsu, T. A.; Ladisch, M.; Tsao, G. T., Alcohol from cellulose. *Chemical Technology* **1980,** 10, (5), 315-309.

22. Zhu, S.; Wu, Y.; Chen, Q.; Yu, Z.; Wang, C.; Jin, S.; Ding, Y.; Wu, G., Dissolution of cellulose with ionic liquids and its applications: a mini-review. *Green Chemistry* **2006,** 8, 325-327.

23. Stuart, E.; Rinaldo, A., E. Device and Method for Treating Biomass. 2005.

24. West, K. N.; Wheeler, C.; McCarney, J. P.; Griffith, K. N.; Bush, D.; Liotta, C. L.; Eckert, C. A., In Situ Formation of Alkylcarbonic Acids with CO_2. *Journal of Physically Chemistry A* **2001,** 105, 3947-3948.

25. Eckert, C. A.; Liotta, C. L.; Bush, D.; Brown, J. S.; Hallett, J. P., Sustainable Reactions in Tunable Solvents. *Journal of Physically Chemistry B* **2004,** 108, 18108-18118.

26. Schuerch, C., The Solvent Properties of Liquids and Their Relation to the Solubility, Swelling, Isolation, and Fractionation of Lignin. *Journal of the American Chemical Society* **1952,** 74, 5061-7.

27. Eckert, C. A.; Liotta, C. L.; Ragauskas, A. J.; Hallett, J. P.; Kitchens, C.; Hill, E.; Draucker, L. C., Tunable solvents for fine chemicals from the biorefinery. *Green Chemistry* **2007,** DOI: 10.1039/b614051c.

28. Yang, H.; Yan, R.; Chen, H.; Zheng, C.; Lee, D. H.; Liang, D. T., in-Depth investigation of Biomass Pyrolysis Based on Three Major Components: Hemicellulose, Cellulose and Lignin. *Energy and Fuels* **2005,** 20, 388-393.

29. Eaton, D. C., *Laboratory Investigations in Organic Chemistry*. McGraw Hill: New York, 1989.

30. Gallezot, P., Process options for converting renewable feedstocks to bioproducts. *Green Chemistry* **2007,** 9, 295-302.

31. Falk, O.; Meyer-Pittroff, R., The effect of fatty acid composition on biodiesel oxidative stability. *European Journal of Lipid Science and Technology* **2004,** 106, 837-843.

32. Choo, Y. M.; Ma, A. N.; Basiron, Y.; Yung, C. L.; Cheng, S. F. Palm-based Biodiesel Foundation. 2006.

33. Marchetti, J. M.; Miguel, V. U.; Errazu, A. F., Heterogenous esterfication of oil with high amount of free fatty acids. *Fuel* **2007,** 86, 906-910.

34. Snare, M.; Kubickova, I.; Maki-Arvela, P.; Eranen, K.; Murzin, D. Y., Hetergenous Catalytic Deoxygenation of Stearic Acid for Production of Biodiesel. *Industrial & Engineering Chemistry Research* **2006,** 45, 5708-5715.

35. Ledakowicz, S.; Michniewicz, M.; Jagiella, A.; Stufka-Olczyk, J.; Martynelis, M., Elimination of resin acids by advanced oxidation processes and their impact on subsequent biodegradation. *Water Research* **2006,** 40, 3439-3446.

36. Coll, R.; Udas, S.; Jacoby, W. A., Conversion of the Rosin Acid Fraction of Crude Tall Oil into Fuels and Chemicals. *Energy and Fuels* **2001,** 15, (1166-1172).

37. Savluchinske-Feio, S.; Curto, M. J. M.; Gigante, B.; Roseiro, J. C., Antimicrobial activity of resin acid derivatives. *Applied Microbiology and Biotechnology* **2006,** 72, 430-436.

38. Palmqvist, E.; Hahn-Hagerdal, B., Fermentation of includes hydrolysates. II: inhibitors and mechanisms of inhibition. *Bioresource Technology* **2000,** 74, 25-33.

39. *Biomass Analysis Technology Team Laboratory Analytical Procedure: Determination of Extractives in Biomass*; National Renewable Energy Lab, http://www1.eere.energy.gov/biomass/analytical_procedures.html, 2005.

40. Guss, L. S.; Kolthoff, I. M., Sulfur Dioxide as an Acid in Methanol. *Journal of the American Chemical Society* **1944,** 66, 1484-1488.

41. Gattow, G.; Behrendt, W., Methyl Hydrogen Carbonate. *Angewandte Chemie International Edition* **1972,** 11, (6), 534-535.

CHAPTER VI

CONCLUSIONS AND RECOMMENDATIONS

Interest in sustainable development has grown beyond the scientific community with increased public awareness of insecure oil supplies, climate change, and overall inadequate environmental stewardship. As researchers in chemical engineering, we can create technological solutions for many existing environmentally unfriendly processes, two of which are discussed in Chapters II and III. Perhaps more importantly, we have the skill set to revolutionize the biofuel industry and create affordable options for domestic fuel. Therefore, we recommend for future research not only ideas specific to the work presented here, but additional research ideas that may improve our ability to create cost-efficient biofuels.

In Chapter II, we present a solid solubility model capable of predicting qualitatively the solubility of complex solutes in a wide range of pure and mixed solvents. We show this model having several distinct advantages over models currently used, and we hope the work published here will increase awareness of the MOSCED model. There are several opportunities to use this model for future work, the most interesting of which is predicting melting point depressions in ionic liquids and solid mixtures. It has been shown that ionic liquids melt at much lower temperatures when exposed to modest CO_2 pressure, a phenomena that could be used to run reactions without solvents[1]. However, to test all the possible cation/anion pairs and determine each individual melting point depression would be extremely time consuming. MOSCED model parameters have been regressed for a few ionic liquids[2], but the lack of sufficient solubility data for ionic solids in general makes any type of modeling a challenge.

Therefore, experimental data are needed for the solubilities of ionic solids (as most ionic liquids are unless they melt below room temperature) in several different solvents to regress MOSCED parameters. Once parameters are established, melting point depressions in CO_2 and other gases as well as solubility in solvent mixtures can be predicted. Furthermore, solubility measurements may be able to establish a pattern for certain cations and anions that would aid in ionic liquid pair selection. Another application for the MOSCED model is in the design of solid separations, most specifically vanillin and syringaldehyde from the solvent mixture discussed in Chapter IV. Solubility data are being collected, and once parameters are regressed for both solids we hope to find the optimal solvent or solvent mixture for separation.

Chapter III reports phase behavior data that aids in the reaction design of fluorous biphasic systems where a CO_2 co-solvent is used to induce miscibility and improve reaction rate and catalyst recovery. In these systems, a fluorocarbon is used because it has significant miscibility with CO_2; however, fluorocarbons have environmental disadvantages and high costs that make them poor targets for use in industrial applications[3, 4]. Therefore, researchers are continuing to find other CO_2-philic chemicals that are benign and cheap in nature, and can be used as either solvents or catalysts[5-7]. Poly(ethylene glycol) (PEG) has been investigated as a possible solvent for CO_2 systems[8, 9], and we report some phase behavior data for PEG and CO_2 in Appendix F. As other chemicals arise that show promise in these applications, more phase behavior will need to be performed to accurately assess the miscibility of the systems.

Chapters IV and V report preliminary work on using novel solvents in different applications as a way to improve the pulp and paper industry and create a commercially

viable biorefinery, and most of our future recommendations stem from this work. In Chapter IV, we developed a process for the extraction of vanillin and syringaldehyde from organosolv lignin using GX-methanol. We did a preliminary economic analysis on these data to determine if work should be continued, and the results were positive.

We outlined two industries in which this process could be implemented, the biorefinery and the pulp and paper mill. If this process is to be developed for implementation in the pulp and paper mill, determining whether vanillin and syringaldehyde can be purified from lignin after treatment with white liquor is essential. Treating wood with white liquor impregnates the lignin with sulfur that has proven difficult to remove downstream[10]. Furthermore, more experimental data will need to be taken using kraft black liquor as the starting material instead of organosolv lignin. It is important to see what additional challenges this may add, as well as determining if lignin removal from black liquor as described in the literature can be combined with our process[11, 12].

As discussed in Chapter IV, if more experimental data are to be collected a new analytical technique is needed. For the preliminary analysis, a gas chromatography/mass spectrometry (GM-MS) was used to determine vanillin and syringaldehyde concentrations, and the lignin concentrations were determined gravimetrically. Although these methods gave satisfactory preliminary results, the error was large and the lignin clogged the liner of the GC-MS several times further reducing the accuracy of our results. Several techniques have been described in the literature, with the most popular for lignin in biomass samples being pyrolysis-GC-MS (where the sample is heated to high temperatures in the absence of air to remove volatile gases and char) combined with

NMR for full characterization[13, 14]. Additionally, Kakola et al. analyzed for aliphatic acids in black liquor using high-performance liquid chromatography-mass spectrometry(LC-MS)[15]. A similar technique, using either pyrolysis–GC-MS or LC-MS, should be developed for future work in valuable chemical determination and quantification from biomass.

Assuming black liquor as a feedstock produces similar results to that of organosolv lignin, and a cost-effective separation and purification technique is established, an in-depth economic analysis combined with pilot scale process design would need to be performed. This will determine whether the addition of this process into the pulp and paper industry will result in profit gain. Furthermore, this analysis should indicate whether a process like this could be beneficial in a biorefinery.

While completing this work it became apparent how similar the potential products from a pulp and paper mill and a lignocellulosic biorefinery actually are. Figure 6-1 shows a comparison between the two. The paper mill is an established industry with the main goal of converting cellulose to paper. However, many of the waste products from the paper mill have potential to be used as biofuels and/or valuable side product (as indicated in red italics). The lignocellulosic biorefinery is still a research concept, and it seems the biggest focus right now is converting cellulose and hemicellulose into bio-ethanol. Just like the paper mill, however, the lignocellulosic biorefinery has the potential to produce a wide range of valuable fuels and side products. It is important when researching in this area to consider both industries; for some technologies that may not work for the biorefinery could be beneficial to the pulp and paper plant, and vice-versa. From this work, it may not be practical to separate vanillin and syringaldehyde from

black liquor because of the sulfur content, but they could be excellent side products from lignin processed in the biorefinery.

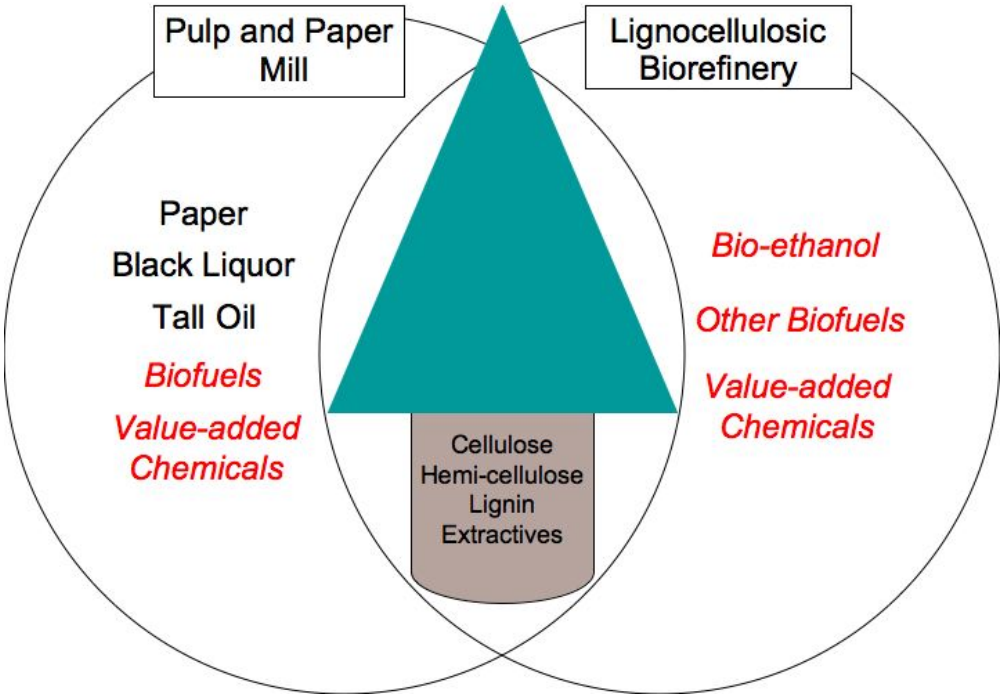

Figure 6-1. Comparison between the paper mill and the lignocellulosic biorefinery: products in black, currently produced; products in red italics, research goals.

So how can we turn this renewable waste into valuable products? The answer to this is in sustainable research, and we recommend several ways to contribute. Besides lignin, hemicellulose is a waste product in the pulp and paper mill that could be used for valuable products. Since hemicellulose is made up of sugars, the obvious use would be to covert those sugars to alcohols for fuel[16]; however, once the wood is treated with white liquor, the hemicellulose is degraded into low value acids and conversion is impractical[17]. Therefore, a pretreatment technique is needed to remove hemicellulose from wood chips before kraft pulping. As long as cellulose is not hydrolyzed during pretreatment, this technology would not only improve profit by producing bio-ethanol but could also

improve the overall efficiency of the pulping process by reducing cook times, enhancing liquor penetration, and increasing pulp production by reducing waste loads to the recovery furnace[17]. We recommend the use of CO_2-enhanced nearcritical water (NCW) for this pretreatment. Although there have been some attempts in the past to use very hot water for pretreatment, large amounts of water consumption and sugar degradation at high temperatures have limited the effectiveness of this process[18]. The addition of CO_2 has been demonstrated to accelerate the acid-catalyzed reaction in hot water,[19, 20] and of course it is easily and benignly reversed by depressurization. Thus, the addition of CO_2 would provide stronger acid at lower temperatures, which could aid in the breakdown of hemicellulose without causing sugar degradation. Along with CO_2-enhanced NCW, other novel solvent systems should be tested as possible pretreatments for pre-pulped wood. Some possibilities include work already being done in our research group with supercritical CO_2/organic co-solvent mixtures, the novel solvent piperylene-sulfone[21], and some unique deep-eutectic systems.

Once hemicellulose is removed from the wood via pretreatment it could be used for the production of many products besides just bio-ethanol. Several literature reviews name many platform molecules and biomaterials that could be derived from hemicellulose[22-25]. These include, but are not limited to, hydrogels, hydroxymethylfurfural (HMF), levullinic acid, furfural, Nylon 6, and lactic acid. As more interest develops in renewable plastics, markets for these bio-based chemicals will growth. Furthermore, this same pretreatment technique could easily be applied to a biorefinery. We described one pretreatment technique in Chapter V, and although the results were not promising for bio-ethanol production, they did cultivate ideas for other novel pretreatment techniques. When testing

new pretreatment techniques for use in a biorefinery it is imperative that we investigate the effect our pretreatment has on the hydrolysis and fermentation of cellulose[26]. We recommend combining any pretreatment with the final two steps for conversion into ethanol to ensure adequate yields and reactions rates. Even a pretreatment that does not show promise (like GX-methanol in Chapter V) may still increase the yield of bio-ethanol by removing extractives, and may be used as a preliminary pretreatment step for valuable chemical production. We recommend collaboration with a research group that is well versed in bio-ethanol fermentation.

In Chapter IV we speculated that removing a 15 to 25% slipstream of black liquor would be sufficient to extract the valuable chemicals vanillin and syringaldehyde from lignin. The literature states that removing up to 42 % of the black liquor waste stream would have a negligible effect on the heat duty from the recovery furnace[12], and they assume that the lignin removed (or remaining after valuable chemical extract in this case) could be sold as biofuel feedstock. This is an assumption because lignin is not yet used as a fuel other than with on-site combustion, but there are several research groups looking into ways to use lignin's natural energy in a more productive way. Some of these include pyrolysis and/or gasification into biohydrogen[27, 28], and gasification into syngas to be used in the Fischer-Tropsch synthesis of renewable diesel[29-31]. Furthermore, lignin also has uses as valuable chemicals beyond vanillin and syringaldehyde including blended polymers and resins[32, 33]. It is imperative that we combine the chemistry behind lignin to biofuel or biomaterials with the separation techniques described in this work. Also, when developing pretreatment techniques we recommend considering how they may effect the removal of lignin. Removing lignin prior to kraft pulping, as previously described with

hemicellulose, would greatly increase the profit margin on these biofuels and biomaterials by lowering the sulfur content.

One last pulp and paper product not yet discussed is tall oil, which could have the largest impact on profitability for the paper mill, especially those located in the southeastern United States. Tall oil is produced from the resinous materials in wood (mostly pine), which is converted into sodium soaps during kraft cooking. As black liquor is evaporated before burning in the recovery furnace it is also skimmed to remove these soaps. The soaps are either sold as is, or sent thru an acidulation reaction to reverse the saponification and create crude tall oil[34]. Crude tall oil from the southern United States consists of approximately 46 % resin acids, 40 % fatty acids, and 14% neutral products (unsaponifiable hydrocarbons and long chain alcohols)[34]. The pulp and paper industry produces approximately 140 million gallons/year of tall oil, and although some can be sold for various applications, in the early 90's mills started burning excess tall oil to save storage costs due to more supply then demand[35]. In the mid-80's crude tall oil was tested for use in the automobile industry, but deposits in the combustion chamber and fuel pump wear caused that idea to be abandoned[36]. However, research continues to find more profitable uses for tall oil. Figure 6-2 breaks down all the possible uses for tall oil, the most predominate being for the production of biodiesel.

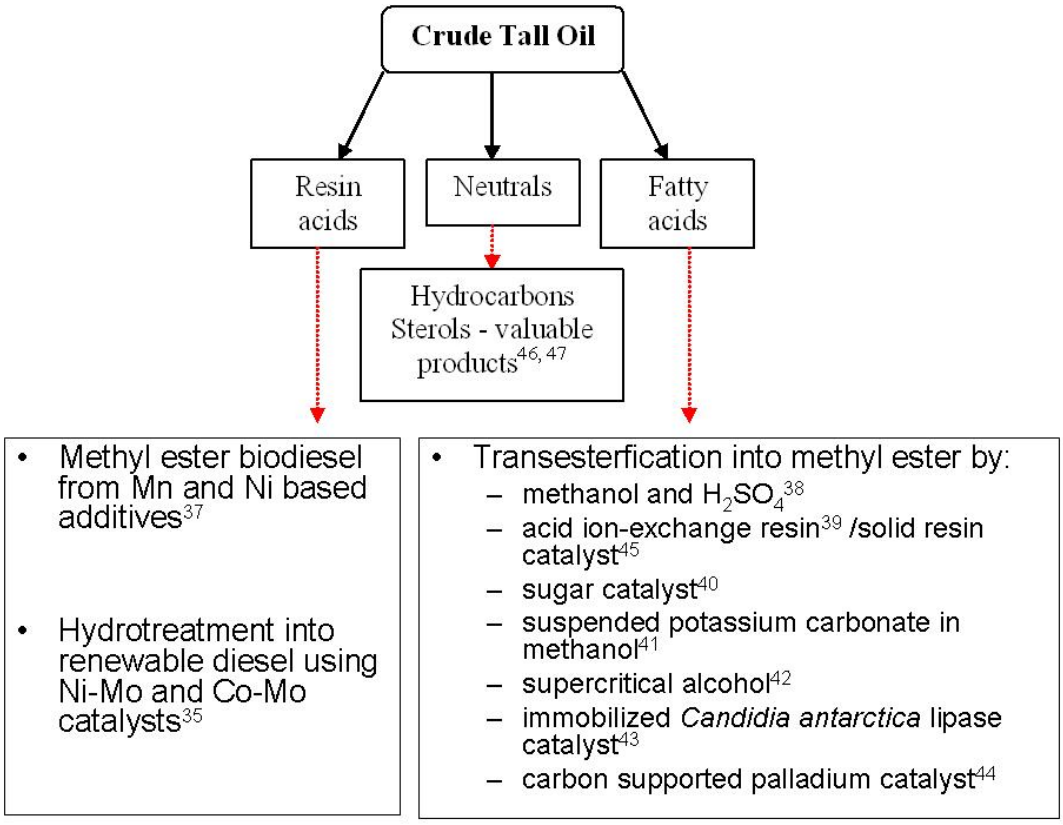

Figure 6-2. Tall oil components and promising product streams.

The largest barrier to producing these valuable products seems to be the separation of the tall oil components. Although some work is being done on creating biodiesel from the entire mixture[36], it seems a cost-effective separation combined with several simple processing streams would be more practical and lucrative. A review by J. M. F. Nogueira outlined research done in the area of tall oil separation, and he concluded that industrially only distillation under high vacuum is practical (which is already done)[46]. He mentioned positive preliminary results were obtained when extracting tall oil with supercritical CO_2 [47], which leads to the recommendation of using our novel solvent systems, like GXLs, for the separation of tall oil. Whether we combine the separation of tall oil with the removal of lignin from black liquor, or look at pre-treatment techniques

that remove the tall oil components before the cooking process (which we show preliminary results for in Chapter V), our process could provide innovation to the pulp and paper industry in a variety of ways. Once preliminary work is preformed on tall oil separation, an in-depth process design will need to be developed to determine exactly how to efficiently combine all or some of the processes discussed in this work.

In conclusion, we recommend the following to improve production of biofuels and biomaterials from the biorefinery and pulp and paper mill:

- research the use of novel pretreatment techniques for the removal of hemicellulose and/or from pre-pulped wood,
- research novel pretreatment techniques for their use in a lignocellulosic biorefinery by testing their effect on bio-ethanol fermentation,
- apply novel solvent separations to tall oil for the product of biodiesel and valuable products, and
- combine our work with processes being developed to form biofuels and biochemicals from lignin, hemicellulose, and tall oil components.

With collaboration, innovative science, and attention to sustainable development, chemical engineers have the power to greatly influence the future of our country and environment. The work presented here will not solve any problem alone, but together with other research ideas and a positive overall vision we are hopeful that the future will bring sustainable solutions to many environmental issues.

References

1. Scurto, A. M.; Leitner, W., Expanding the useful rand of ionic liquids: met ling point depression of organic salts with carbon dioxide for biphasic catalytic reactions. *Chemical Communications* **2006**, 3681-3683.

2. Lazzaroni, M. J.; Bush, D.; Eckert, C. A.; Frank, T. C.; Gupta, S. K.; Olson, J. D., Revision of MOSCED Parameters and Extension to Solid Solubility Calculations. *Industrial & Engineering Chemistry Research* **2005,** 44, (11), 4075-4083.

3. Ravishankara, A. R.; Solomon, S.; Turnipseed, A. A.; Warren, R. F., Atmospheric lifetimes of long-lived halogenated species. *Science* **1993,** 259, 194-199.

4. Cavalli, F.; Glasius, M.; Hjorth, J.; Rindone, B.; Jensen, N. R., Atmospheric lifetimes, infrared spectra and degradation products of a series of hydrofluoroethers. *Atmospheric Environment* **1998,** 32, (21), 3767-3773.

5. Fan, X.; Potluri, V. K.; Mcleod, M. C.; Wang, Y.; Liu, J.; Enick, R. M.; Hamilton, A. D.; Roberts, C. B.; Johnson, J. K.; Beckman, E. J., Oxygenated Hydrocarbon Ionic Surfactants Exhibit CO_2 Solubility. *Journal of the American Chemical Society* **2005,** 127, 11754-11762.

6. Alblan, C. D.; Sheppard, D.; Beckman, E. J.; Olmstead, M. M.; Jessop, P. G., Solubility of several analogues of triphenylphosphine in carbon dioxide. *Green Chemistry* **2005,** 7, 590-594.

7. Sarbu, T.; Styranec, T. J.; Beckman, E. J., Design and Synthesis of Low Cost, Sustainable CO_2-philes. *Industrial & Engineering Chemistry Research* **2000,** 39, 4678-4683.

8. Heldebrant, D. J.; Jessop, P. G., Liquid Poly(ethylene glycol) and Supercritical Carbon Dioxide: A Benign Biphasic Solvent System for Use and Recycling of Homogeneous Catalysts. *Journal of the American Chemical Society* **2003,** 125, 5600-5601.

9. Hou, Z.; Theyssen, N.; Brinkman, A.; Leitner, W., Biphasic Aerobic Oxidation of Alcohols Catalyzed by Poly(ethylene glycol)-Stabilized Palladium Nanoparticles in Supercritical Carbon Dioxide. *Angew. Chem. Int. Ed.* **2005,** 44, 1346-1349.

10. Moosavifar, A.; Sedin, P.; Brelid, H.; Theliander, H., Modification of precipitated kraft lignin through the addition of calcium-reduction of SO_2 emission. *Nordic Pulp and Paper Research* **2006,** 21, (4), 493-495.

11. Olsson, M. R.; Axelsson, E.; Berntsson, T., Exporting lignin or power from heat-integrated kraft pulp mills: A techno-economic comparison using model mills. *Nordic Pulp and Paper Research* **2006,** 21, (4), 476-484.

12. Axelsson, E.; Olsson, M. R.; Berntsson, T., Increased capacity in kraft pulp mills: Lignin separation and reduced steam demand compared with recovery boiler upgrade. *Nordic Pulp and Paper Research* **2006,** 21, (4), 485-492.

13. del Rio, J. C.; Gutierrez, A.; Martinez, A. T., Identifying acetylated lignin units in non-wood fibers using pyrolysis-gas chromatography/mass spectrometry. *Rapid Communications in Mass Spectrometry* **2004,** 18, 1181-1185.

14. Ralph, J.; Hatfield, R. D., Pyrolysis-GC-MS Characterization of Forage Materials. *Journal of Agriculture and Food Chemistry* **1991,** 39, 1426-1437.

15. Kakola, J.; Alen, R.; Pakkanen, H.; Matilainen, R.; Lahti, K., Quantitative determination of the main aliphatic carboxylic acids in wood kraft black liquors by high-performance liquid chromatography- mass spectrometry. *Journal of Chromatography A* **2007,** 1139, 263-270.

16. Thorp, B., Biorefinery Offers Industry Leaders Business Model for Major Change. *Pulp and Paper* **2005**, 35-39.

17. Ragauskas, A. J.; Nagy, M.; Kim, D. H.; Eckert, C. A.; Hallett, J. P.; Liotta, C. L., From wood to fuels: Integrating biofuels and pulp production. *Industrial Biotechnology* **2006,** 2, (1), 55-65.

18. Liu, C.; Wyman, C., Partial flow of compressed-hot water through corn stover to enhance hemicellulose sugar recovery and enzymatic digestibility of cellulose. *Bioresource Technology* **2005,** 96, 1978-1985.

19. Hunter, S. E.; Savage, P. E., Acid-Catalyzed Reactions in Carbon Dioxide-Enriched High-Temperature Liquid Water. *Industrial & Engineering Chemistry Research* **2003,** 42, (2), 290-294.

20. Hunter, S. E.; Ehrenberger, C. E.; Savage, P. E., Kinetics and Mechanism of Tetrahydrofuran Synthesis via 1,4-Butanediol Dehydration in High-Temperature Water. *Journal of Organic Chemistry* **2006,** 71, (16), 6229-6239.

21. Vinci, D.; Donaldson, M.; Hallett, J. P.; John, E. A.; Pollet, P.; Thomas, C. A.; Grilly, J. D.; Jessop, P. G.; Liotta, C. L.; Eckert, C. A., Piperylene sulfone: a labile and recyclable DMSO substitute. *Chemical Communications* **2007,** 14, 1427-1429.

22. Clark, J. H.; Budarin, V.; Deswarte, F. E. I.; Hardy, J. J. E.; Kerton, F. M.; Hunt, A. J.; Luque, R.; Macquarrie, D. J.; Milkowski, K.; Rodriguez, A.; Samuel, O.; Tavener, S. J.; White, R. J.; Wilson, A. J., Green chemistry and the biorefinery: a partnership for a sustainable future. *Green Chemistry* **2006,** 8, 853-860.

23. Gallezot, P., Process options for converting renewable feedstocks to bioproducts. *Green Chemistry* **2007,** 9, 295-302.

24. Kamm, B.; Kamm, M., Principles of biorefineries. *Applications of Microbiology and Biotechnology* **2004,** 64, 137-145.

25. Gabrielii, I.; Gatenholm, P., Preparation and Properties of Hydrogels Based on Hemicellulose. *Journal of Applied Polymer Science* **1998,** 69, 1661-1667.

26. Mosier, N.; Wyman, C.; Dale, B.; Elander, R.; Lee, Y. Y.; Holtzapple, M.; Ladisch, M., Features of promising technologies for pretreatment of lignocellulosic biomass. *Bioresource Technology* **2005,** 96, 673-686.

27. Dowaki, K.; Ohta, T.; Kasahara, Y.; Kameyama, M.; Sakawaki, K.; Mori, S., An economic and energy analysis on bio-hydrogen fuel using a gasification process. *Renewable Energy* **2007,** 32, 80-94.

28. Demirbas, A., Hydrogen Production from Biomass via Supercritical Water Extraction. *Energy Sources* **2005,** 27, 1409-1417.

29. Ledford, H., Making it up as you go along. *Nature* **2006,** 444, (7), 677-678.

30. Petrus, L.; Noordermeer, M. A., Biomass to biofuels, a chemical perspective. *Green Chemistry* **2006,** 8, 861-867.

31. Hamelinck, C. N.; Faaij, A. P. C.; den Uil, H.; Boerrigter, H., Production of FT transportation fuels from biomass; technical options, process analysis and optimisation, and development potential. *Energy* **2004,** 29, 1743-1771.

32. Tejado, A.; Pena, C.; Labidi, J.; Echeverria, J. M.; Mondragon, I., Physico-chemical characterization of lignins from different sources for used in phenol-formaldehyde resin synthesis. *Bioresource Technology* **2007,** 98, 1655-1663.

33. Kadla, J. F.; Kubo, S., Poly(Ethylene Oxide)/Organosolv Lignin Blends: Relationship between Thermal Properties, Chemical Structure, and Blend Behavior. *Macromolecules* **2004,** 37, 6904-6911.

34. Smook, G. A., *Handbook for Pulp and Paper Technology*. 2nd ed.; Angus Wilde Publications: 1992.

35. Coll, R.; Udas, S.; Jacoby, W. A., Conversion of the Rosin Acid Fraction of Crude Tall Oil into Fuels and Chemicals. *Energy and Fuels* **2001,** 15, 1166-1172.

36. Sharma, R. K.; Bakhshi, N. N., Efficient utilization of waste tall oil from the kraft pulp industry. *Tappi Journal* **1990**, 175-180.

37. Keskin, A.; Guru, M.; Altiparmak, D., Biodiesel production from tall oil with synthesized Mn and Ni based additives: Effects of the additives on fuel consumption and emissions. *Fuel* **2007,** 86, 1139-1143.

38. Altiparmak, D.; Keskin, A.; Koca, A.; Guru, M., Alternative fuel properties of tall oil fatty acid methyl ester-diesel fuel blends. *Bioresource Technology* **2007,** 98, 241-246.

39. Tesser, R.; Di Serio, M.; Guida, M.; Nastasi, M.; Santacesaria, E., Kinetics of Oleic Acid Esterification with Methanol in the Presence of Triglycerides. *Industrial & Engineering Chemistry Research* **2005,** 44, 7978-7982.

40. Zong, M.-H.; Duan, Z.-Q.; Lou, W.-Y.; Smith, T. J.; Wu, H., Preparation of a sugar catalyst and its use for highly efficient production of biodiesel. *Green Chemistry* **2007,** DOI: 10.1039/b615447f.

41. Kurzin, A. V.; Evdokimov, A. N.; Pavlova, O. S.; Antipina, V. B., Esters of Sucrose and Tall Oil Fatty Acids. *Russian Journal of Applied Chemistry* **2007,** 80, (2), 344-245.

42. Warabi, Y.; Kusdiana, D.; Saka, S., Biodiesel Fuel from Vegetable Oil by Various Supercritical Alcohols. *Applied Biochemistry and Biotechnology* **2004,** 113-116, 793-801.

43. Watanabe, Y.; Pinsirodom, P.; Nagae, T.; Yamauchi, A.; Kobayashi, T.; Nishida, Y.; Takagi, Y.; Shimada, Y., Conversion of acid oil by-produced in vegetable oil refining to biodiesel fuel by immobilized *Candida antarctica* lipase. *Journal of Molecular Catalysis B: Enzymatic* **2007,** 44, 99-105.

44. Snare, M.; Kubickova, I.; Maki-Arvela, P.; Eranen, K.; Murizin, D. Y., Heterogeneous Catalytic Deoxygenation of Stearic Acid for Production of Biodiesel. *Industrial & Engineering Chemistry Research* **2006,** 45, 5708-5715.

45. Marchetti, J. M.; Miguel, V. U.; Errazu, A. F., Heterogeneous esterification of oil with high amounts of free fatty acids. *Fuel* **2007,** 86 , 906-910.

46. Nogueria, J. M. F., Refining and Separation of Crude Tall-Oil Components. *Separation Science and Technology* **1996,** 31, (17), 2307-2316.

47. Harvala, T.; Alkio, M.; Komppa, V., Extraction of Tall Oil with Supercritical Carbon Dioxide. *Chemical Engineering Research and Design* **1987,** 65, 386-389.

APPENDIX A

EXPERIMENTAL AND PREDICTED DATA FOR SOLID SOLUBILITY IN PURE AND MIXED SOLVENTS USING THE MOSCED MODEL WITH WILSON G^E PARAMETERS

Table A-1: Experimental and Regressed Solid-Liquid Equlibria for the given solutes in pure solvents at various temperatures.

Solvent	T (K)	x_1 (exp)	x_1 (fit)	Error (%)	Solvent	T (K)	x_1 (exp)	x_1 (fit)	Error (%)
Benzimidazole									
2-butanone	283	0.0217	0.0147	32.4	ethanol	283	0.0713	0.0257	63.9
2-butanone	298	0.0242	0.0263	-8.7	ethanol	298	0.0859	0.0426	50.4
2-butanone	313	0.0352	0.0446	-26.6	ethanol	313	0.0930	0.0676	27.3
acetonitrile	283	0.0055	0.0085	-53.5	ethyl acetate	283	0.0124	0.0055	55.7
acetonitrile	313	0.0304	0.0278	8.6	ethyl acetate	298	0.0140	0.0111	20.6
chloroform	283	0.0029	0.0022	25.1	ethyl acetate	313	0.0266	0.0212	20.2
chloroform	298	0.0044	0.0052	-17.5	heptane	283	0.0001	0.0000	63.3
chloroform	313	0.0077	0.0113	-47.0	heptane	298	0.0002	0.0002	14.5
cyclohexane	283	0.0000	0.0000	-1.2	heptane	313	0.0007	0.0005	19.0
cyclohexane	298	0.0002	0.0002	-17.3	isopropanol	283	0.0581	0.0225	61.2
dichloromethane	283	0.0040	0.0021	48.0	isopropanol	298	0.0754	0.0376	50.1
dichloromethane	298	0.0109	0.0049	55.1	isopropanol	313	0.0832	0.0602	27.7
dichloromethane	313	0.0119	0.0106	11.1	methanol	298	0.1375	0.0421	69.4
dioxane	283	0.0199	0.0201	-1.0	methanol	313	0.2453	0.0674	72.5
dioxane	313	0.0516	0.0565	-9.6	nitromethane	283	0.0058	0.0027	53.7
DMF	283	0.1497	0.0865	42.2	nitromethane	298	0.0074	0.0056	24.0
DMF	298	0.1864	0.1187	36.3	nitromethane	313	0.0100	0.0111	-10.8
DMF	313	0.2057	0.1568	23.8	toluene	283	0.0004	0.0004	-20.7

Solvent	T (K)	x_1 (exp)	x_1 (fit)	Error (%)	Solvent	T (K)	x_1 (exp)	x_1 (fit)	Error (%)
3-Nitrophthalimide									
2-butanone	283	0.0057	0.0026	54.6	DMF	298	0.1340	0.0853	36.3
2-butanone	298	0.0129	0.0054	58.1	DMF	313	0.2029	0.1067	47.4
2-butanone	313	0.0231	0.0104	55.0	ethanol	283	0.0015	0.0008	47.1
acetonitrile	283	0.0050	0.0045	9.5	ethanol	298	0.0017	0.0018	-9.1
acetonitrile	298	0.0058	0.0090	-55.2	ethanol	313	0.0038	0.0038	-1.1
acetonitrile	313	0.0104	0.0170	-63.2	ethyl Acetate	283	0.0083	0.0047	43.0
benzyl alcohol	298	0.0102	0.0028	72.5	ethyl Acetate	298	0.0090	0.0089	1.2
benzyl alcohol	313	0.0118	0.0057	51.6	ethyl Acetate	313	0.0125	0.0159	-27.5
chloroform	313	0.0010	0.0010	-1.0	isopropanol	283	0.0012	0.0006	49.8
dichloromethane	283	0.0009	0.0003	68.2	isopropanol	298	0.0011	0.0014	-33.3
dichloromethane	298	0.0023	0.0008	66.2	methanol	283	0.0021	0.0009	58.5
dichloromethane	313	0.0024	0.0019	19.8	methanol	298	0.0022	0.0019	12.4
dioxane	283	0.0073	0.0027	62.9	methanol	313	0.0074	0.0041	44.6
dioxane	298	0.0107	0.0056	47.7	nitromethane	283	0.0039	0.0012	68.9
dioxane	313	0.0214	0.0107	50.0	nitromethane	298	0.0049	0.0027	45.0
DMF	283	0.0882	0.0670	24.0	nitromethane	313	0.0088	0.0056	36.2

Solvent	T (K)	x_1 (exp)	x_1 (fit)	Error (%)	Solvent	T (K)	x_1 (exp)	x_1 (fit)	Error (%)
5 - fluoroisatin									
2-butanone	283	0.0065	0.0112	-72.4	ethanol	283	0.0038	0.0012	68.2
acetonitrile	283	0.0054	0.0029	45.8	ethanol	298	0.0042	0.0024	43.4
acetonitrile	298	0.0060	0.0057	5.0	ethanol	313	0.0056	0.0046	18.1
acetonitrile	313	0.0085	0.0106	-24.2	ethyl acetate	283	0.0085	0.0052	38.9
benzyl alcohol	298	0.0086	0.0069	20.1	ethyl acetate	298	0.0102	0.0094	7.5
chloroform	283	0.0016	0.0027	-69.0	ethyl acetate	313	0.0133	0.0162	-22.0
chloroform	313	0.0082	0.0101	-22.5	isopropanol	298	0.0030	0.0023	23.2
dichloromethane	283	0.0036	0.0027	25.5	isopropanol	313	0.0045	0.0045	-0.8
dichloromethane	298	0.0171	0.0055	67.9	methanol	283	0.0058	0.0011	81.1
dioxane	283	0.0188	0.0169	10.2	methanol	298	0.0065	0.0022	65.9
dioxane	298	0.0274	0.0272	0.6	methanol	313	0.0077	0.0042	45.2
dioxane	313	0.0426	0.0421	1.3	nitromethane	283	0.0073	0.0014	80.7
DMF	283	0.0434	0.0285	34.3	nitromethane	298	0.0050	0.0030	40.0
DMF	298	0.0718	0.0428	40.4	nitromethane	313	0.0086	0.0060	29.9
DMF	313	0.1076	0.0610	43.3					

Solvent	T (K)	x_1 (exp)	x_1 (fit)	Error (%)	Solvent	T (K)	x_1 (exp)	x_1 (fit)	Error (%)
2 -amino 5- nitrobenzophenone									
2-propanol	283	0.0006	0.0006	0.7	DMF	313	0.1092	0.1032	5.5
2-propanol	298	0.0012	0.0014	-21.2	ethanol	283	0.0006	0.0005	22.7
2-propanol	313	0.0042	0.0033	22.2	ethanol	298	0.0013	0.0012	9.5
benzonitrile	298	0.0529	0.0307	42.0	ethanol	313	0.0032	0.0028	13.5
benzyl alcohol	298	0.0170	0.0020	88.2	ethyl acetate	283	0.0223	0.0182	18.5
chlorobenzene	298	0.0059	0.0037	37.7	ethyl acetate	298	0.0307	0.0311	-1.2
chloroform	283	0.0072	0.0016	77.7	ethyl acetate	313	0.0474	0.0502	-5.9
chloroform	298	0.0077	0.0038	50.3	methanol	283	0.0006	0.0004	35.8
chloroform	313	0.0119	0.0086	27.5	methanol	298	0.0017	0.0009	44.2
dichloromethane	298	0.0380	0.0060	84.2	methanol	313	0.0015	0.0021	-42.6
dichloromethane	313	0.0426	0.0131	69.2	nitromethane	283	0.0101	0.0036	64.3
dioxane	283	0.0279	0.0280	-0.2	nitromethane	298	0.0190	0.0084	55.9
dioxane	298	0.0422	0.0429	-1.8	nitromethane	313	0.0223	0.0180	19.4
dioxane	313	0.0566	0.0637	-12.5	toluene	283	0.0021	0.0010	53.0
DMF	283	0.0618	0.0482	22.0	toluene	298	0.0022	0.0024	-11.4
DMF	298	0.0934	0.0724	22.5	toluene	313	0.0038	0.0055	-44.9

Table A-2: Experimental and Predicted Solid-Liquid Equlibria for the given solutes in mixed solvents at various temperatures.

Solvent 1	Solvent 2	Mole Fraction Solvent 1	283 K			298 K			313 K		
			x^{exp}	x^{pred}	% AD	x^{exp}	x^{pred}	% AD	x^{exp}	x^{pred}	% AD
Benzimidazole											
Ethanol	Ethyl Acetate	0	0.0124	0.0055	55.5	0.0140	0.0112	19.8	0.0266	0.0214	19.6
		0.25	0.0529	0.0166	68.7	0.0543	0.0281	48.3	0.0810	0.0461	43.1
		0.5	0.0726	0.0241	66.8	0.1097	0.0398	63.7	0.1126	0.0632	43.9
		0.75	0.0985	0.0269	72.7	0.1369	0.0444	67.5	0.1691	0.0701	58.6
		1	0.0713	0.0256	64.1	0.0859	0.0426	50.4	0.0930	0.0675	27.4
Dioxane	2-Butanone	0	0.0217	0.0148	31.9	0.0242	0.0264	-9.3	0.0352	0.0448	-27.2
		0.25	0.0256	0.0168	34.4	0.0451	0.0296	34.4	0.0457	0.0494	-8.1
		0.5	0.0261	0.0185	29.2	0.0488	0.0321	34.2	0.0536	0.0531	1.0
		0.75	0.0215	0.0196	8.8	0.0381	0.0339	11.1	0.0559	0.0555	0.7
		1	0.0199	0.0201	-1.2	0.0233	0.0346	-48.1	0.0516	0.0565	-9.6
Iso-propanol	Nitro-methane	0	0.0058	0.0024	59.3	0.0074	0.0050	31.5	0.0100	0.0100	-0.3
		0.25	0.0364	0.0091	75.1	0.0543	0.0164	69.8	0.0630	0.0284	54.9
		0.5	0.0724	0.0160	77.8	0.1017	0.0280	72.5	0.1069	0.0466	56.4
		0.75	0.0652	0.0210	67.8	0.0916	0.0359	60.8	0.0982	0.0584	40.5
		1	0.0581	0.0202	65.2	0.0754	0.0345	54.2	0.0832	0.0561	32.6
DMF	Chloro-form	0	0.0029	0.0023	23.3	0.0044	0.0053	-19.4	0.0077	0.0115	-49.4
		0.25	0.0370	0.0082	77.8	0.0514	0.0177	65.5	0.0620	0.0327	47.2
		0.5	0.0696	0.0242	65.3	0.0833	0.0429	48.6	0.1025	0.0680	33.6
		0.75	0.1085	0.0522	51.9	0.1365	0.0788	42.3	0.1512	0.1118	26.1
		1	0.1497	0.0869	42.0	0.1864	0.1190	36.2	0.2057	0.1571	23.6

Solvent 1	Solvent 2	Mole Fraction Solvent 1	283 K			298 K			313 K		
			x^{exp}	x^{pred}	% AD	x^{exp}	x^{pred}	% AD	x^{exp}	x^{pred}	% AD
3-Nitrophthalimide											
Ethanol	Ethyl Acetate	0	0.0083	0.0047	-75.9	0.0090	0.0088	-1.9	0.0125	0.0158	20.9
		0.25	0.0039	0.0088	56.0	0.0044	0.0154	71.5	0.0178	0.0255	30.2
		0.5	0.0032	0.0086	63.1	0.0039	0.0156	74.8	0.0111	0.0266	58.2
		0.75	0.0018	0.0056	67.9	0.0023	0.0108	79.1	0.0068	0.0194	64.8
		1	0.0015	0.0008	-91.2	0.0016	0.0018	6.6	0.0038	0.0038	0.4
Dioxane	2-Butanone	0	0.0057	0.0026	-120.0	0.0129	0.0054	-140.0	0.0054	0.0104	48.2
		0.25	0.0151	0.0028	-444.0	0.0262	0.0057	-358.4	0.0057	0.0110	48.0
		0.5	0.0124	0.0028	-333.9	0.0188	0.0059	-221.0	0.0059	0.0113	47.9
		0.75	0.0102	0.0028	-262.3	0.0096	0.0058	-64.9	0.0058	0.0112	48.0
		1	0.0073	0.0027	-171.3	0.0107	0.0056	-92.2	0.0056	0.0107	48.1
Iso-propanol	Nitro-methane	0	0.0039	0.0012	-233.1	0.0049	0.0027	-85.4	0.0088	0.0056	-56.4
		0.25	0.0048	0.0023	-108.9	0.0071	0.0050	-41.7	0.0183	0.0100	-82.6
		0.5	0.0037	0.0024	-55.6	0.0064	0.0052	-22.7	0.0146	0.0106	-37.9
		0.75	0.0014	0.0017	17.0	0.0031	0.0038	18.8	0.0078	0.0079	1.2
		1	0.0012	0.0006	-102.7	0.0010	0.0014	26.3	0.0017	0.0031	44.9
DMF	Chloro-form	0	0.000012	0.0001	91.2	0.000024	0.0004	93.8	0.0010	0.0010	0.0
		0.25	0.0064	0.0032	-95.9	0.0081	0.0064	-27.9	0.0162	0.0116	-39.4
		0.5	0.0373	0.0156	-138.6	0.0429	0.0247	-73.8	0.0587	0.0370	-58.6
		0.75	0.0443	0.0390	-13.4	0.0609	0.0534	-14.0	0.1133	0.0711	-59.3
		1	0.0882	0.0670	-31.7	0.1338	0.0853	-56.9	0.2029	0.1067	-90.3

Solvent 1	Solvent 2	Mole Fraction Solvent 1	283 K			298 K			313 K		
			x^{exp}	x^{pred}	% AD	x^{exp}	x^{pred}	% AD	x^{exp}	x^{pred}	% AD
5 - fluoroisatin											
Ethanol	Ethyl Acetate	0	0.0085	0.0052	38.9	0.0102	0.0095	7.0	0.0133	0.0163	-22.3
		0.25	0.0085	0.0069	19.2	0.0091	0.0121	-33.5	0.0109	0.0202	-84.3
		0.5	0.0085	0.0059	30.5	0.0100	0.0107	-6.3	0.0118	0.0182	-54.1
		0.75	0.0068	0.0038	44.4	0.0074	0.0071	4.4	0.0095	0.0125	-31.6
		1	0.0038	0.0012	68.1	0.0042	0.0024	42.7	0.0056	0.0046	17.4
Dioxane	2-Butanone	0	0.0065	0.0112	-73.2	0.0068	0.0188	-176.7	0.0154	0.0299	-94.9
		0.25	0.0124	0.0127	-2.3	0.0165	0.0209	-26.7	0.0208	0.0331	-59.1
		0.5	0.0154	0.0141	8.5	0.0212	0.0230	-8.8	0.0256	0.0361	-41.0
		0.75	0.0206	0.0155	24.8	0.0241	0.0252	-4.6	0.0296	0.0392	-32.4
		1	0.0188	0.0169	10.0	0.0274	0.0273	0.4	0.0426	0.0422	1.2
Iso-propanol	Nitro-methane	0	0.0073	0.0014	80.3	0.0050	0.0030	39.3	0.0086	0.0060	30.1
		0.25	0.0067	0.0023	65.9	0.0108	0.0047	56.7	0.0162	0.0089	44.9
		0.5	0.0139	0.0024	82.5	0.0161	0.0050	69.3	0.0175	0.0094	46.1
		0.75	0.0061	0.0021	66.5	0.0095	0.0042	56.0	0.0117	0.0079	32.0
		1	0.0027	0.0011	58.9	0.0030	0.0023	22.9	0.0045	0.0045	-0.1
DMF	Chloro-form	0	0.0016	0.0027	-66.2	0.0017	0.0053	-220.9	0.0082	0.0101	-22.0
		0.25	0.0082	0.0043	47.7	0.0114	0.0082	28.5	0.0158	0.0146	7.4
		0.5	0.0227	0.0086	61.9	0.0395	0.0151	61.7	0.0371	0.0250	32.7
		0.75	0.0379	0.0166	56.3	0.0534	0.0267	50.0	0.0761	0.0408	46.4
		1	0.0434	0.0286	34.2	0.0718	0.0428	40.3	0.1076	0.0611	43.2

Solvent 1	Solvent 2	Mole Fraction Solvent 1	283 K			298 K			313 K		
			x^{exp}	x^{pred}	% AD	x^{exp}	x^{pred}	% AD	x^{exp}	x^{pred}	% AD
2 -amino 5- nitrobenzophenone											
Ethanol	Ethyl Acetate	0	0.0223	0.0184	17.5	0.0307	0.0313	-1.8	0.0474	0.0505	-6.4
		0.25	0.0056	0.0126	-125.6	0.0095	0.0232	-143.6	0.0123	0.0400	-225.6
		0.5	0.0044	0.0059	-34.8	0.0082	0.0123	-49.6	0.0094	0.0236	-150.4
		0.75	0.0031	0.0021	33.1	0.0039	0.0047	-20.8	0.0059	0.0101	-71.5
		1	0.0006	0.0005	21.9	0.0013	0.0012	8.4	0.0032	0.0028	13.4
Dioxane	2-Butanone	0	0.0169	0.0337	-100.0	0.0220	0.0508	-130.5	0.0353	0.0741	-110.1
		0.25	0.0121	0.0348	-187.9	0.0235	0.0518	-119.9	0.0329	0.0747	-127.5
		0.5	0.0160	0.0343	-114.5	0.0242	0.0509	-110.4	0.0359	0.0734	-104.2
		0.75	0.0153	0.0321	-109.2	0.0292	0.0480	-64.4	0.0374	0.0698	-86.6
		1	0.0279	0.0282	-0.9	0.0422	0.0432	-2.4	0.0566	0.0640	-13.1
Iso-propanol	Nitro-methane	0	0.0101	0.0036	63.8	0.0190	0.0084	55.7	0.0223	0.0180	19.6
		0.25	0.0035	0.0046	-30.2	0.0053	0.0107	-101.5	0.0101	0.0225	-122.7
		0.5	0.0034	0.0038	-11.7	0.0050	0.0091	-83.2	0.0094	0.0198	-111.8
		0.75	0.0020	0.0023	-14.0	0.0043	0.0057	-30.6	0.0053	0.0128	-141.6
		1	0.0006	0.0006	-0.5	0.0012	0.0014	-23.9	0.0042	0.0034	20.7
DMF	Chloro-form	0	0.0072	0.0016	78.0	0.0077	0.0038	49.7	0.0119	0.0087	27.0
		0.25	0.0099	0.0053	46.7	0.0152	0.0111	26.8	0.0196	0.0216	-9.9
		0.5	0.0183	0.0136	25.8	0.0237	0.0251	-5.8	0.0338	0.0431	-27.5
		0.75	0.0412	0.0282	31.5	0.0475	0.0465	2.2	0.0569	0.0716	-25.7
		1	0.0618	0.0485	21.6	0.0934	0.0728	22.1	0.1092	0.1035	5.2

APPENDIX B

EXAMPLE CALCULATION FOR DETERMINING SOLID SOLUBILITY USING THE MOSCED MODEL WITH THE WILSON G^E EQUATION

Steps with Examples

1. Define solubility system

Solvent: 2-butanone

Solute: benzimidazole

Temperature: 298 K

2. Obtain pure component data for solute and solvent

MOSCED parameters	2-butanone (1)	benzimidazole(2)
λ $(J/cm^3)^{0.5}$	14.74	16.21
τ $(J/cm^3)^{0.5}$	6.64	4.22
α $(J/cm^3)^{0.5}$	0	12.15
β $(J/cm^3)^{0.5}$	9.7	11.12
q	1	0.9
v (cm^3/mol)	90.2	92
ΔH^{fus}(kJ/mol)	---	22.7
T^m(K)	---	444

3. Calculate infinite dilution activity coefficients using MOSCED

Calculation of γ_1^{∞}

$$R = 8.314 \frac{\text{J}}{\text{mol} \cdot \text{K}}$$

$$\alpha_1^T = \alpha_1 \left(293 / T \right)^{0.8} = 0$$

$$\beta_1^T = \beta_1 \left(293 / T \right)^{0.8} = 9.57$$

$$\tau_1^T = \tau_1 \left(293 / T \right)^{0.4} = 6.6$$

$$POL_1 = q^4\left(1.15 - 1.15\exp\left(-0.002337(\tau_1^T)^3\right)\right) + 1 = 1.56$$

$$\psi_1 = POL_1 + 0.002629\alpha_1^T\beta_1^T = 1.56$$

$$\xi_1 = 0.68\left(POL_1 - 1\right) + \left[3.24 - 2.4\exp\left(-0.002687\left(\alpha_1\beta_1\right)^{1.5}\right)\right]^{\left(293/T\right)^2} = 1.23$$

$$aa_1 = 0.953 - 0.002314\left((\tau_1^T)^2 + \alpha_1^T\beta_1^T\right) = 0.85$$

$$d_{21} = \ln\left(\frac{v_1}{v_2}\right)^{aa_1} + 1 - \left(\frac{v_1}{v_2}\right)^{aa_1} = -0.00014$$

$$\ln\gamma_1^{\infty} = \frac{v_1}{RT}\left[\left(\lambda_2 - \lambda_1\right)^2 + \frac{q_2^2q_1^2\left(\tau_2^T - \tau_1^T\right)^2}{\psi_2} + \frac{\left(\alpha_2^T - \alpha_1^T\right)\left(\beta_2^T - \beta_1^T\right)}{\xi_2}\right] + d_{21} = 0.36$$

$$\gamma_1^{\infty} = 1.43$$

Calculation of γ_2^{∞}

$$\alpha_2^T = \alpha_2\left(293/T\right)^{0.8} = 11.99$$

$$\beta_2^T = \beta_2\left(293/T\right)^{0.8} = 10.97$$

$$\tau_2^T = \tau_2\left(293/T\right)^{0.4} = 4.19$$

$$POL_2 = q^4\left(1.15 - 1.15\exp\left(-0.002337(\tau_2^T)^3\right)\right) + 1 = 1.12$$

$$\psi_2 = POL_2 + 0.002629\alpha_2^T\beta_2^T = 1.47$$

$$\xi_2 = 0.68\left(POL_2 - 1\right) + \left[3.24 - 2.4\exp\left(-0.002687\left(\alpha_2\beta_2\right)^{1.5}\right)\right]^{\left(293/T\right)^2} = 3.16$$

$$aa_2 = 0.953 - 0.002314\left((\tau_2^T)^2 + \alpha_2^T \beta_2^T\right) = 0.62$$

$$d_{12} = \ln\left(\frac{v_2}{v_1}\right)^{aa_2} + 1 - \left(\frac{v_2}{v_1}\right)^{aa_2} = -7.4 \cdot 10^{-5}$$

$$\ln \gamma_2^{\infty} = \frac{v_2}{RT}\left[(\lambda_1 - \lambda_2)^2 + \frac{q_1^2 q_2^2 \left(\tau_1^T - \tau_2^T\right)^2}{\psi_1} + \frac{\left(\alpha_1^T - \alpha_2^T\right)\left(\beta_1^T - \beta_2^T\right)}{\xi_1}\right] + d_{12} = 0.65$$

$$\gamma_2^{\infty} = 1.91$$

4. Calculate Wilson parameters from predicted infinite dilution activity coefficients

Solve the Wilson equation for two unknown interaction parameters.

$$\ln \gamma_1^{\infty} = 1 - \ln \Lambda_{12} - \Lambda_{21} = 0.36$$

$$\ln \gamma_2^{\infty} = 1 - \ln \Lambda_{21} - \Lambda_{12} = 0.65$$

Solving for Λ_{12} and Λ_{21} yields

$$\Lambda_{12} = 1.28$$

$$\Lambda_{21} = 0.396$$

5. Calculate solubility using Wilson equation and ideal solubility

Solve for x_2 in

$$x_2 \gamma_2 = x_2^{ideal}$$

where

$$\ln \gamma_2 = -\ln(x_2 + \Lambda_{21} x_1) - x_1\left(\frac{\Lambda_{12}}{x_1 + \Lambda_{12} x_2} - \frac{\Lambda_{21}}{\Lambda_{21} x_1 + x_2}\right) \text{ and}$$

$$x_2^{ideal} = \exp\left[\frac{-\Delta H_{fus}}{RT_m}\left(\frac{T_m}{T} - 1\right)\right]$$

$$x_2^{ideal} = 0.04854$$

Solution is x_2=0.027 and γ_2=1.79

APPENDIX C

SOLUBILTY DATA FOR SOLIDS IN MIXED SOLVENTS COMPARED TO PREDICTIONS BY THE MOSCED MODEL WITH WILSON G^E PARAMETERS

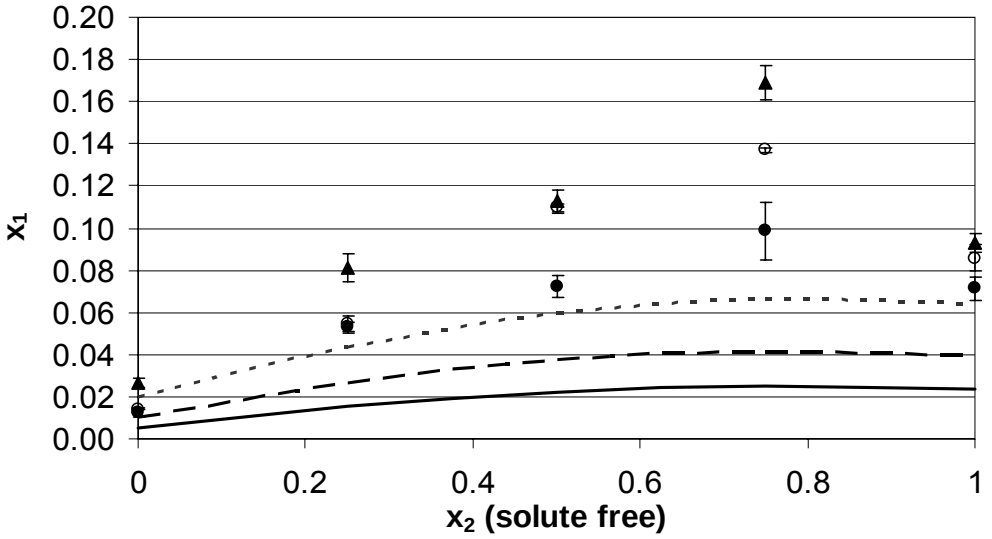

Figure C-1. Benzimidazole (1) solubility in mixtures of ethanol(2) and ethyl acetate (3): ●, 283 K; ○, 298 K;▲, 313 K; this work; lines predicted with MOSCED + Wilson.

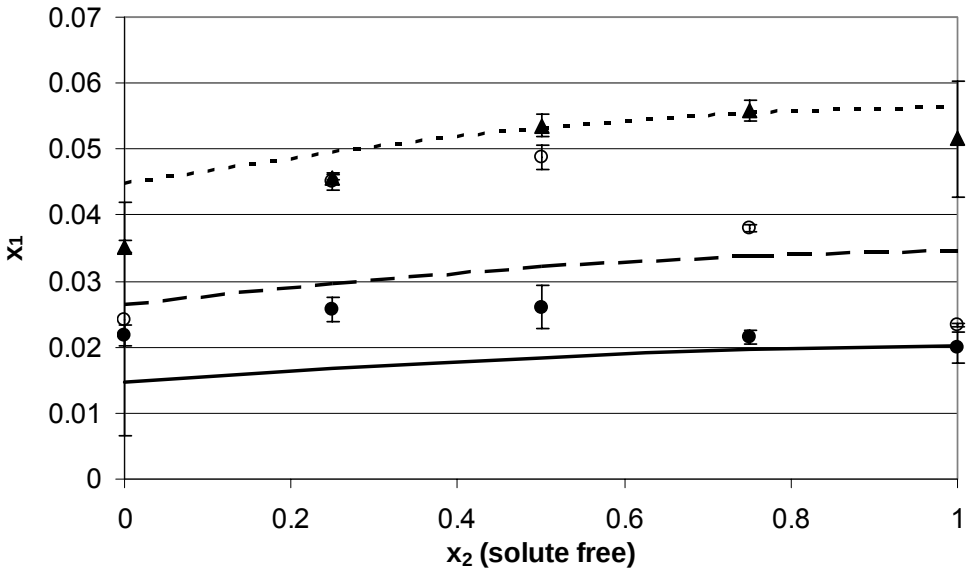

Figure C-2. Benzimidazole (1) solubility in mixtures of dioxane (2) and 2-butanone (3): ●, 283 K; ○, 298 K;▲, 313 K; this work; lines predicted with MOSCED + Wilson.

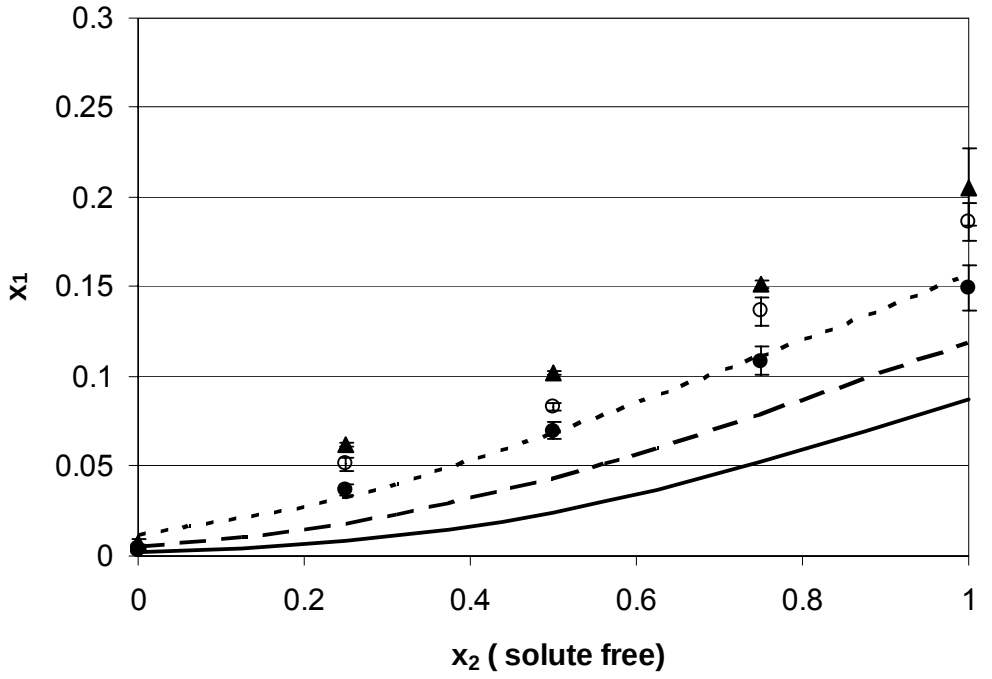

Figure C-3. Benzimidazole (1) solubility in mixtures of DMF(2) and chloroform (3): ●, 283 K; ○, 298 K;▲, 313 K; this work; lines predicted with MOSCED + Wilson.

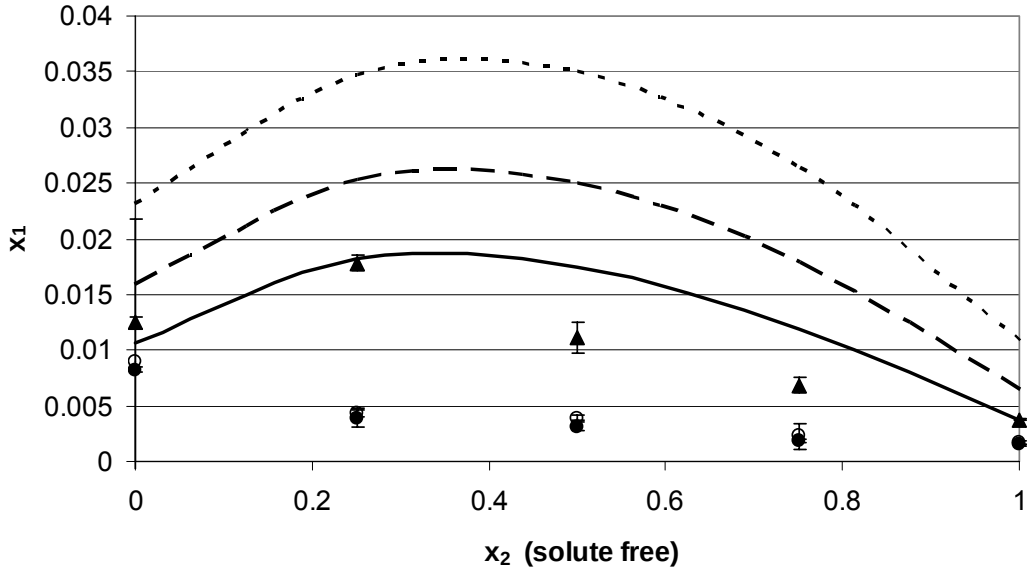

Figure C-4. 3-Nitrophthalimide (1) solubility in mixtures of ethanol(2) and ethyl acetate (3): ●, 283 K; ○, 298 K;▲, 313 K; this work; lines predicted with MOSCED + Wilson.

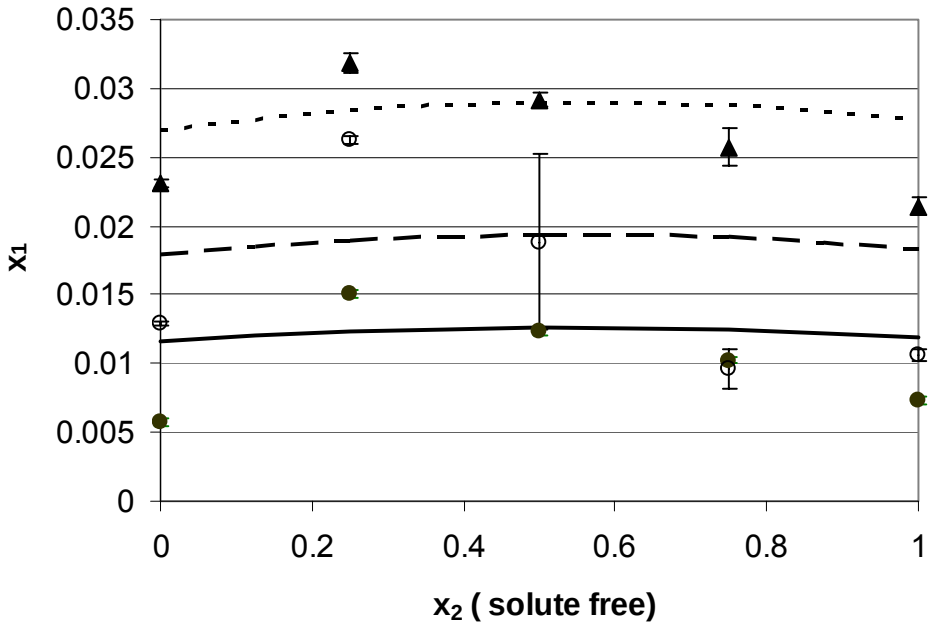

Figure C-5. 3-Nitrophthalimide (1) solubility in mixtures of dioxane (2) and 2-butanone (3): ●, 283 K; ○, 298 K;▲, 313 K; this work; lines predicted with MOSCED + Wilson.

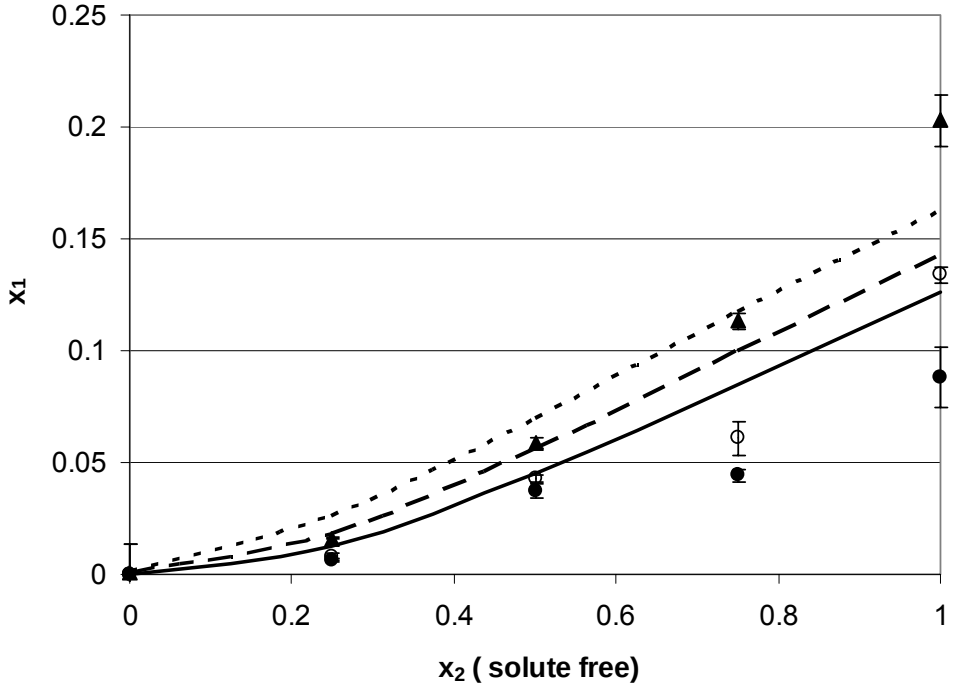

Figure C-6. 3-Nitrophthalimide (1) solubility in mixtures of DMF(2) and chloroform (3): ●, 283 K; ○, 298 K;▲, 313 K; this work; lines predicted with MOSCED + Wilson.

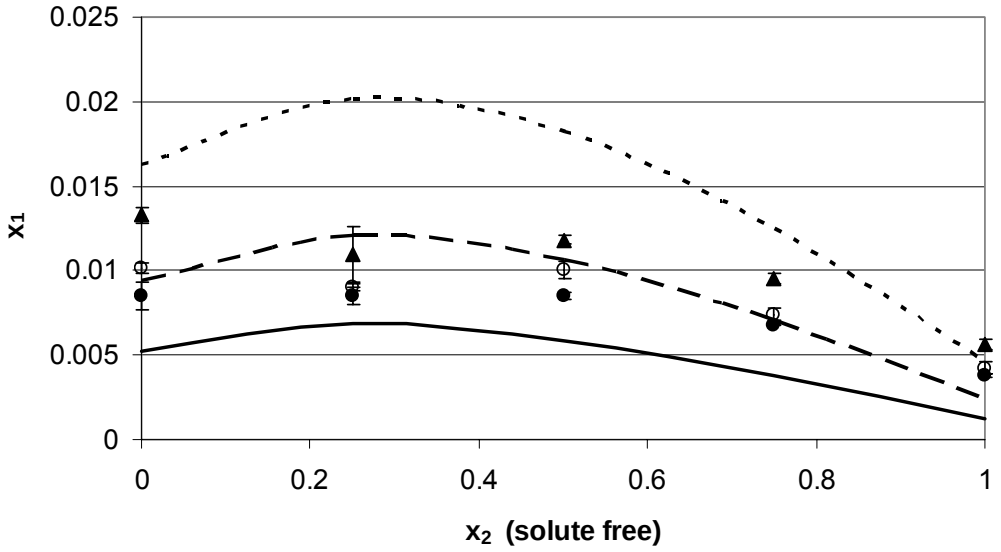

Figure C-7. 5-Fluoroisatin(1) solubility in mixtures of ethanol(2) and ethyl acetate (3): ●, 283 K; ○, 298 K;▲, 313 K; this work; lines predicted with MOSCED + Wilson.

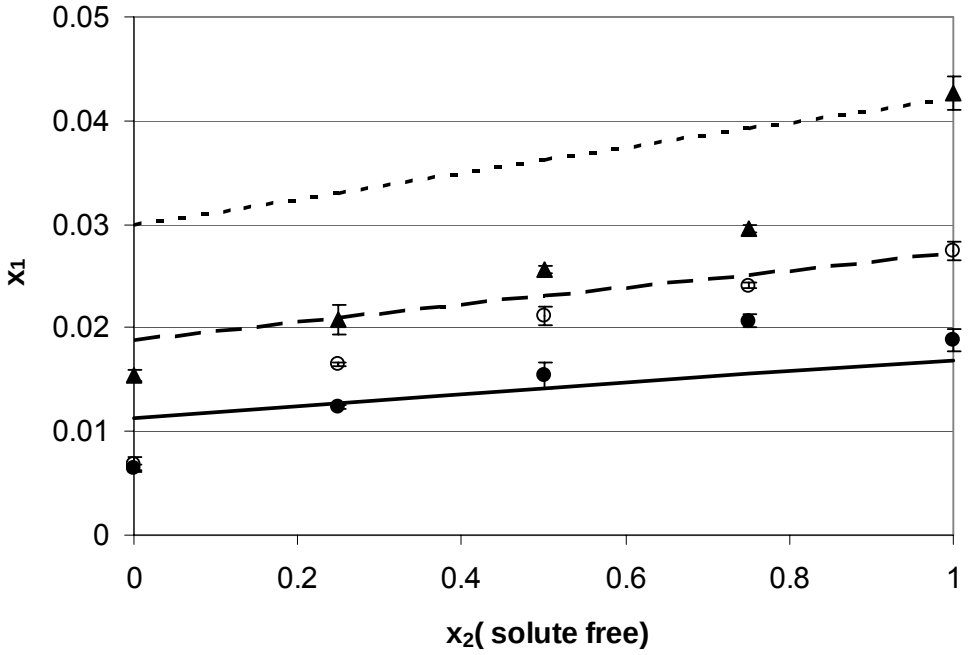

Figure C-8. 5-Fluoroisatin(1) solubility in mixtures of dioxane (2) and 2-butanone (3): ●, 283 K; ○, 298 K;▲, 313 K; this work; lines predicted with MOSCED + Wilson.

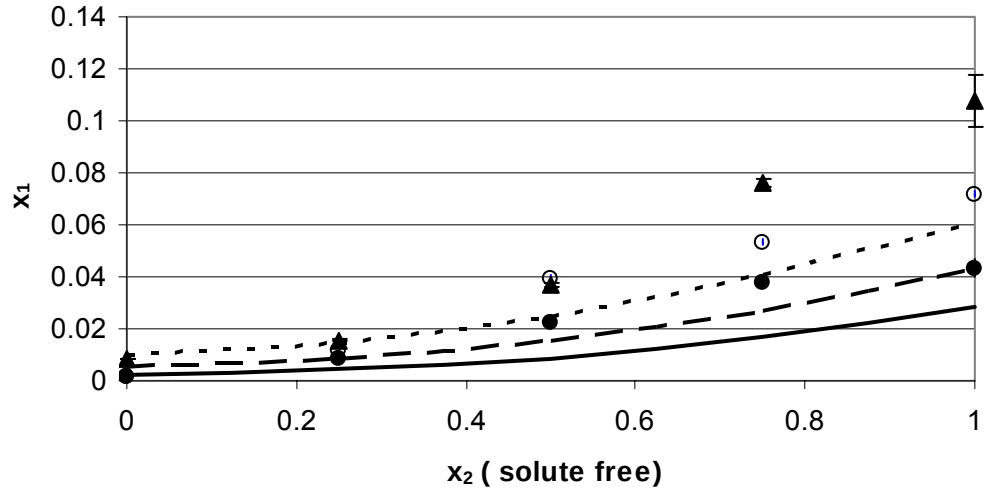

Figure C-9. 5-Fluoroisatin(1) solubility in mixtures of DMF (2) and chloroform (3): ●, 283 K; ○, 298 K;▲, 313 K; this work; lines predicted with MOSCED + Wilson.

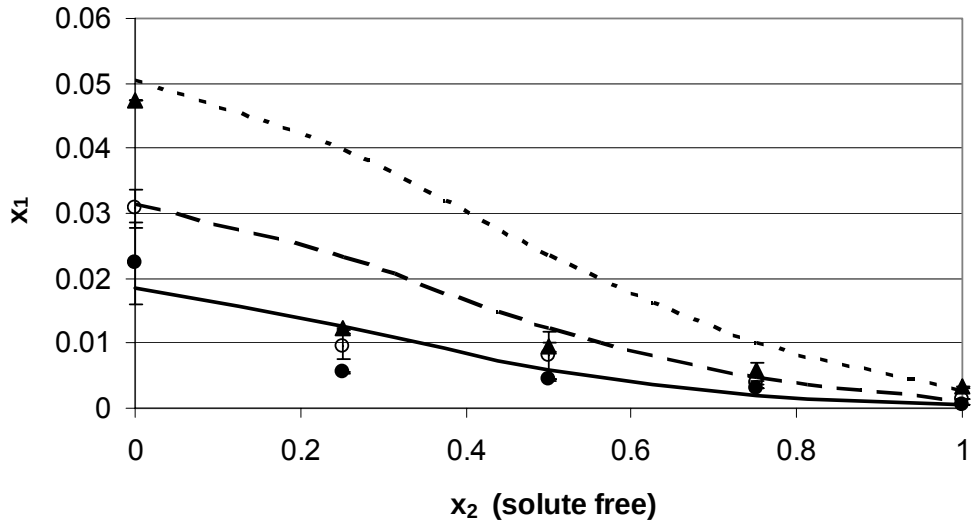

Figure C-10. 2-amino-5-nitrobenzophenone (1) solubility in mixtures of ethanol (2) and ethyl acetate (3): ●, 283 K; ○, 298 K;▲, 313 K; this work; lines predicted with MOSCED + Wilson.

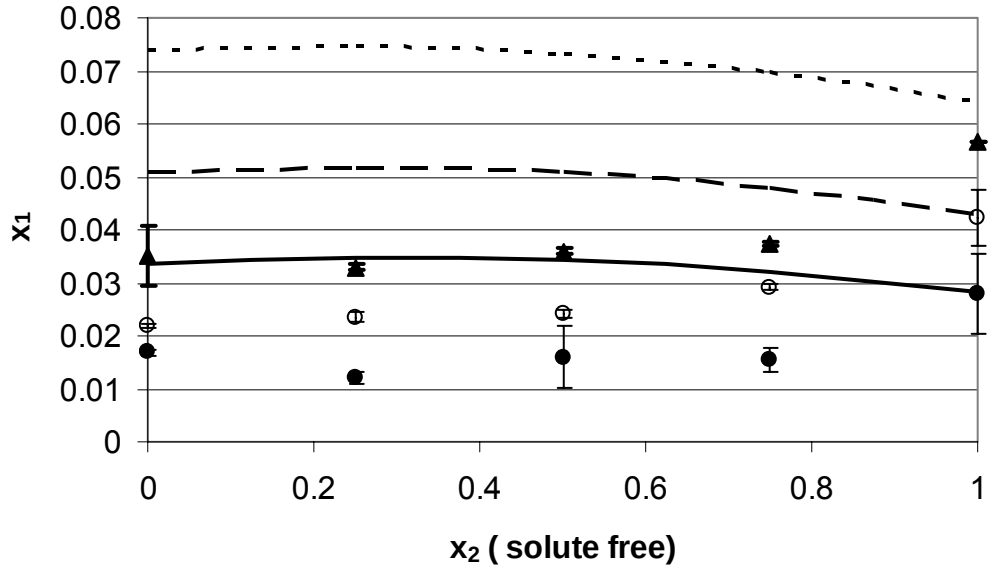

Figure C-11. 2-amino-5-nitrobenzophenone (1) solubility in mixtures of dioxane (2) and 2-butanone (3): ●, 283 K; ○, 298 K;▲, 313 K; this work; lines predicted with MOSCED + Wilson.

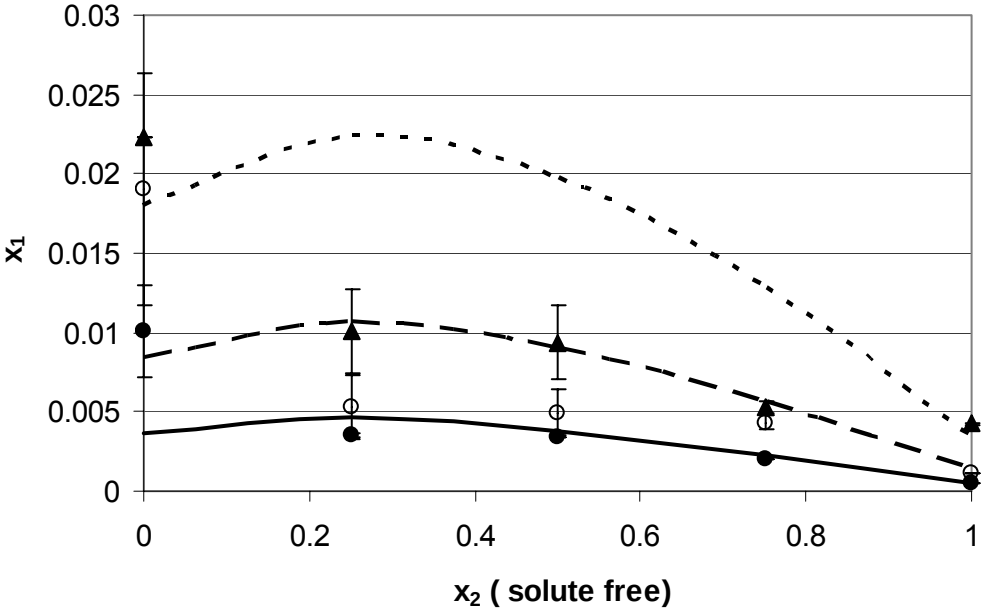

Figure C-12. 2-amino-5-nitrobenzophenone (1) solubility in mixtures of 2-propanol (2) and nitromethane (3): ●, 283 K; ○, 298 K;▲, 313 K; this work; lines predicted with MOSCED + Wilson.

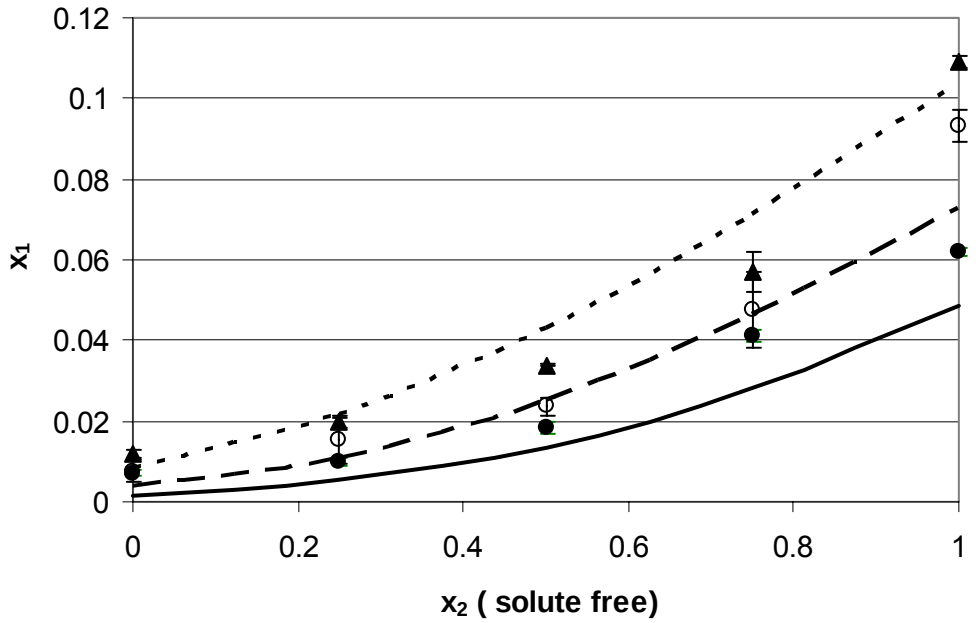

Figure C-13. 2-amino-5-nitrobenzophenone (1) solubility in mixtures of DMF (2) and chloroform (3): ●, 283 K; ○, 298 K;▲, 313 K; this work; lines predicted with MOSCED + Wilson.

APPENDIX D

SAFE ASSEMBLY AND OPERATING PROCEDURE FOR THE SAPPHIRE CELL HIGH PRESSURE APPARATUS

Safety Precautions

Safe Operating Conditions*

Max pressure: **2500 psia**.

Max temperature: **120 °C**

*As estimated upon initial testing. Conditions are a safe rule-of-thumb when using this equipment; other options may be available with a thorough screening process. If current sapphire cell is replaced, these conditions will need to be reevaluated.

Procedure for Handling Sapphire Cell

- **Always were gloves when handling the cell.** Never touch the cell with bare skin, as this can result in transfer of oils to the cell surface and may cause micro-cracks or scratches on the surface.
- **Inspect cell for any defects prior to use.** Make sure there are no chips or scratches in the cell surface prior to pressurization.
- **Never place cell on unprotected bench top.** Place towels or cloth on laboratory bench.

Pressure Testing

The cell should be periodically pressure tested. It is recommended that the cell is tested every four months or 12 pressure cycles. A pressure cycle is considered to be an experiment where the pressure is raised above atmospheric conditions and then depressurized back to atmospheric pressure. This procedure is written for a cell fit with a Swagelok R-series proportional relief valve (SS-RL3M4F4-BUMO). If a different type of relief valve is used, this procedure is no longer valid.

Pressure Testing Procedure

1. The cell is assembled as normal. The operating side is filled with a liquid, such that no vapor space is present, in other words liquid full. Typically water is the liquid of choice.

2. Raise the pressure to 2000 psia and allow the cell to rest at this pressure for approximately 1 hour.

3. Raise the pressure slowly to the relief valve pressure. At the relief valve pressure setting (2780 psia as of January 2007) the valve will unseat and reduce the pressure.

4. To ensure the relief valve reseats, raise the pressure again to a pressure below the relief pressure and watch for any pressure drop.

Assembly Procedures

Parts list

1 sapphire cell

1 stainless steel piston

2 stainless steel end caps

1 multi-port fitting

3 O-rings (size 210) (ethylene propylene, buna-N)

3 backing rings (116 size for piston; 2 8210 size for end caps)

4 aluminum spacer rods

4 stainless steel bolts, 4 nuts, 2 washers

1 Mounting bracket (UNI-STRUT)

For part specifications refer to Lazzaroni[1].

Assembly

1. Place 116 size backing ring and 210 size O-ring onto piston (EPR- ethylene propylene for polar). Place the backing ring flat edge down and the curved edge against the O-ring. Thread rod into back-side of piston and insert piston into cell. This may require some force to overcome the friction of the O-ring against the cell wall. Take caution that piston does not contact cell wall and only the O-ring is in contact with the cell wall.

2. Place 8210 size backing ring and 210 size O-ring onto bottom end cap. Insert bottom end-cap (the water-side and so still has the fitting in it) into cell, which is the side of the piston with the hole. Again, take care not to contact steel to the sapphire cell. A twisting motion may be helpful but make sure you are pushing evenly.

3. Place 8210 size backing ring and 210 size O-ring onto top end cap. Insert top end-cap into cell. Again, take care not to contact steel to the sapphire cell. A twisting motion may be helpful but make sure you are pushing evenly.

4. Align end-caps and insert two bolts through UNISTRUT mounting bracket into end cap alignment holes and through aluminum spacers and through opposing end cap. Loosely attach nuts.

5. Insert two remaining bolts through washers and end cap alignment holes, through aluminum spacers and through opposing end cap. Loosely attach nuts.

6. Tighten all four nuts evenly to 8-10 ft/lbs torque.

7. Mount assembled cell to bracket on rotating shaft. Attach all tubing, multi-port fitting to top end cap, and thermocouples.

Disassembly

1. Discharging: You can only run water back when the cell is under pressure so you need to do that before you discharge. Attach the funnel apparatus to the outside value. Position the cell upside down to avoid letting the vapor space out first. Open the value and let the organic and $C0_2$ go into the funnel.

2. Unhook the thermal couple, multi-port fitting, and tubing.

3. Undo the bolts on the underside on the cell until you can slide the cell off the uni-strut.

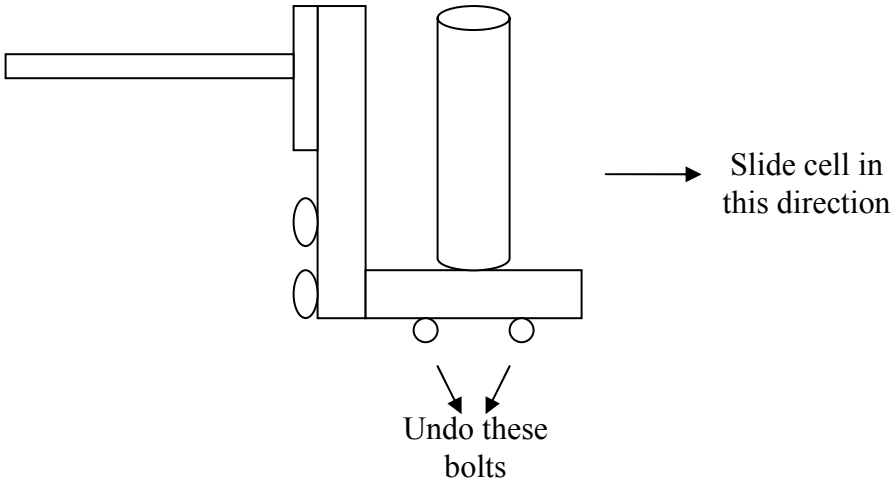

5. Loosen and remove the nuts on the spacer bolts.

6. Take out bolts, making sure the spacers are secure and not going to hit the cell. It may be necessary to get someone else to hold the spacers. If the screws will not come out easily you can hit them gently with a rubber mallet**.** Make sure you hit only the screws!!

7. Take off caps straight out and with out touching the cell. A slight twisting motion may help.

8. Take out the piston with the piston extraction rod.

9. Rinse off the cell with a solvent and place in its box until future use.

10. Flush the outside value and line that you discharged the cell thru with solvent and $C0_2$ before using the cell again.

Operating Procedure

1. Attach the water line loosely to the water side of the cell and run the ISCO pump until water begins to drip out of the tube to insure no air is in the water line. Attach the tubing and fill the cell with water.

2. Evacuate the cell by attaching the vacuum pump to the value attached directly to the top fitting. Make sure all other values are closed and all the fittings are tight to insure that you are actually pulling a vacuum in the cell. Run the pump for at least 30 minutes.

3. Add the organic phase thru the value attached directly to the top fitting. Squirt a little bit of organic into the value to make up for organic left in the syringe. Weigh the syringe before and after you insert the organic.

4. Adding $C0_2$: Attach the tube loosely to the outside valve. Open the valve on the $C0_2$ ISCO and run $C0_2$ thru the tube the get the air out. Attach the tube tightly and open the value on the $C0_2$ ISCO. Record the volume of $C0_2$ after the ISCO levels. Open the outside value letting the desired amount of $C0_2$ into the cell. Always mix the cell contents well when adding pressure to make sure you reach equilibrium.

Note. If you are running the piston down, run it up a small amount before recording pressure to avoid an incorrect reading caused by static pressure effects.

References

1.Lazzaroni, M. J. Optimizing Solvent Selection for Separation and Reaction. Georgia Institute of Technology, Atlanta, 2004.

APPENDIX E

FLUOROUS PHASE BEHAVIOR DATA TABLES

Table E-1. CO_2(1) + perflurohexane (2) + methanol (3) at 313 K.

P(MPa)	Liquid Phase 1 (L_1)			Liquid Phase 2 (L_2)			Vapor
	x_1	x_2	v (cm_3/mol)	x_1	x_2	v (cm_3/mol)	v (cm^3/mol)
2.13	0.310	0.690	202.1	0.119	0.022	40.1	1061.7
2.76	0.341	0.656	182.3	0.164	0.016	40.7	785.7
3.45	0.503	0.495	142.1	0.205	0.01	42.2	596.0
4.14	0.594	0.402	122.7	0.247	0.009	43.4	469.2
4.83	0.653	0.271	102.9	0.306	0.017	45.5	377.2
5.17	0.656	0.215	90.0	0.368	0.019	46.8	338.3
5.52	0.679	0.161	80.7	0.415	0.027	49.0	303.9

Table E-2. CO_2 (1) + perflurohexane (2) + acetone (3) 313 K.

P(MPa)	Liquid Phase 1 (L_1)			Liquid Phase 2 (L_2)			Vapor
	x_1	x_2	v (cm_3/mol)	x_1	x_2	v (cm_3/mol)	v (cm^3/mol)
1.24	0.299	0.622	154.6	0.2	0.029	73.5	1984.1
1.55	0.309	0.584	156.8	0.232	0.037	72.3	1563.5
1.90	0.379	0.444	135.4	0.329	0.052	70.2	1257.1
2.07	0.396	0.387	126.1	0.349	0.062	71.0	1142.1

Table E-3. CO_2 (1) + perflurohexane (2) + toluene (3) at 313 K.

P(MPa)	Liquid Phase 1 (L_1)			Liquid Phase 2 (L_2)			Vapor
	x_1	x_2	v (cm_3/mol)	x_1	x_2	v (cm_3/mol)	v (cm^3/mol)
1.13	0.193	0.746	173.8	0.125	0.013	102.2	2189.1
1.57	0.231	0.594	154.9	0.181	0.019	103.6	1247.2
3.21	0.426	0.369	119.9	0.405	0.024	85.8	688.8
3.51	0.456	0.287	112.3	0.428	0.046	85.6	618.9

Table E-4. CO_2 (1) + FC-43 (2) + methanol (3) at 313 K.

P(MPa)	Liquid Phase 1 (L_1)			Liquid Phase 2 (L_2)			Vapor v (cm^3/mol)
	x_1	x_2	v (cm_3/mol)	x_1	x_2	v (cm_3/mol)	
1.03	0.122	0.878	459.3	0.063	0.024	42.6	2366.9
3.02	0.564	0.436	232.4	0.176	0.017	42.6	730.0
3.80	0.612	0.388	194.8	0.195	0.010	43.5	551.6
5.11	0.741	0.259	142.3	0.26	0.005	47.4	370.0
6.28	0.734	0.114	99.1	0.462	0.012	47.9	266.9

Table E-5. CO_2 (1) + FC-75 (2) + methanol (3) at 313 K.

P(MPa)	Liquid Phase 1 (L_1)			Liquid Phase 2 (L_2)			Vapor v (cm^3/mol)
	x_1	x_2	v (cm_3/mol)	x_1	x_2	v (cm_3/mol)	
1.93	0.224	0.776	227.6	0.102	0.011	42.3	1232.9
3.09	0.454	0.546	166.7	0.172	0.005	43.6	721.6
5.60	0.600	0.195	102.9	0.411	0.018	46.1	328.3

APPENDIX F

BINARY PHASE BEHAVIOR MEASUREMENTS FOR PEG 300-CO_2 AND PEG 400-CO_2 SYSTEMS

Introduction

The following binary phase behavior measurements were taken for PEG 300 /$C0_2$ and PEG 400/CO_2 systems. The experiment procedure was the same as reported by Lazzaroni et al.[1]; however, instead of performing these measurements in the Jergurson cell we used the sapphire cell apparatus (as described in detail in Chapter III). We assumed that neither PEG 300 nor PEG 400 would enter into the vapor phase at these modest temperatures and pressures, making it possible to calculate the liquid phase compositions without data reduction using an EOS model. These measurements complement ternary phase behavior for PEG/organic/CO_2 systems taken by another group member.

Data Tables

Table F-1. Composition and pressure of CO_2 (1) + PEG 300 (2) at 298 K.

T/K	P/bar	x_1
298	12.9	0.174
298	23.9	0.326
298	38.3	0.493
298	52.5	0.588
298	64.1	0.681

Table F-2. Composition and pressure of CO_2 (1) + PEG 300 (2) at 313 K.

Run Number	T/K	P/bar	x_1
1	313	75.5	0.664
	313	86.3	0.656
	313	98.8	0.692
	313	109.7	0.714
	313	123.8	0.730
	313	136.9	0.730
	313	159.7	0.736
2a	313	14.7	0.177
	313	25.9	0.297
	313	36.7	0.416
	313	49.2	0.481
	313	62.4	0.545
	313	75.9	0.618
	313	85.6	0.614
	313	94.7	0.652
2b	313	76.6	0.632
	313	85.2	0.626
	313	96.3	0.670
	313	106.5	0.691
	313	128.4	0.709
	313	154.1	0.715

Table F-3. Composition and pressure of CO_2 (1) + PEG 400 (2) at 313 K.

T/K	P/bar	x_1(this work)	x_1(literature[2])
313	18.6	0.308	---
313	29.9	0.420	---
313	43.0	0.524	---
313	50.1	0.552	---
313	60.9	0.602	---
313	70.8	0.628	---
313	79.7	0.637	---
313	89.9	0.681	---
313	102.1	0.735	---
313	123.5	0.772	---
313	141.1	0.776	---
313	155.7	0.783	---
313	52	---	0.601
313	100	---	0.750
313	160	---	0.769
313	197	---	0.785
313	240	---	0.796

Figures

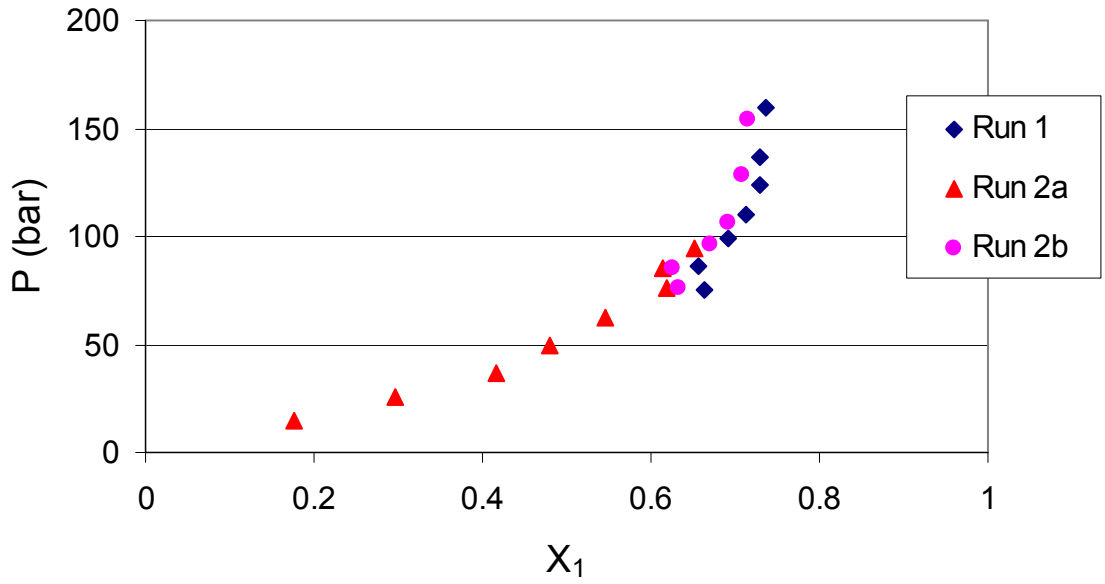

Figure F-1. Composition versus pressure for CO_2 (1) + PEG 300 (2) at 298 K.

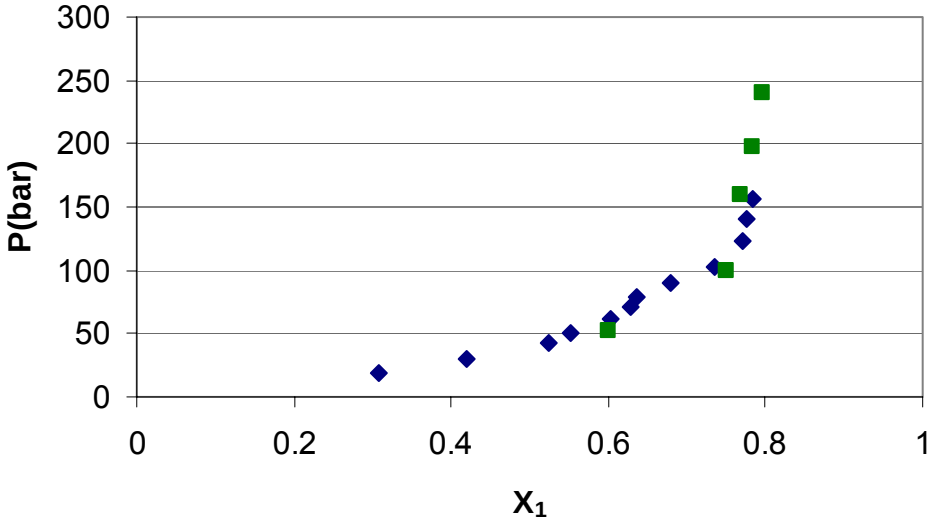

Figure F-2. Composition versus pressure for CO_2 (1) + PEG 400 (2) at 298 K; (◆) this work, (■) literature values[2].

References

1. Lazzaroni, M. J.; Bush, D.; Brown, J. S.; Eckert, C. A., High-pressure vapor-liquid equilibria of some carbon dioxide + organic binary systems. *Journal of Chemical and Engineering Data* **2005,** 50, (1), 60-65.

2. Daneshvar, M.; Kim, S.; Gulari, E., High-Pressure Phase Equilibria of Poly(ethylene glycol)-Carbon Dioxide Systems. *Journal of Physical Chemistry* **1990,** 94, 2124-2128.

APPENDIX G

DATA TABLES FOR LIGNIN, VANILLIN, AND SYRINGALDEHYDE CONCENTRATIONS IN GXL SYSTEMS

Table G-1. Concentration of lignin in GX-methanol as a function of CO_2 pressure at various temperatures.

T/°C	P/bar	mg lignin/mL solvent in GXL phase	Error (±)
25	1.0	144.8	0
	11.5	110.0	2.3
	20.4	93.0	2.3
	34.7	66.5	3.6
	41.4	61.4	3.2
	48.6	49.4	3.6
35	1.0	165.8	7.7
	19.3	98.7	8.1
	37.3	84.4	4.5
	51.7	67.4	4.7
	61.8	57.6	8.3
	70.1	24.9	0.7
40	1.0	157.5	2.8
	20.7	114.7	1.7
	32.6	92.2	4.6
	46.0	76.6	4.0
	61.0	57.6	3.7
	76.8	18.3	3.9
48	1.0	140.8	7.4
	30.5	91.0	5.4
	46.4	82.1	4.3
	62.4	70.5	4.6
	77.8	47.9	6.5
	88.8	35.6	13.3

Table G-2. Concentration of lignin in GX-ethanol at 25 °C and GX-acetone at 40°C as a function of CO_2 pressure.

Solvent	T/°C	P/bar	mg lignin/mL solvent in GXL phase	Error (±)
Ethanol	25	1.0	45.4	9.1
		12.2	62.6	3.9
		20.5	53.3	10.1
		27.5	39.5	5.4
		34.5	43.6	10.1
		41.5	36.8	---
		48.0	37.0	2.4
Acetone	40	1.0	224.3	---
		17.5	139.5	---
		52.3	85.5	---
		67.9	75.4	---

Table G-3. Vanillin and syringaldehyde concentrations in GX-methanol at 25°C using the general, timed, and staged GXL procedures.

Procedure	Run number	Time/hr	P/bar	mg vanillin /mL methanol	Error (±)	mg syringaldehyde /mL methanol	Error (±)
General	1	N/A	20.5	1.01	0.29	2.42	0.18
			27.6	0.62	0.18	2.13	0.17
			34.4	0.37	0.16	1.94	0.24
			41.4	0.28	0.18	1.75	0.52
			48.9	0.19	0.11	1.63	0.26
	2		1.0	0.66	0.23	2.64	0.25
			12.3	0.81	0.15	2.85	0.39
			20.8	0.65	0.36	2.57	0.42
			28.3	0.15	0.12	1.94	0.29
			34.3	0.17	0.17	1.93	0.39
			41.2	0.12	0.04	1.77	0.34
			48.4	---	---	1.42	0.47
Timed	1	0	1.0	0.48	0.12	2.09	0.09
		1	18.4	0.36	0.15	1.76	0.34
		3	18.4	0.67	0.06	1.54	0.08
		24	18.4	0.73	0.17	1.63	0.30
	2	0	1.0	0.27	0.14	1.57	0.09
		1	38.4	0.25	0.04	1.12	0.26
		3	38.4	0.14	0.06	1.02	0.16
		24	38.4	0.24	0.09	0.93	0.12
Staged	1	N/A	1.0	0.24	0.15	0.88	0.67
			7.4	0.42	0.03	1.21	0.09
			10.4	0.43	0.03	1.16	0.11
			15.9	0.32	0.27	1.12	0.12
	2		1.0	0.28	0.10	1.21	0.11
			6.1	0.41	0.03	1.44	0.08
			8.5	0.38	0.09	1.34	0.11
			11.7	0.36	0.03	1.31	0.08
			16.5	0.32	0.09	1.30	0.08
			19.0	0.28	0.06	1.24	0.17

Table G-4. Vanillin and syringaldehyde concentrations in GX-methanol at 40 and 48 °C using the general GXL procedure.

T /°C	Run number	P/bar	mg vanillin /mL methanol	Error (±)	mg syringaldehyde /mL methanol	Error (±)
40	1	1.0	0.52	0.04	1.47	0.30
		20.8	0.54	0.05	1.38	0.41
		32.7	0.51	0.02	1.15	0.05
		45.6	0.54	0.02	1.22	0.12
		60.9	0.64	0.01	1.37	0.06
	2	1.0	0.51	0.03	1.25	0.15
		20.6	0.51	0.02	1.35	0.16
		32.6	0.51	0.01	1.26	0.13
		46.5	0.55	0.01	1.16	0.20
		61.1	0.65	0.02	1.41	0.08
47	1	1.0	0.27	0.03	2.71	0.56
		30.5	0.30	0.08	2.26	0.43
		46.4	0.31	0.06	2.22	0.45
		62.4	0.39	0.05	2.08	0.44
		77.8	0.37	0.01	1.71	0.55
	2	1.0	0.31	0.09	2.70	0.87
		29.9	0.29	0.07	2.37	0.54
		46.1	0.32	0.10	2.12	0.48
		62.9	0.35	0.09	1.84	0.29
		76.9	0.25	0.03	1.28	0.20

VITA

Laura Christine Draucker was born on August 18th, 1981 in Salisbury, Maryland to William (Bill) and Sheree Draucker. She spent her entire childhood and adolescence there, attending public school in Wicomico County and graduating from James M. Bennett Senior High School in 1999. She then moved to Pennsylvania where she attended Villanova University, majoring in Chemical Engineering and receiving her Bachelors of Science in 2003. In the fall of 2003 she came down south to Atlanta to attend graduate school at Georgia Institute of Technology, where she researched in the school of Chemical and Biomolecular Engineering under the advisement of Dr. Charles A. Eckert and Dr. Charles L. Liotta. While at Georgia Tech she minored in public policy and met her fiancé, Marcus E. B. Smith. She will complete a Ph. D. in the summer of 2007 in Chemical Engineering. Selected publications and presentations follow.

Publications

Laura C. Draucker, Jason P. Hallett, David Bush, Charles A. Eckert, Vapor-liquid-liquid equilibria of perfluorohexane + CO_2 + methanol, + toluene,+ acetone at 313 K, *Fluid Phase Equilibria* **2006**, 241(1-2), 20-24.

Laura C. Draucker, Malina Janakat, Michael J. Lazzaroni, David Bush, and Charles A. Eckert, Timothy C. Frank and James D. Olson, Experimental Determination and Model Prediction of Solid Solubility of Multi-functional Compounds in Pure and Mixed Non-electrolyte Solvents**,** *Industrial Engineering and Chemistry Research* **2007,** 46 (7), 2198-2204.

Charles Eckert, Charles Liotta, Arthur Ragauskas, Jason Hallett, Christopher Kitchens, Elizabeth Hill, and Laura Draucker, Tunable Solvents for Fine Chemicals from the Biorefinery**,** *Green Chemistry* **2007**, 9, 545 – 548.

Aaron M. Scurto, Elizabeth Newton, Ross R. Weikel, Laura C. Draucker, Jason P. Hallett, Charles L. Liotta, Walter Leitner, Charles A. Eckert, Melting Point Depression of Ionic Liquids with CO_2: Phase Equilibria, *Industrial Engineering and Chemistry Research* (accepted for publication).

Presentations

Laura C. Draucker(speaker), Jason P. Hallett, David Bush, Charles A. Eckert and Charles L. Liotta, Cost effective extraction of high value-added chemicals from lignin with gas-expanded liquids, *231st ACS National Meeting,* Atlanta, GA, United States, March 26-30**, 2006.**

Laura C. Draucker(speaker), Jason P. Hallett, Christopher L. Kitchens, David Bush, Arthur J. Ragauskas, Charles A. Eckert, and Charles Liotta, Cost Effective High Value-Added Chemical Extraction from Lignin with Gas Expanded Liquids, *AIChE Annual Meeting*, San Francisco, CA, United States, November 12-17**,** **2006**.

Laura C. Draucker(speaker), Jason P. Hallett, David Bush, and Charles A. Eckert, Vapor-Liquid-Liquid Equilibria of Ternary Fluorous, Organic, and Carbon Dioxide Systems, *AIChE Annual Meeting*, San Francisco, CA, United States, November 12-17, **2006**.

Eckert, Charles A. (speaker), Liotta, Charles L., Ragauskas, Arthur J., Hallett, Jason P., Kitchens, Christopher L., Hill, Elizabeth M., Draucker, Laura C., Tunable solvents for fine chemicals from the biorefinery**.** *232nd ACS National Meeting*, San Francisco, CA, United States, September 10-14, **2006.**